Canada

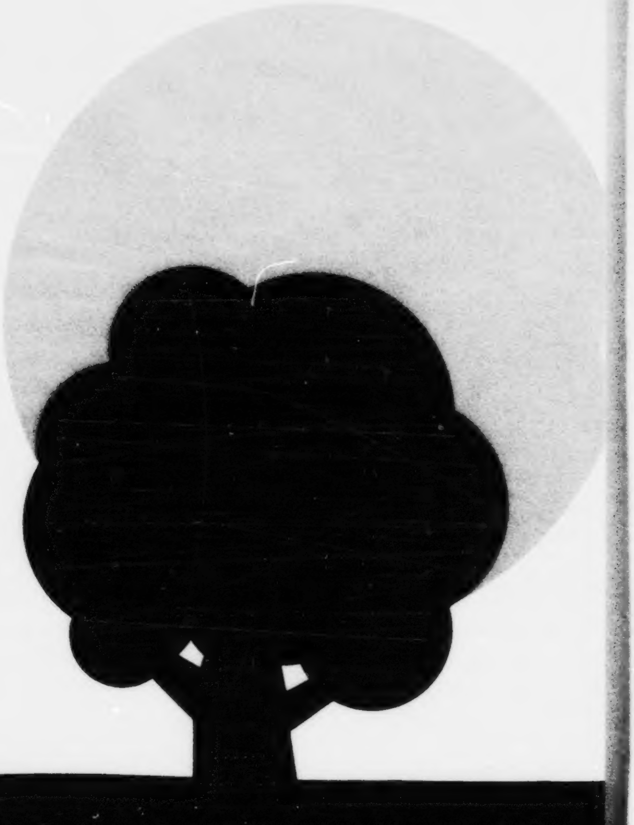

Energy, Mines and
Resources Canada

Énergie, Mines et
Ressources Canada

TECHNICAL EVALUATION OF THE WATERLOO FAST PYROLYSIS PROCESS

RENEWABLE ENERGY BRANCH

PREPARED FOR:

Bioenergy Development Program
Renewable Energy Branch
Energy, Mines and Resources Canada
Ottawa, Ontario
DSS Contract File No: 20ST.31926-3-5026
January 1987

PREPARED BY:

Waterloo Research Institute
Donald S. Scott, Principal Investigator
Department of Chemical Engineering
University of Waterloo
Waterloo, Ontario N2L 3G1
(510) 885-1211 Ext. 2914

SCIENTIFIC AUTHORITY:

1. Dr. R.P. Overend
National Research Council
Division of Energy Research
& Development
Bldg. M55, Ottawa, Ontario

2. E. Hogan
Renewable Energy Branch
Energy,Mines and Resources Canada
555 Booth Street
Ottawa, Ontario

CITATION

Scott, D.S. Technical Evaluation of the Waterloo Fast Pyrolysis Process. Report of Contract File # 20ST.31926-3-5026. Renewable Energy Branch; Energy, Mines and Resources Canada, Ottawa, Ontario, 1986 (210 pp).

Copies of this report may be obtained through:

Bioenergy Development Program
Renewable Energy Branch
Energy, Mines and Resources Canada
580 Booth Street
Ottawa, Ontario
K1A 0E4
(613) 995-9447

or

Interlibrary Loans
CISTI Library
National Research Council
Bldg. M-55, Montreal Road
Ottawa, Ontario
K1A 0S2
(613) 993-1585

This report is distributed for informational purposes only and does not necessarily reflect the views of the Government of Canada nor constitute an endorsement of any commercial product or person. Neither Canada nor its ministers, officers, employees or agents makes any warranty in respect of this report or assumes any liability arising out of this report.

©Minister of Supply and Services Canada 1987

Catalogue No. M91-7/4-1987E
ISBN 0-662-15614-5

ACKNOWLEDGEMENTS

The principal investigator wishes to acknowledge that the work reported here is the result of a true team effort, and the contributions of every member of the team were of importance in the final results. The members of the University of Waterloo Pyrolysis Group whose achievements are recorded here are Jan Piskorz, Dr. Desmond Radlein, Dr. Franco Berruti, Anna Grinshpun, Gunnar Lidén, Peter Majerski and Betty Maugham.

The Pyrolysis Group also wishes to extend their thanks to the National Research Council and to Dr. R.P. Overend, for their initial financial support and advice; to the Renewable Energy Division of Energy, Mines and Resources for continuing financial support, and to Mr. E. Hogan for his advice; and to the Natural Sciences and Engineering Research Council of Canada for a Strategic Research Grant which made possible some of the more fundamental studies.

TABLE OF CONTENTS

Page

ACKNOWLEDGEMENTS

PREFACE iii

ABSTRACT v

EXECUTIVE SUMMARY vi

RESUME A L'INTENTION DE LA DIRECTION xi

1. INTRODUCTION 1

2. OBJECTIVES 4

3. OPTIMIZATION OF THE WATERLOO FAST PYROLYSIS PROCESS 6

3.1 Statistical Studies and Kinetic Model 6

3.2 Temperature as a Variable in Fast Pyrolysis Processes 21

3.2.1 Introduction 21

3.2.2 Experimental 24

3.2.3 Results 25

3.2.4 Discussion 36

3.2.5 Literature Cited 47

4. MIXING AND SCALE-UP IN SHALLOW FLUIDIZED BEDS 48

4.1 Introduction 48

4.2 Modelling of the Pyrolysis Reactor 49

Appendix 4-A - Measuring and Modelling Lateral Solids Mixing in a Three-Dimensional Batch Gas-Solid Fluidized Bed Reactor 52

Appendix 4-B - Measuring and Modelling Residence Time Distribution of Low Density Solids in a Fluidized Bed Reactor of Sand Particles 62

5. ADDITIONAL ASPECTS OF THE WATERLOO FAST PYROLYSIS PROCESS 90

5.1 Effect of Moisture Content of the Feed 90

5.2 Pyrolysis of Softwood. Comparison of Liquid Product from Different Feeds 91

5.3 Genotoxicity Testing of Pyrolysis Oils 99

5.4 Alternative Product Recovery Methods for WFPP 100

Appendix 5 -A - Genotoxicity Testing of Pyrolysis Oils 104

6. CHARACTERIZATION OF PYROLYSIS PRODUCT OILS 124

6.1 Introduction 124

6.2 On the Presence of Anhydrodisaccharides in WFPP Pyrolysis Oils 127

6.3 Lignin Derived Product from the Fast Pyrolysis of Poplar Wood 127

6.4 Yields of Individual Components of Cellulose Pyrolysis Oils as a Function of Temperature 128

Appendix 6-A - On the Mechanism of Rapid Pyrolysis of Cellulose 131

Appendix 6-B - On the Presence of Anhydro-oligosaccharides in the Sirups from the Fast Pyrolysis of Cellulose 149

Appendix 6-C - Lignin Derived Oils from the Fast Pyrolysis of Poplar Wood 173

7. PRELIMINARY CONCEPTUAL DESIGN AND ECONOMIC FEASIBILITY STUDY FOR THE WFPP (BBC ENGINEERING LTD.) 192

7.1 Executive Summary and Comments 192

Appendix 7-A - Consultant's Report 195

8. CONCLUSIONS AND RECOMMENDATIONS 205

PREFACE

This report summarizes the results of two years intensive study of the Waterloo Fast Pyrolysis Process for the thermal conversion of biomass to liquids. In particular, various aspects of three areas of work are described. First, studies using statistically designed experiments were carried out to determine the optimal reaction conditions, particle size and feed conditions for a maximum production of organic liquids from poplar wood. The range of conditions considered was limited by the operating limitations of fluidized beds, by the limitations of our equipment and by economic considerations. Secondly, detailed characterization of the pyrolysis oils produced was made possible in the second part of the program when an NSERC grant allowed the acquisition of appropriate analytical equipment. The oils produced in the WFPP have now been more completely characterized than any previous biomass liquids. Thirdly, scale up considerations of the process, and modelling of the kinetics and heat transfer behaviour during fast pyrolysis, have been done with considerable success.

Some related studies have also been completed in this work, namely, pyrolysis studies of softwoods and a number of commercial celluloses; a preliminary study of the carcinogenic and mutagenic properties of our pyrolysis oil, and a preliminary conceptual and economic feasibility study for a full scale pyrolysis plant (the latter by an independent consultant).

The process in its present form appears to be one of the most economic methods of converting biomass to a liquid substitute fuel oil. In addition. the oils contain useful amounts of potentially significant chemicals. Further, a lignin fraction very similar to lignin from steam explosion processes, and a sugar containing aqueous solution potentially useful as a cheap fermentation substrate can be readily recovered from pyrolysis oils.

This work places the Waterloo Fast Pyrolysis Process in the forefront of thermal conversion methods for biomass. In addition, it shows that oils of considerable potential value as sources of specific chemicals can be made cheaply from wood. Some unique contributions have been made to the understanding of the basic mechanism of fast pyrolysis processes. The pyrolysis oil has been well characterized. On the other hand, very little work has been done to evaluate the properties of the char (10%-15% of the yield).

In our opinion, the Waterloo Fast Pyrolysis Process is now ready for a demonstration plant scale-up, possibly to about 5 tonnes/day size. When recovery methods for chemicals are developed, or when there is some increase in fuel oil prices, the economics of the process will become viable. The WFPP is currently the most economically attractive method of producing an alternative fuel oil from waste wood or biomass.

ABSTRACT

The fluidized bed fast pyrolysis process for the thermal conversion of biomass to liquids which is being developed at the University of Waterloo has been evaluated more fully in a number of ways. Optimal operating conditions for the maximum yield of liquids from hardwood or softwood have been determined by statistically designed experimentation in a 3 kg/hr reactor. The nature of the liquid product has been characterized, and from 80%-90% of the composition quantitatively identified. Similar studies have been done for some commercial celluloses. Scale-up criteria for shallow fluidized beds have been studied, and the results used to develop a model of the fluidized bed reactor process. A preliminary study of the carcinogenic and mutagenic properties of the oils has been carried out. A preliminary conceptual design and economic feasibility study have also been done for a full scale process.

It is concluded that the Waterloo Fast Pyrolysis Process is currently the most economic method of converting biomass to an alternative fuel oil. In addition, the pyrolysis oils show a unique potential to serve as a feedstock for the recovery of chemicals, or as an inexpensive fermentation substrate.

EXECUTIVE SUMMARY

Over the past several years, the Waterloo Fast Pyrolysis Process (WFPP) has been developed as one of the most successful and potentially the most economical ways of thermally converting biomass to liquids. During the course of the present work, two units were routinely operated - a 50-100 gm/hr bench scale fluid bed unit and a 3 kg/hr fluid bed pilot plant unit. Past studies showed that higher liquid yields than any other reported thermal conversion process were obtained in simple low cost equipment at moderate conditions - 75-80% liquid yield, with 60-65% of the wood converted to organic liquid. The principal objectives of the present study were to determine optimal conditions for maximum liquid yields, to model the process and to investigate important scale-up parameters, to carry out a preliminary conceptual design and economic feasibility study, and to better characterize the liquid product. Some additional features of the process were also investigated.

An extensive series of pilot plant tests, using a whole tree poplar feed, was carried out according to an optimal statistical plan. The variables studied were temperature, residence time and feed rate. The latter two could be varied only over limited ranges because of both equipment design limitations and the limitations of good fluidization behaviour. The tests for statistical significance showed clearly that in terms of yield of organic liquid, the temperature of reaction was the single most important variable. Within the feasible operating ranges, neither feed rate nor residence time were as important. Optimal

conditions were determined to be, for poplar wood at least, 500°-525°C, 0.4-0.6 seconds residence time and a feed rate up to about 3.0 kg of dry wood per litre of expanded bed volume.

A kinetic model of the reactor was developed based on a simple scheme of two parallel decomposition reactions to volatiles or to char + gas; with a second consecutive decomposition step of the volatiles to gases (very little secondary char is formed in the WFPP). With an assumption of first order kinetics, this model successfully described the yield of liquid product from about 450°C to 850°C.

A detailed study of lateral mixing in shallow fluidized beds was carried out, and a new mixing coefficient correlation proposed. A mixing model was also proposed which appeared best to fit the observed phenomena. The techniques developed in these studies were then used to measure the mixing behaviour of mixtures of low and high density solids in fluidized beds, and to measure the residence time distribution of wood particles in a fluidized bed of sand. These latter values were then employed in testing the kinetic model.

In brief, the WFPP operates at optimal conditions so that biomass feed particles and sand particles are always fully mixed in the fluid bed, and the wood particles are never eluted from the bed. However, as pyrolysis proceeds the wood particle loses 80%-90% of its mass, but retains much of its original geometric shape. When the density of the particle is low enough, it is eluted from the bed, a process representing particle mean residence times of 2 to 6 seconds. The system is therefore self-regulating, in that biomass particles are retained in the bed until they are fully reacted. Volatiles liberated are swept from the bed with a mean vapour residence time of about 0.6 seconds.

Other aspects of the WFPP process investigated included the effect of moisture content of the feed. Except as a diluent and possible heat sink, there is no chemical effect of moisture content at optimal conditions up to at least 25% moisture. Spruce sawdust and mill waste were pyrolysed with organic liquid yields very similar to those obtained from hardwoods. Some differences in liquid product acid content were noted for the two cases, however (less acetic acid and more formic acid were obtained from softwood).

Preliminary tests on the genotoxicity of pyrolysis oils were carried out by the Environmental Monitoring Division of the British Columbia Cancer Institute of Vancouver, B.C. Tests for carcinogenic properties showed very little effect, with only a narrow dosage range showing an effect of marginal statistical significance. Preliminary tests of mutagenicity again showed some effects in a narrow dosage range. In summary, more extensive testing would be required for a clear assessment, but preliminary results show surprisingly low genotoxicity of this oil. These results are in agreement with similar tests done by U.S. workers.

Electrostatic precipitation was tested as a means of collecting the oil fog normally formed when pyrolysis volatiles are quickly cooled. Because of the highly polar nature of the pyrolysis product, it can be very easily collected with a very high efficiency at low (non-corona) voltages in a simple collector. Electrostatic precipitation is now used routinely in the bench scale apparatus.

A great deal of work was carried out characterizing pyrolysis oils after an NSERC grant allowed the acquisition of HPLC and GC-MS analytical equipment. As a result of these studies, about 90% of the liquid product has been quantitatively identified. About 20-25% is water, 18-25% is derived from lignin, and the balance is derived from cellulose primarily, and to a lesser extent from hemicellulose. Of the individual compounds identified, the presence of anhydrocellobiosan as the major disaccharide product was demonstrated for the first time. Significant amounts of hydroxyacetaldehyde (up to 15% of the oil) were also present, and suggest this compound as a major potential commercial chemical. The presence of such large yields also led to the publication of some speculations concerning the mechanisms of fast pyrolysis of cellulose.

The lignin fraction of the pyrolysis oil can be readily separated and recovered from the carbohydrate fraction by water extraction. This lignin product gave an NMR spectra which was essentially identical to that obtained from the lignin recovered from steam exploded poplar wood. The aqueous carbohydrate fraction has a sugar content such that it may be a very economical substrate for a fermentation process.

Finally, a conceptual preliminary and economic feasibility study was carried out by BBC Engineering Ltd. (Toronto). This study was based on a 100 dry t/day or 500 dry t/day plant sizes, and assumed a feed of green wood waste at 40% moisture at a cost of $40 per dry tonne. Scale up rules might be adequate for a 100 t/day fluidized bed reactor, but at 500 t/day feed rate, probably a circulating fluid bed might be a better choice. This option is now being investigated experimentally on a laboratory scale. Approximately one third of the capital cost goes for wood grinding, about one third for wood drying and handling, and about one third for the actual pyrolysis unit. The cost of the wood feed is a major operating cost - about 50% for a 500 t/day plant and about 30% for a 100 t/day unit.

On the basis of a 50% equity and a 30% DCF rate of return, the cost of production of a pyrolysis oil (about 24% water) would be about \$92/tonne or 10.8 ¢/litre (S.G.=1.18) or \$5.7/million BTU. This production cost would be \$8-\$9/million BTU for a 100 tonne/day plant, if the same conceptual design and economic criteria were used.

It is concluded that the Waterloo Fast Pyrolysis Process is potentially the cheapest present method of converting biomass to a substitute fuel oil. Further, the pyrolysis oil can also serve as a feedstock for the recovery of chemicals, for the production of a lignin product, or as a source of fermentable sugars. The low capital cost and simplicity of the WFPP suggests that it would be particularly suitable for use as one of a number of small scale units located near the sites of waste biomass production. The collective liquid product could then be further processed. The next stage of development of the WFPP should therefore be a 5 to 10 t/day mobile demonstration unit.

RÉSUMÉ À L'INTENTION DE LA DIRECTION

Au cours des dernières années, on a mis au point le procédé de pyrolyse rapide Waterloo (Waterloo Fast Pyrolysis Process, WFPP) qui constitue l'une des méthodes les plus efficaces et potentiellement les plus économiques de transformer la biomasse en liquides par traitement thermique. Au cours des présents travaux, on a fait régulièrement fonctionner deux unités : une unité de laboratoire à lit fluidisé d'une capacité de 50 à 100 g/h, et une unité pilote à lit fluidisé d'une capacité de 3 kg/h. Des études antérieures ont montré que ce procédé, qui utilise un matériel simple et peu coûteux, et des conditions modérées, permet d'obtenir des rendements en liquides plus élevés que tout autre procédé de conversion thermique connu (rendement en liquides de 75-80 % et transformation de 60-65 % du bois en liquide organique). La présente étude visait principalement à déterminer les conditions qui permettraient d'obtenir les rendements maximums en liquides, à modéliser le procédé et à étudier les importants paramètres de mise à l'échelle, à effectuer une étude préliminaire de faisabilité technique et de rentabilité et à mieux caractériser le produit liquide. Certaines autres caractéristiques du procédé ont aussi été étudiées.

De nombreux essais ont été réalisés à l'échelle pilote suivant un plan statistique optimal, avec des peupliers entiers. Les variables étudiées étaient la température, le temps de séjour et le taux d'alimentation. On n'a pu faire varier ces deux dernières variables qu'à l'intérieur de gammes limitées, à cause de contraintes liées à la conception du matériel et à la fluidisation. Les tests de signification statistique ont clairement montré qu'en ce qui concerne le

rendement en liquide organique, c'est la température de réaction qui était la variable la plus importante. À l'intérieur des gammes de traitement possibles, ni le taux d'alimentation et ni le temps de séjour n'étaient aussi importants. On a déterminé que les conditions optimales étaient les suivantes, du moins dans le cas du bois de peuplier : température de 500-525 °C, temps de séjour de 0,4-0,6 seconde et taux d'alimentation allant jusqu'à 3,0 kg de bois sec par litre de lit expansé.

Un modèle cinétique du réacteur a été élaboré à partir d'un schème simple comprenant deux réactions parallèles de décomposition en produits volatils ou en produits de carbonisation + gaz et une étape consécutive de décomposition des produits volatils en gaz (le procédé WFPP donne très peu de produits de carbonisation secondaires). En supposant que les réactions suivent une cinétique du premier ordre, ce modèle décrit fidèlement le rendement en produits liquides, d'une température d'environ 450 jusqu'à 850 °C.

On a étudié en détail le mélange latéral dans les lits fluidisés peu profonds et on a proposé une nouvelle corrélation entre les coefficients de mélange. On a également proposé un modèle qui semblait représenter le mieux le phénomène observé. Les techniques mises au point au cours de ces études ont ensuite été utilisées pour déterminer le comportement de mélanges de solides de faible masse volumique et de masse volumique élevée dans les lits fluidisés et pour mesurer la répartition des temps de séjour des particules de bois dans un lit fluidisé de sable. Ces dernières valeurs ont ensuite été employées pour vérifier le modèle cinétique.

En bref, le procédé WFPP fonctionne dans des conditions optimales de sorte que les particules de biomasse et les particules de sables sont toujours parfaitement mélangées dans le lit fluidisé et que les particules de bois ne sont jamais éluées du lit. Cependant, durant la pyrolyse, les particules de bois perdent 80-90 % de leur masse, mais conservent en grande partie leur forme géométrique. Lorsque la masse volumique d'une particule est assez faible, cette particule est éluée du lit, ce qui correspond à un temps de séjour moyen de 2 à 6 secondes. Il y a donc autorégulation du système, en ce sens que les particules de biomasse sont retenues dans le lit jusqu'à ce qu'elles aient complètement réagi. Les produits volatils libérés sont balayés du lit, le temps de séjour moyen des vapeurs étant d'environ 0,6 seconde.

L'effet de la teneur en humidité de la charge d'alimentation est un autre aspect du procédé WFPP qui a été étudié. Outre son effet de dilution et peut-être de puits thermique, la teneur en humidité n'a aucun effet chimique dans des conditions optimales, jusqu'à un taux d'humidité d'au moins 25 %. La pyrolyse de bran de scie d'épinette et de déchets des usines de conversion du bois d'épinette a donné des rendements en liquides organiques très analogues à ceux qu'on obtient avec des feuillus. On a toutefois constaté certaines différences dans la teneur en acide des produits liquides obtenus dans ces deux cas (on obtient moins d'acide acétique et davantage d'acide formique avec des résineux).

Des essais préliminaires visant à évaluer la génotoxicité des huiles obtenues par pyrolyse ont été effectués par la Environmental Monitoring Division du Cancer Institute de Colombie-Britannique à Vancouver (C.-B.). Des essais visant à déceler les propriétés cancérogènes ont révélé très peu d'effets, et un effet de signification statistique marginale a été observé uniquement dans une gamme étroite de doses. Des essais préliminaires de mutagénicité ont aussi mis en évidence certains effets à l'intérieur d'une gamme étroite de doses. En résumé, il faudrait effectuer des essais plus approfondis pour bien évaluer les risques, mais les résultats préliminaires révèlent que la génotoxicité de l'huile obtenue par pyrolyse est étonnament faible. Ces résultats concordent avec des essais analogues réalisés par des chercheurs des É.-U.

On a déterminé dans quelle mesure la précipitation électrostatique permettrait de recueillir le brouillard d'huile qui se forme normalement lorsque les liquides volatils produits pendant la pyrolyse sont rapidement refroidis. En raison de leur nature hautement polaire, les produits de pyrolyse peuvent être très facilement et très efficacement recueillis par un simple collecteur réglé à basse tension (sans effet couronne). La précipitation électrostatique est maintenant utilisée régulièrement dans l'unité de laboratoire.

Après l'acquisition d'appareils d'analyse par CLHP et par CG-SM, rendue possible grâce à une subvention du CRSNG, on a effectué de nombreux travaux visant à caractériser les huiles obtenues par pyrolyse. Ces études ont permis d'identifier quantitativement 90 % environ du produit liquide. Ce dernier est constitué d'environ 20-25 % d'eau et renferme 18-25 % d'une substance provenant de la lignine, tandis que le reste dérive principalement de la cellulose et, dans une moindre mesure, de l'hémicellulose. Pour ce qui est des composés individuels, on a décelé pour la première fois la présence d'anhydrocellulobiose, qui est le principal dissaccharide dans ce produit. Le produit renferme aussi une quantité importante d'hydroxy-acétaldéhyde (jusqu'à 15 % de l'huile), ce qui donne à penser que ce composé pourrait être important du point de vue commercial. L'obtention de rendements aussi élevés a aussi amené la publication de certaines hypothèses concernant les mécanismes de pyrolyse rapide de la cellulose.

On peut facilement séparer et récupérer la fraction de lignine de l'huile obtenue par pyrolyse, en procédant par extraction à l'eau de la fraction glucidique. Cette fraction possède un spectre RMN essentiellement identique à celui de la lignine récupérée à partir du bois de peuplier éclaté à la vapeur. La teneur en sucres de la fraction glucidique aqueuse est telle que cette dernière pourrait constituer un substrat très économique pour un procédé de fermentation.

Finalement, une étude préliminaire de faisabilité technique et de rentabilité a été réalisée par la BBC Engineering Ltd (Toronto). Cette étude était basée sur une capacité de 100 t sèches/jour ou de 500 t sèches/jour et supposait une charge d'alimentation de déchets de bois vert renfermant 40 % d'humidité, au coût de 40 $ la tonne sèche. Les règles de mise à l'échelle sont peut-être adéquates pour un réacteur à lit fluidisé de 100 t/jour, mais pour un taux d'alimentation de 500 t/jour, il serait peut-être préférable de choisir un lit fluidisé à recirculation. Cette option fait actuellement l'objet d'une étude à l'échelle du laboratoire. Environ un tiers des dépenses en capital sont affectées au broyage du bois, environ un tiers au séchage et à la manipulation du bois, et environ un tiers à l'unité de pyrolyse. Le bois représente une part importante des frais d'exploitation, soit 50 % environ pour une usine de 500 t/jour et 30 % environ pour une unité de 100 t/jour.

Si l'on suppose un taux de fonds propres de 50 % et une rentabilité du flux monétaire actualisé de 30 %, le coût de production de l'huile de pyrolyse (renfermant environ 24 % d'eau) s'élèverait à environ 92 $ la tonne, soit 10,8 ¢ le litre (densité=1,18) ou 5,7 $ le million de BTU. Pour une usine de 100 tonnes/jour, le coût de production serait de 8-9 $ le million de BTU, si les mêmes critères techniques et économiques étaient appliqués.

On conclut que le procédé de pyrolyse rapide Waterloo est potentiellement la méthode la moins chère qui existe actuellement pour transformer la biomasse en un substitut du mazout. De plus, l'huile obtenue par pyrolyse peut servir de charge de départ pour la récupération de produits chimiques, pour la production d'un produit de lignine ou comme source de sucres fermentescibles. La faible dépense en capital et la simplicité du procédé WFPP laissent penser qu'il s'agit d'une méthode particulièrement appropriée dans le cas d'un certain nombre de petites unités situées à proximité de sites où l'on produit des déchets de biomasse. On pourrait ensuite faire subir un traitement plus poussé à l'ensemble du produit liquide. La prochaine étape de la mise au point du procédé WFPP devrait donc être la fabrication d'une unité mobile de démonstration d'une capacité de 5-10 t/jour.

TECHNICAL EVALUATION OF THE WATERLOO FAST PYROLYSIS PROCESS

by Donald S. Scott, University of Waterloo

1. INTRODUCTION

Since 1979, a fluidized bed flash pyrolysis process for the production of pyrolytic liquids from biomass has been under development at the University of Waterloo. Initially, a bench scale mini-fluidized bed was developed patterned after that used by Tyler (1979) for the flash pyrolysis of coal. A novel entrained flow low rate biomass feeder was also developed, capable of feeding biomass particles at rates of 5 to 100 grams/hour with an accuracy of 5% (Scott and Piskorz, 1982a). Initial studies done with this bench scale pyrolysis apparatus using maple and hybrid poplar wood showed that up to 65% yields of organic liquids could be obtained from hardwoods at temperatures of about 500°C and 0.5 seconds apparent residence time. Details of this work are given in the final report for ENFOR Project No. C-28 (Scott, 1981), as well as in several publications e.g. Scott and Piskorz (1982b), Scott et al. (1984). In the course of bench scale work, the effects on the liquid yield of particle size, residence time, reaction atmosphere and of various additives were reported. In addition to maple and poplar wood, wheat straw, corn stover, poplar bark, bagasse and peat moss were also evaluated for conditions giving maximum yields of liquids.

As a result of the promising results obtained in the bench scale work, funding was received in April, 1981, to design, construct and operate a larger continuous unit with a throughput of 1-3 kg/hr. of biomass (ENFOR Project C-223). This work was completed in early 1983, and has been reported (Scott, 1984a; Scott and Piskorz, 1984).

Additional work was undertaken in 1983 to 1984 to extend the knowledge of the nature of the pyrolysis products, how these products might be altered to a more desirable liquid fuel, and to participate in the International Energy Agency Biomass Direct Liquefaction Test Facility Evaluation Program (IEA BLTF project). All of these objectives were met to the extent that our facilities allowed. In terms of product analysis, it was necessary to rely on external agencies for the more sophisticated work e.g. GC-MS, HPLC or NMR analysis. However, a number of useful results were obtained. More extensive work was done than required by the original contract on chemical modification of the liquid product, both by liquid phase and vapour phase reactions. Also more pilot plant tests were done in the IEA program than required, both to give a better picture of possible yields, and to supply the required quantities of pyrolytic oil for other tests. In addition, some pilot plant runs were done using whole tree poplar aspen wood in order to obtain pyrolytic oil samples which might be more representative of those produced in a larger scale unit. All this work has been described in a major contract report (Scott, 1984a) and in publications (Scott et al., 1985; Scott and Piskorz, 1984b).

The work on the Waterloo Fast Pyrolysis Process was resumed in January, 1984, when additional funds were received from the National Research Council (later transferred to the Renewable

Energy Division of Energy, Mines and Resources). The present report describes the development of the Waterloo Fast Pyrolysis Process from January 19th, 1984 to March 31st, 1986. In late 1984, funds were also received from the Strategic Grant Program of the Natural Sciences and Engineering Research Council for the purchase of a GC/MS unit as well as an HPLC unit (jointly with Prof. M. Moo Young). This equipment became operational in April, 1985, and has played a major role in the characterization studies of the oils produced from the Waterloo Fast Pyrolysis Process (WFPP).

2. OBJECTIVES

The work reported here had a number of objectives which are listed below.

1. Further investigation of the WFPP with respect to yields from poplar including a set of statistically designed experiments intended to locate optimal operating conditions for maximum liquid yields
2. Evaluation of the WFPP yields for alternative feedstocks, especially softwood
3. Evaluation of the effect of moisture content on yields from the WFPP
4. Characterization of pyrolysis oils with respect to conversion to fermentable sugars, and possible formation and recovery of derivatives
5. Evaluation of alternate product recovery systems for the WFPP
6. Evaluation of tar and tar fractions for mutagenic properties
7. Evaluation of pyrolysis oils as fuels - storage stability, limited firing tests, cooperation with Canadian Combustion Laboratories, Ottawa
8. Experimental modelling of shallow fluidized bed reactors; and determination of important scale-up parameters
9. Carrying out an engineering technical feasibility study and an economic evaluation of a conceptual process.

In our opinion all of these objectives have been met to some degree, and in some cases have been considerably exceeded.

During the course of the work, some fundamental studies were carried out employing a variety of celluloses, in an attempt to better understand the decomposition mechanisms occurring in flash pyrolysis. In addition, kinetic modelling studies were also done for the WFPP. Much of this work was carried out with the aid of an NSERC Strategic Grant, but a summary of many of the results are included here, since they are complementary to this work. Therefore, the results of some investigations are included in this report which do not fall directly under the above objectives, and which were not directly a part of the proposed contract work.

A great deal of both fundamental and developmental work has been done since January, 1984. Because full details could become very voluminous, reporting is confined primarily to results obtained and discussions of these results. Specific procedural and analytical details can be found in the included publications in most cases.

3. OPTIMIZATION OF THE WATERLOO FAST PYROLYSIS PROCESS

3.1 Statistical Studies and Kinetic Model

A complete 2^n factorial design was used for a set of experiments employing poplar wood feed in the pilot plant reactor. The number of factors studied was $n = 3$, with the chosen variables being temperature, feed rate and gas residence time. The range of values of the latter two variables which could be covered was restricted by the design limitations of the fluid bed reactor. On the basis of sixteen runs, it was found that temperature was by far the controlling variable.

A kinetic model was developed, based on first order kinetics and two parallel reaction sequences. Published rate equations were reviewed, and one of these selected to describe the initial decomposition of the wood to volatiles or to char + gas by parallel reactions. The kinetic parameters for the decomposition of volatiles (tars) to light liquids and gas were deduced from our pilot plant results.

A complete modelling of the heat transfer to a wood particle was carried out, and from this a criterion was developed for a probable maximum particle size. Wood particle residence times in the fluid bed were estimated from a series of direct measurements.

Some experimental runs were also done in order to determine the heat of reaction of pyrolysis in the WFPP. This measurement was not highly accurate because the net heat of reaction is nearly zero when liquid production is at a maximum.

All of these results are contained in detail in the MASc thesis of A.G. Liden. The Abstract, Table of Contents and final Summary for this thesis are attached. One copy of the full thesis has been submitted with the original of this report.

ABSTRACT

A statistical analysis of wood pyrolysis runs in a fast pyrolysis process, the Waterloo Fast Pyrolysis Process, is presented. The investigated factors were temperature, feedrate and gas residence time. The statistical analysis showed only a significant effect of the temperature. Optimum temperature for production of tar was found to be 506 C for Brockville poplar.

A kinetically motivated model which considers secondary tar cracking reactions is presented. The secondary reaction rate constant is estimated for the tar cracking of poplar tar. The secondary rate constant is found to be

$k_2 = 4.28 \cdot 10^6 \exp(-107.5 \cdot 10^3/(RT))$ (s^{-1})

The optimum tar yield for poplar is estimated to be 0.703.

The heat requirement for the pyrolysis process is estimated. The heat requirement of pyrolysis of poplar at a temperature of 500 C, with an initial wood temperature of 21 C was found to be about 900 J/g calculated on a moisture free basis.

Heat transfer to a wood particle in a fluidized bed is discussed. It is recommended that the particle size to be used in a fluidized bed pyrolysis process aiming at a high tar production should be smaller than 2 mm

TABLE OF CONTENTS

PAGE

List of Tables xii

List of Figures xv

I. Introduction 1

  1. Biomass as a Fuel Resource 1

  2. Fluidized Bed Technology 2

  3. Waterloo Pilot Plant Unit 7

  4. Objectives of This Work 11

II. Statistical Analysis of Waterloo Pilot Plant Runs 12

  1. Background 12

  2. Theory 13

    2.1. Factorial Design 13

      2.1.1. Introduction 13

      2.1.2. Definitions 13

      2.1.3. Waterloo Experimental Design . 15

      2.1.4. Basic Notation 16

      2.1.5. Method of Analysis. 18

    2.2. The D-optimality Design 20

      2.2.1. Notation and Model 21

3. Result and Analysis of Waterloo Data . . 24

4. Conclusions 30

III. Pyrolysis Kinetics 32

1. Background 32

2. Studies to Determine an Overall Decomposition Rate 48

2.1. TGA-studies 48

2.2. Other Methods 50

3. Studies to Determine Rate Constants for Different Product Groups 53

4. Studies to Determine Rate Constants for Primary and Secondary Reactions 55

5. Discussion 56

IV. Kinetic Modelling 58

1. Background 59

2. Derivation of Model 60

2.1. Assumptions 61

2.2. Steady State, Secondary Reactions Neglected 61

2.3. Steady State, Secondary Reactions Considered 63

3. Model Parameters 66

3.1. Secondary Reaction Parameters . . 66

3.2. Primary Reaction Parameters . . . 68

4. Residence Time of Solids in the Reactor. . 69

5. Proposed Model 71

6. Discussion 78

V. Unsteady State Heat Transfer 83

1. Background 87

2. Problem Definition 87

2.1. Initial Conditions 87

2.2. Basic Equations 89

2.3. Essential Physical Properties Needed . 95

3. Physical Properties of Wood 95

3.1. Density 95

3.2. Heat Capacity and Thermal Conductivity . 97

3.3. Recommended Values 100

4. Physical Properties of Product Gases . . 101

4.1. Density 101

4.2. Thermal Conductivity 102

4.3. Dynamic Viscosity 108

4.4. Recommended Values 110

5. Heat Transfer to Particles Immersed in a Fluidized Bed 110

5.1. Modes of Heat Transfer 110

5.2. Homogeneous Gas-Solid Heat Transfer . 112

5.2.1. Single Sphere 112

5.2.2. Fixed Bed 113

5.2.3. Fluidized Bed 115

5.3. Models for Heat Transfer to Immersed Particles 119

6. Calculation of Temperature Profiles for Waterloo Pilot Plant Conditions 130

7. Gas Radiation 139

8. Conclusions for Size Limitations Due to Heat Transfer Effects 143

VI. Heat Requirements for Pyrolysis Reactions . 149

1. Heat of Reaction 150

2. Experimental 151

3. Calculations 154

4. Results and Discussion 162

VII. General Discussion and Recommendations for Scale-Up 170

1. Proposition for Future Work 170

2. Proposed Models for Pyrolysis in a Fluidized Bed with Particular Reference to Poplar . 171

2.1. Unstructured or Polynomial Model . . 171

2.2. Structured Model 172

2.2.1. Kinetic Model 172

2.2.2. Reactor Conditions and Yield Expressions 173

2.2.3. Heat Transfer to a Particle in the Bed 173

2.2.4. Heat Requirements for the Process . 174

2.3. General Design Considerations . . 174

References 176

Appendices 188

Appendix II 188

Appendix IV 202

Appendix V 208

Appendix VI 231

VII. GENERAL DISCUSSION AND RECOMMENDATIONS FOR SCALE-UP

1. Proposition for Future Work

Production of liquid fuel from biomass is with today's oil prices not economically attractive other than under special circumstances. According to Klass (35) biomass will not play any important role as an energy source until after 1990. However, the importance of biomass as an energy source will no doubt increase in the coming years.

The breakdown of the cellulose chain to shorter fractions can also find other applications than merely fuel production. Oil from pyrolysis contains a wide range of products, including anhydrosugars. There is a distinct possibility that the oil can be used in fermentation. Until more is known about the chemical structure of the oil, it is difficult to predict usage of it, but it is rather obvious that other organic feedstocks than fossil oil must be found to be used by the petrochemical industry in the future. In this context, oil from biomass is an interesting alternative.

This work has dealt with problems concerning the scale-up of the Waterloo Fast Pyrolysis process. A proposal for a scale-up model will be given here. However, it is recommended that further studies, especially in the field of kinetics, are undertaken to attain complementary knowledge, permitting economical and technical feasability studies and, hopefully, the industrial application of the process. It is the author's belief that the fluidized bed technology will prove highly successful, in comparison to other techniques, in producing tar at a high yield and at a competitive price.

2. Proposed Models for Pyrolysis in a Fluidized Bed with Particular Reference to Poplar

2.1. Unstructured or Polynomial Model.

The simplest possible model to be used for prediction of tar yield from pyrolysis of poplar in a fluidized bed is the polynomial model achieved from the statistical analysis in Chapter II. This model is restricted to gas residence times between 0.5 and 0.7 s, feedrate to bed weight ratio between 0.5 kg wood/kg sand hr and 2.0 kg wood/kg sand hr and temperatures between 450 and 590 C.

The yield prediction is given by Eq. 1.

$$(1)\ Y = (0.542 + 0.215(T - 500) - 0.956(T - 500)^2)/0.2 + 60$$

Y = Tar yield in %

T = Temperature in °C.

Since the model makes no assumption regarding heat transfer or kinetic pathways, the particle size should be that used in the experiments, which was 0.6 - 1.2 mm.

2.2. Structured Model.

A structured model should make predictions regarding kinetic pathways, heat transfer effects and heat of reaction. The model developed in this work is comprised of the above mentioned parts.

2.2.1. Kinetic Model.

The predominant kinetic pathways are assumed to be:

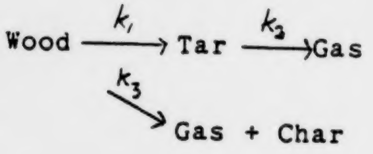

Furthermore, the relations given by Eq. 2 and Eq. 3 are assumed:

(2) $k = k_1 + k_3$

(3) $\bar{\Phi}^{*} = k_1 / k$

The kinetic parameter estimates recommended for the temperature interval 450 - 600 °C are:

(4) $k_1 = 10^{13} \exp(-183300/RT)\ s^{-1}$ (Kosstrin)

(5) $$k_2 = 4.28\times10^{6}\exp(-107500/RT)\ s^{-1}$$

(6) $$\Phi^{**} = 0.703$$

Considering the reasonable extrapolated behaviour of the structured kinetic model and the limited applicable range of the statistical model, it is recommended that the structured model be used for scale-up at the present time.

2.2.2 Reactor Conditions and Yield Expressions

The fluid bed reactor is assumed to give:

* Perfect Backmix of Solids
* Plug Flow of Gas

Depending on the depth of the bed and the size of the freeboard region two different expressions for the tar yield will result. For a reactor with a small freeboard region compared to the bed, the expression for tar yield prediction will be that given by Eq. 7. For a very shallow reactor with a large freeboard region, the expression will be that of Eq. 8.

(7) $$\Phi = \Phi^{*}\Big(1 - \exp(-k\tau_s)\Big)\frac{\Big(1 - \exp(-k_2\tau_g)\Big)}{k_2\tau_g}$$

$$\phi = \phi^{\circ}\left(1 - \exp(-k\tau_{\circ})\right) \cdot \exp(-k_2 \tau_g) \qquad (8)$$

174

2.2.3. Heat Transfer to a Particle in the Bed

The wood particles can be regarded as immersed particles for the low feedrates used in the Waterloo Fast Pyrolysis Process. In this case the heat transfer coefficient describing the total heat transfer to the particle is estimated to be between 300 W/m^2·K and 510 W/m^2·K. These values apply for a sand particle size of 0.45 mm. Larger sand particles will probably lead to decrease in the heat transfer. The above given estimates of the heat transfer coefficients are believed to be the best estimates which can be achieved with the present knowledge of heat transfer to immersed surfaces. However, the uncertainty is still larger than desirable and studies of the heat transfer between sand particles and biomass in a fluidized bed would be highly useful to achieve more precise estimates of the heat transfer coefficient.

Given the criteria that less than 10% of the wood pyrolysis should take place below 450°C, it is recommended that the wood particle size to be used in the process should be less than 2 mm.

2.2.4. Heat Requirements for the Process

For Brockville Poplar with an initial temperature of 21 °C and a pyrolysis temperature of 483 °C, the heat requirement calculated on a moisture free basis was estimated to 940 J/g. For IEA poplar, with the same initial temperature but a pyrolysis temperature of 509 °C, the corresponding estimate was 930 J/g.

With the uncertainty associated with these estimates it is recommended that the heat requirement is taken to be within the interval 700-1100 J/g for the poplar species in question. For pyrolysis of poplar in the Waterloo Fast Pyrolysis Process at 500 C, the value recommended for the heat requirement on a moisture free basis is 900-950 J/g.

2.3. General Design Considerations

Three major design considerations to be taken are :

1. Adequate mixing of solids in the bed. This is necessary to ensure a good heat transfer and thus a complete reaction. For a large scale unit with a diameter/bed height ratio > 1 multiple feeders in the bed will probably be necessary.
2. Adequate operational temperature. Fortunately, the temperature is not very critical as can be seen from graphs in Chapter II and Chapter IV. The operational temperature should be slightly above 500 °C.
3. Adequate gas residence time. For the proper temperature,

the gas residence time is not that crucial for kinetic reasons. The gas residence time will be decided from considerations of minimum fluidization and char entrainment. Generally it can be said that the gas residence time should be as low as possible for kinetical reasons. However, a low gas residence time means a high gas flow rate, which could lead to undesirable entrainment of wood. A probable operational superficial gas velocity is the velocity used in the Waterloo Pilot Plant, that is about 0.6 m/s. However, this value must probably be tested for the specific reactor design in question. Especially the freeboard region height might be important in determining the operational superficial gas velocity.

Furthermore, it might be recommendable for heat transfer reasons to use a relatively small sand particle size.

3.2 Temperature as a Variable in Fast Pyrolysis Processes

3.2.1 Introduction

In rapid pyrolysis processes, the rate of heat transfer is all-important. Ideally, in such a process, the time required for a biomass particle to reach about 95% of the reaction temperature would be much less than the particle residence time itself. The residence times normally quoted in thermal pyrolysis studies are usually mean gas residence times, that is, the net empty reactor volume divided by the volumetric flow rate, usually taken at reactor inlet conditions. Particle residence times are not as precisely known, and will vary with the reactor configuration and type. Measurement of mean particle residence times has not been done in the majority of fast pyrolysis process studies. However, Berruti (1985) measured these residence times in a fluidized sand bed for 1 mm particles, and found that these varied from 2 to 6 s depending on the gas residence time (400 to 800 ms). Recently, Solomon et al. (1986) reported measurements of the velocity of fine coal particles in a downward flow entrained reactor and found these were only about 40% of the gas velocity over most of the reaction period. Therefore, although the residence time of particles is generally not known very precisely in fast pyrolysis processes, it will likely be from 2 to 10 times the apparent gas residence time for most of the applicable reactors, that is, for entrained flow, fluid bed, spouted bed or cyclonic reactors. It is likely, therefore, that given a reactor capable of high heat flux, and particles of appropriate size with the "normal" gas residence time of about 500 ms, the heat-up time may not be a large fraction of the total particle residence time.

Antal (1983, 1985) has pointed out in his excellent reviews of biomass pyrolysis theory and experimentation, that the particle must pass through the same temperature zones regardless of the final reaction temperature. Therefore, given the high rates at which initial thermal decomposition of biomass occurs, it is unlikely that a particle can be still in its primary decomposition phase at any temperature above about 500°C, regardless of the heat flux available. Above this temperature, secondary reactions must occur, in either vapor or solid phases. The heat-up rate of a particle depends, of course, on several factors apart from the available heat flux. Obviously, faster heat-up will occur with smaller particles (higher surface/mass ratio) and with drier particles. It is also of considerable significance that initial decomposition processes of biomass to give a maximum liquid yield at 500°-550°C show a very small net heat of reaction. Secondary decomposition reactions of liquid products, however, are much more endothermic.

In recent articles, Antal (1985) and Kothari and Antal (1985) have mathematically modelled the relationships between the various heat transfer and kinetic parameters, and formulated quantitative criteria for the times required for heat-up and devolatilization. In a similar way, Lidén (1985) has given a criterion for heating-up times of particles of biomass in a fluidized bed reactor.

In summary, it is likely that each process will have its limits such that inadequate heat transfer causes marked changes in the distribution of the pyrolysis products. However, within these limits (which may not differ very much for different reactors capable of high heat transfer rates), the product distribution at a given gas residence time might be expected to be a function of the final reaction temperature only, especially if particles are smaller than about 1 mm and are reasonably dry. The principal criterion for this to be true is that the heat-up time for the particle should be considerably less than the time spent near reaction temperature, possibly only 20% of the total particle reaction time. As a result, the kinetic rate of reaction will probably be the rate limiting process. The present results were obtained to demonstrate whether or not these speculations are confirmed by experiment in different reactors.

3.2.2 Experimental

For this work, two completely different pyrolysis reactors were used, operated by two different research groups. The "ultrapyrolysis" entrained flow reactor was developed by workers at the University of Western Ontario, and was capable of operation to 1000°C with gas residence times of 50 ms to 900 ms. The second reactor was the fluidized bed pyrolysis unit developed at the University of Waterloo for thermal conversion of biomass to liquids. It operated up to 750°C with gas residence times of 300 to 1500 ms. Typical operating ranges for the two reactors are summarized in Table 3.2.1. Details of the operation of these reactors have been given by Graham et al. (1985) and by Scott et al. (1985).

Table 3.2.1 Range of Experimental Parameters

	Ultrapyrolysis	Fluid Bed
Temperature, °C	700-1000	400-750
Reactor Residence Time (Gas), ms	50-900	300-1500
Maximum Feed Rate, kg/hr	1.0	3.0
Estimated Heating Rates, °C/s	10^4-10^5	10^4-10^5
Pressure, atm abs.	1.0	1.0
Reaction Atmosphere	N_2	N_2 or Product Gas

3.2.3 Results

Two feed materials, Avicel cellulose and red maple sawdust, were used in these tests, with properties shown in Table 3.2.2. The Avicel PH-102 used by both research groups was from the same lot. However, the maple, although the same species in both cases, came from different samples of mature trees. Avicel is a highly purified highly crystalline cellulose product, while the maple is a typical Eastern Canadian hardwood.

The pyrolysis experiments in the fluid bed were all carried out at gas residence times of 450-550 ms. In this range, yields of liquid, gas and char show only a small variation with time. A typical experiment in the transport reactor at 700°C is shown in Figure 3.2.1 for maple wood. Over the reaction time span of 350-900 ms, the yields of liquid, char and gas became independent of residence time in the reactor. Accordingly, data from the transport reactor in this asymptotic range were compared to data from the fluidized bed pyrolyzer.

Table 3.2.1 Characteristics of Feed Materials

	Cellulose (Avicel PH-102)		Wood (Eastern Red Maple)	
	Ultra-pyrolysis	Fluid Bed	Ultra-pyrolysis	Fluid Bed
Moisture, %	4.01	2.9	0.9	5.4
Ash, %	<0.1	<0.1		0.59
Particle Size Range, μm	-250+40	-250+40	-180+37	-595
Mean Particle Size, μm	100	100	120	
Elemental Analysis (mf), %				
C	44.24		48.5	
H	6.16		6.1	
N	Tr.		0.50	
O (by difference)	49.6		44.9	

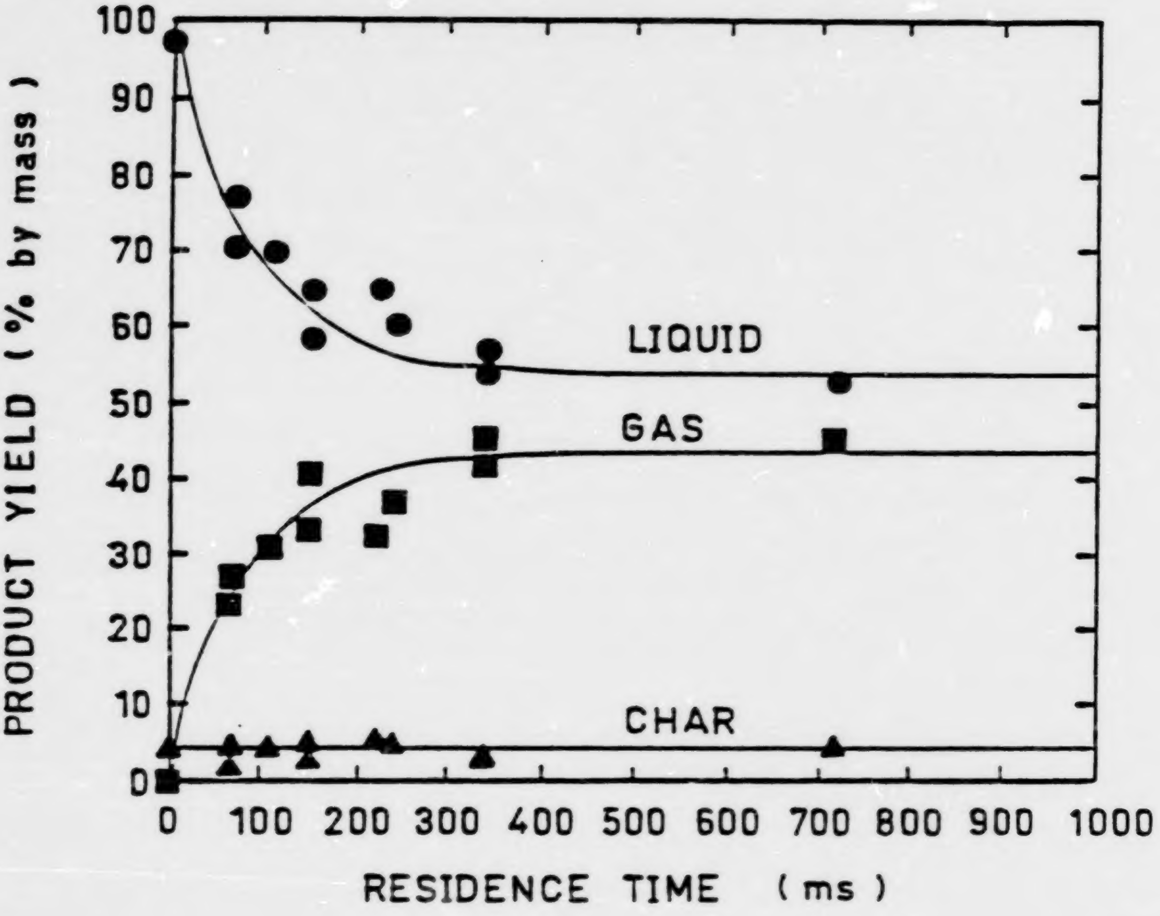

Figure 3.2.1 Typical Results for Ultrapyrolysis of Eastern Red Maple at 700°C - Yields vs. Residence Time

The results of pyrolysis experiments with Avicel cellulose are shown in Figures 3.2.2-3.2.6 with all data presented on a dry feed basis. Figure 3.2.2 shows that over the temperature range of 450°C-900°C the yields of gas, char and liquids from two different reactors, operated by different research groups, are in very close agreement. Figures 3.2.3 and 3.2.4 show the variation in CO and CO_2 yields with temperature over the same range. Again, agreement of the two sets of results is very good. Yields of hydrocarbon gases are shown in Figures 3.2.5 and 3.2.6, and the good agreement of data from the two reactors is again evident for both CH_4 yield (Figure 3.2.5) and C H +C H yield (Figure 3.2.6).

The yields of liquids, gases and char from pyrolysis experiments with maple wood over a range of 400°-800°C are shown in Figure 3.2.7. Although the data from the two reactors does not have the degree of overlap which existed for the Avicel results, the smooth relationship of the two data sets is confirmation of their essential agreement. Figure 3.2.8 shows the yields of CO and CO_2, and Figure 3.2.9 the yields of CH_4 and C_2H_2+C_2H_4. Again the agreement of yield data from the two reactors is very satisfactory.

The results shown in Figures 3.2.2-3.2.9 represent experiments done in two fluidized bed reactors (bench scale and pilot plant) and in a transport reactor. Further, the experiments were done by various workers over a period of time. The agreement of all the results has implications for fast pyrolysis processes where heat transfer is not a rate limiting factor.

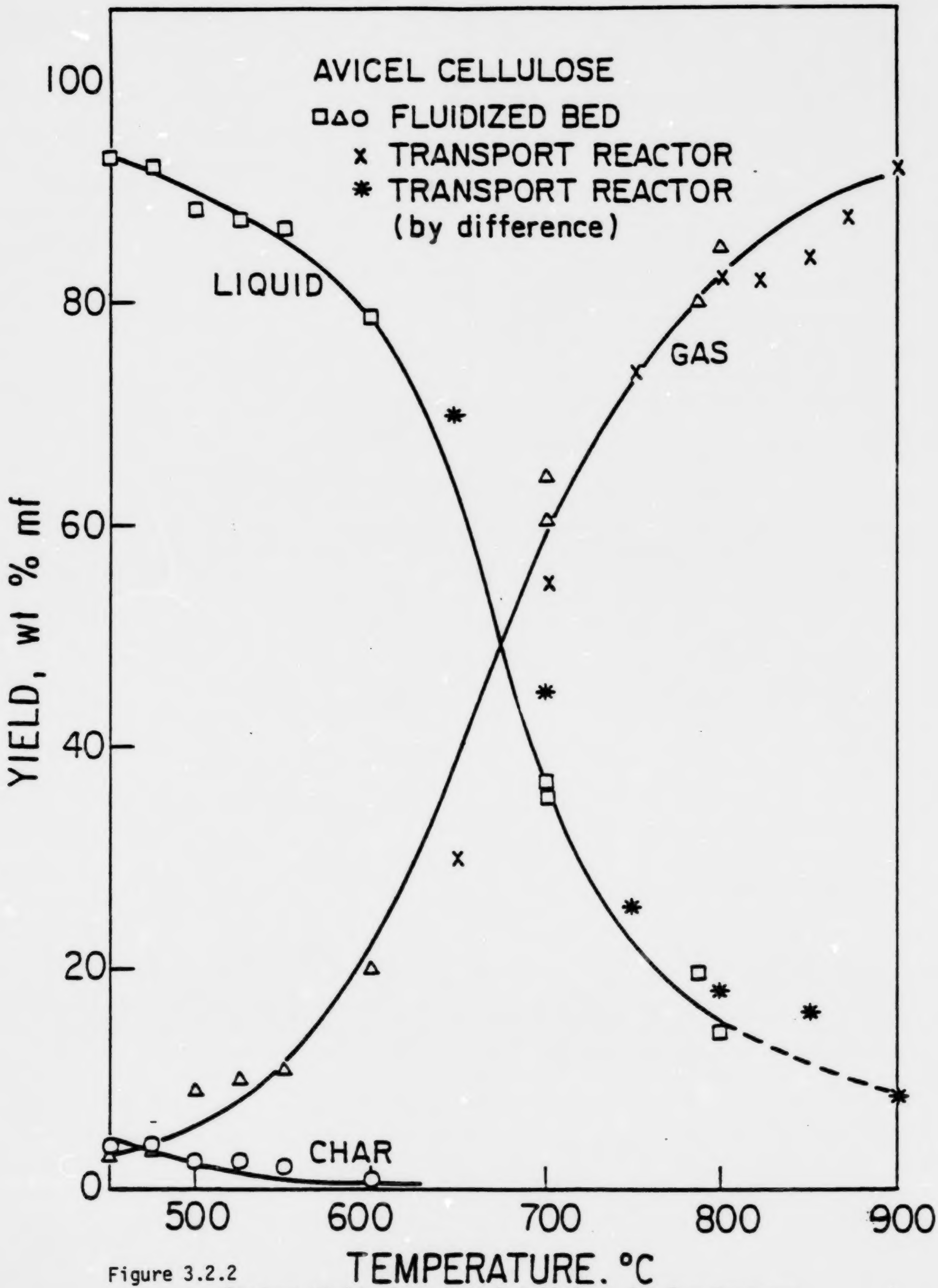

Figure 3.2.2 Product Yields from Avicel Cellulose for Two Reactors, 0.5 s Vapor Residence Time

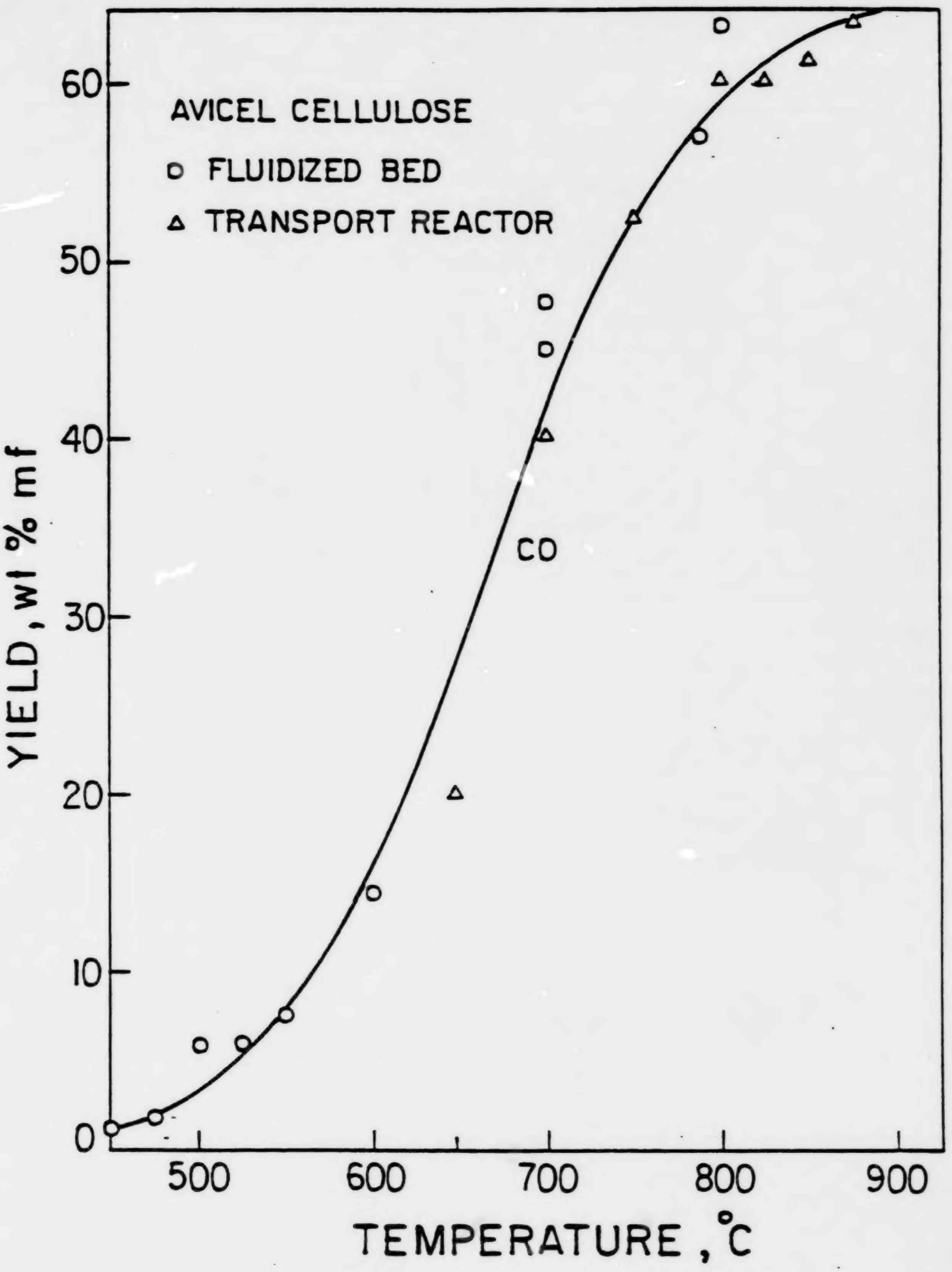

Figure 3.2.3 Yield of CO from Avicel Cellulose

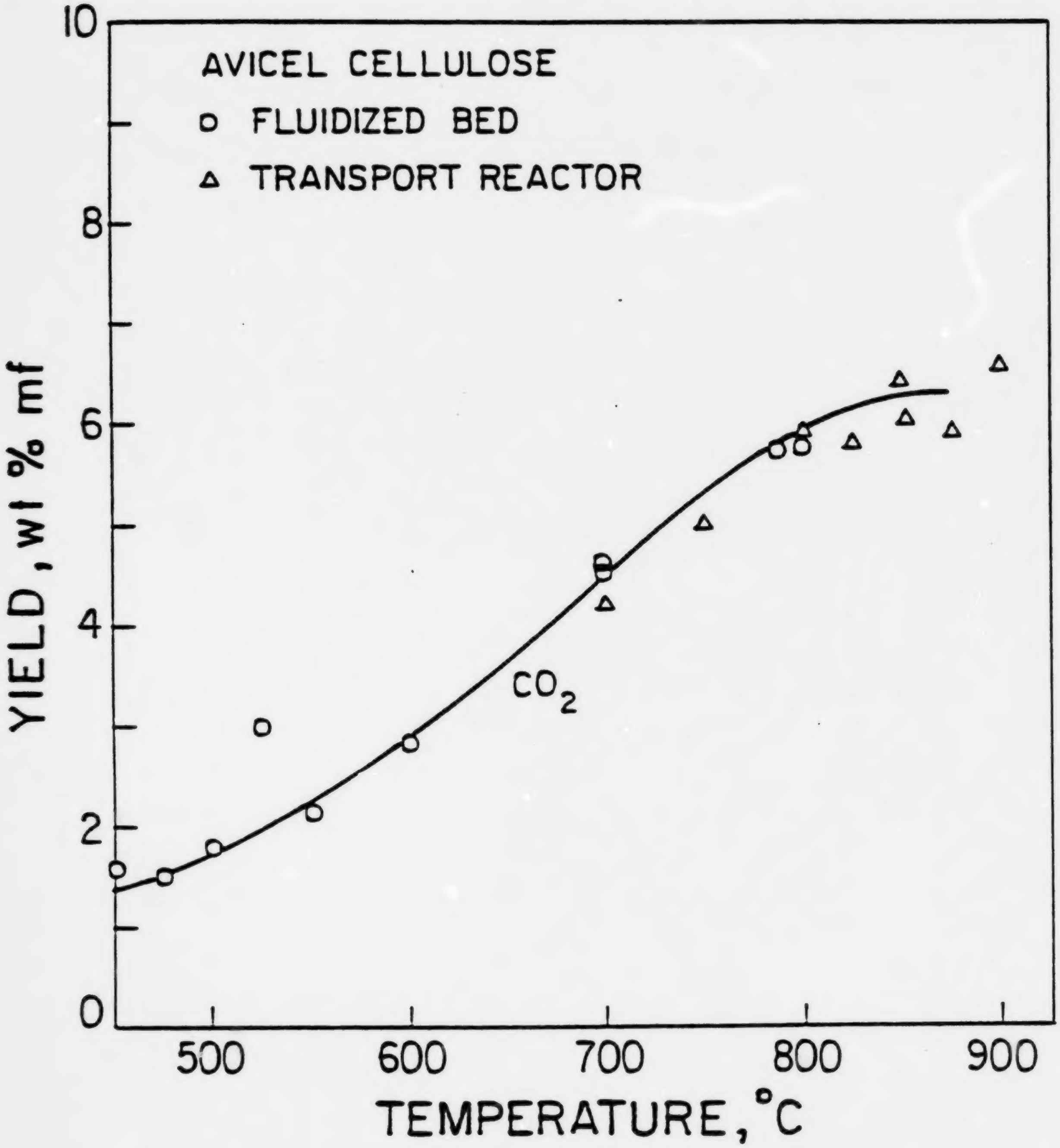

Figure 3.2.4 Yield of CO_2 from Avicel Cellulose

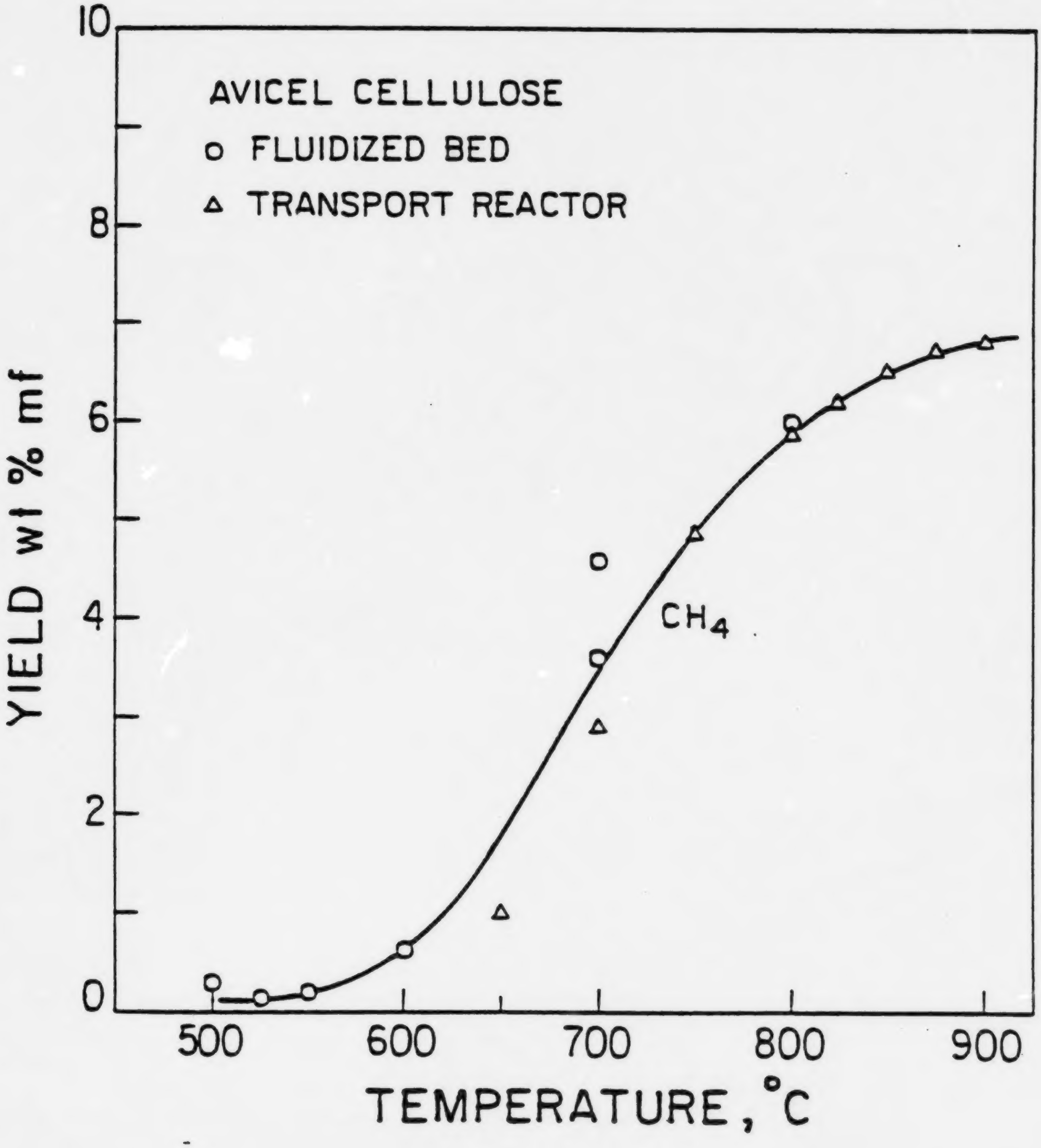

Figure 3.2.5 Yield of CH_4 from Avicel Cellulose

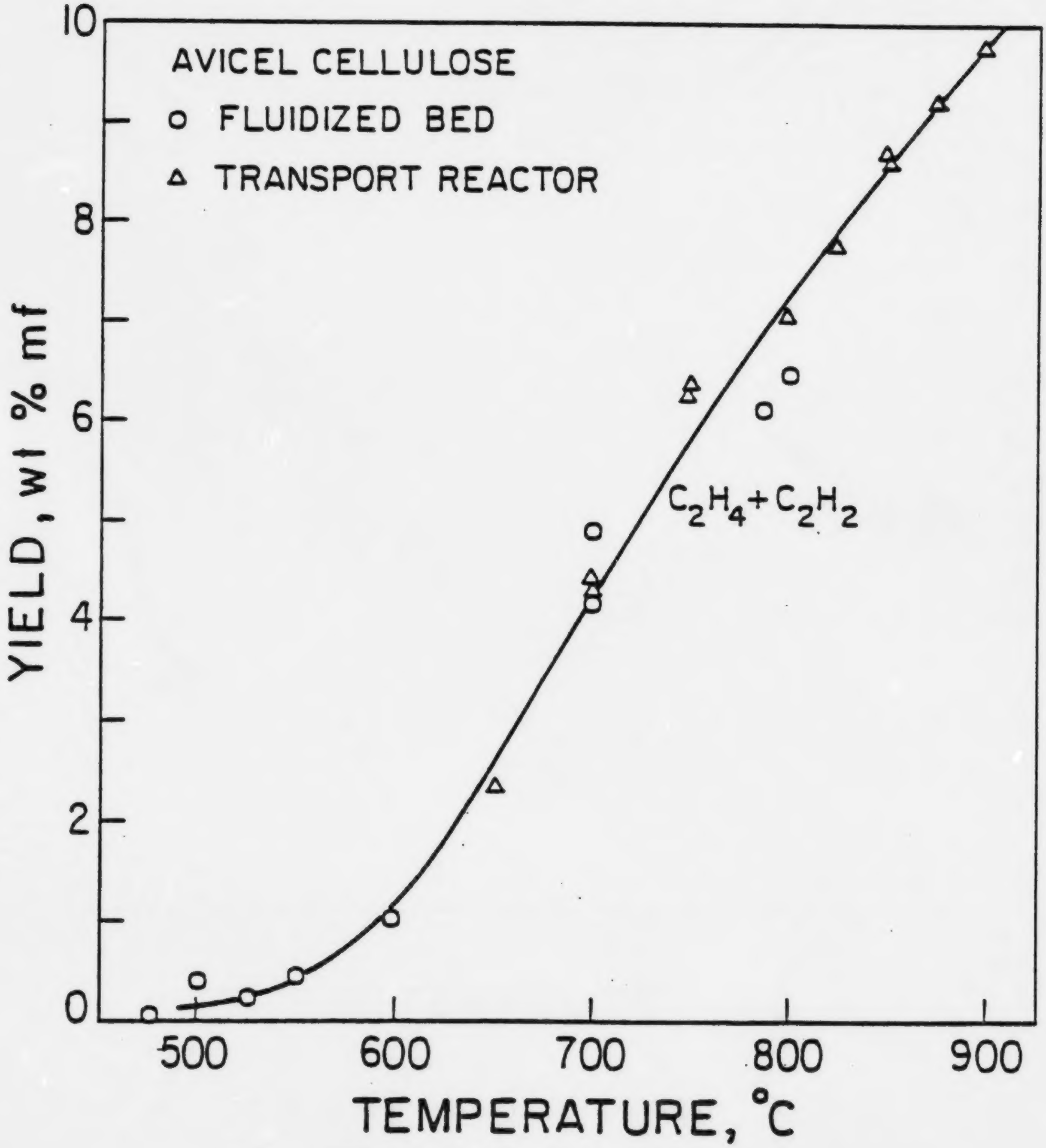

Figure 3.2.6 Yield of $C_2H_4 + C_2H_2$ from Avicel Cellulose

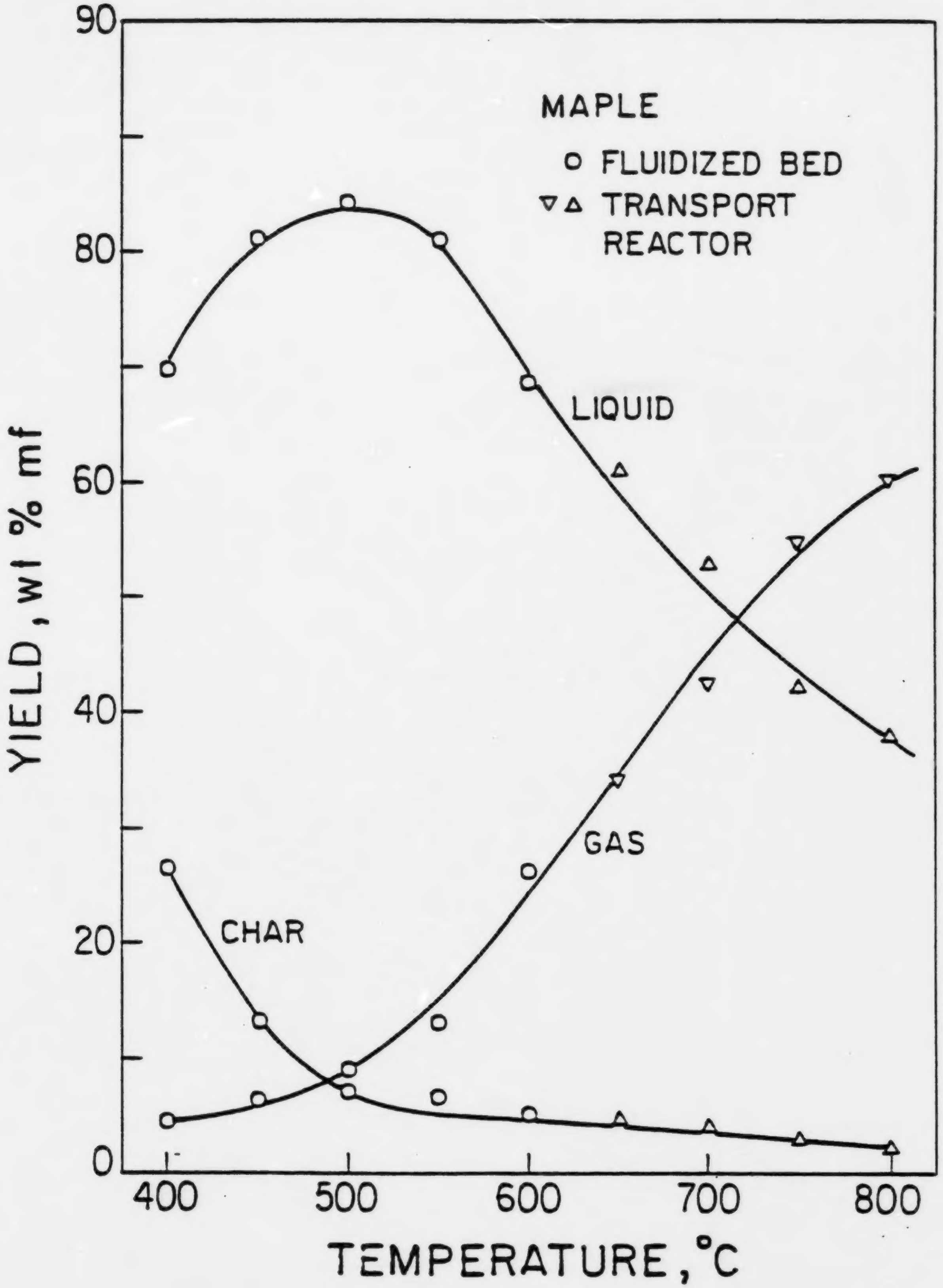

Figure 3.2.7 Product Yields from Eastern Red Maple from Two Reactors, 0.5 Vapor Residence Time

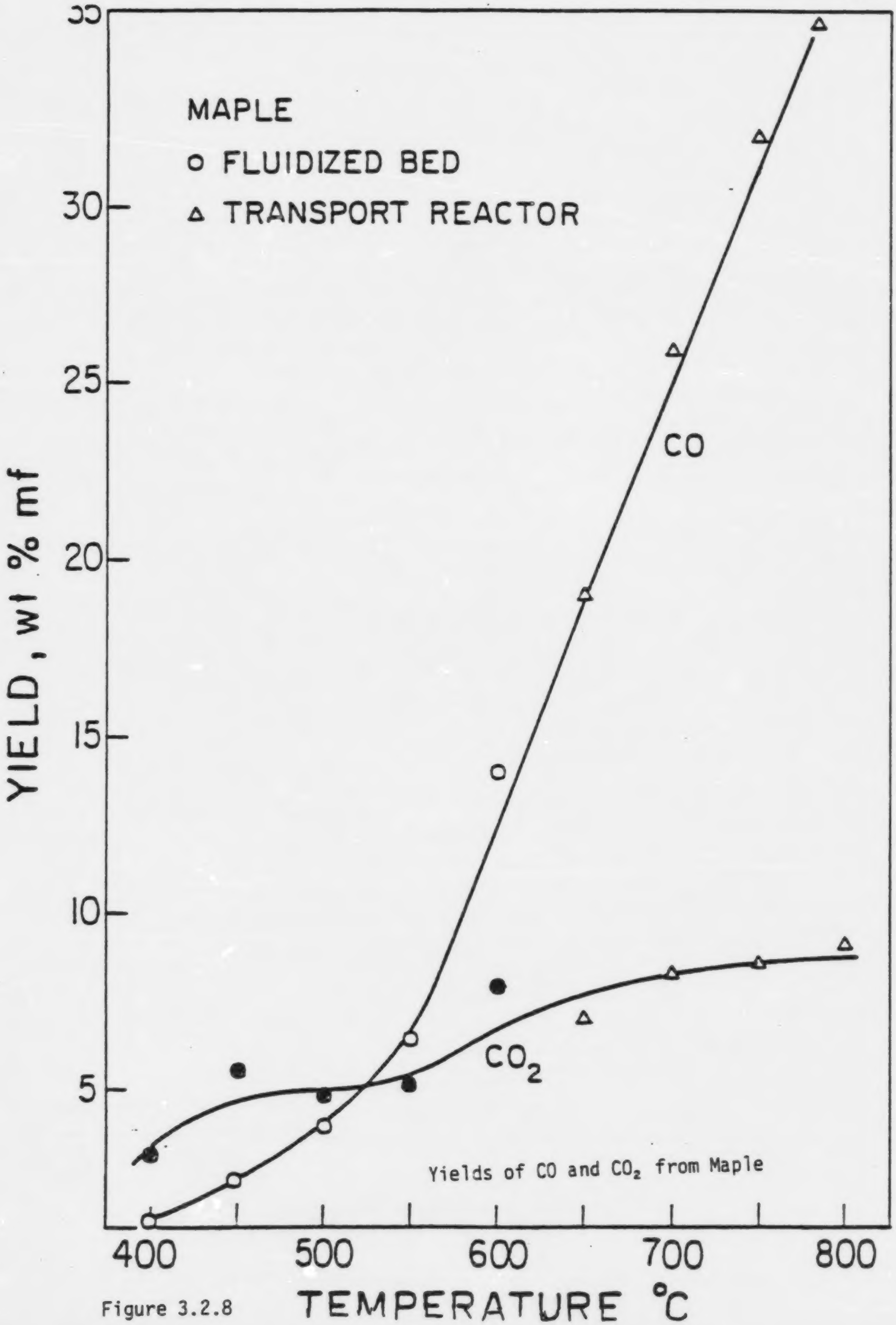

Yields of CO and CO_2 from Maple

Figure 3.2.8

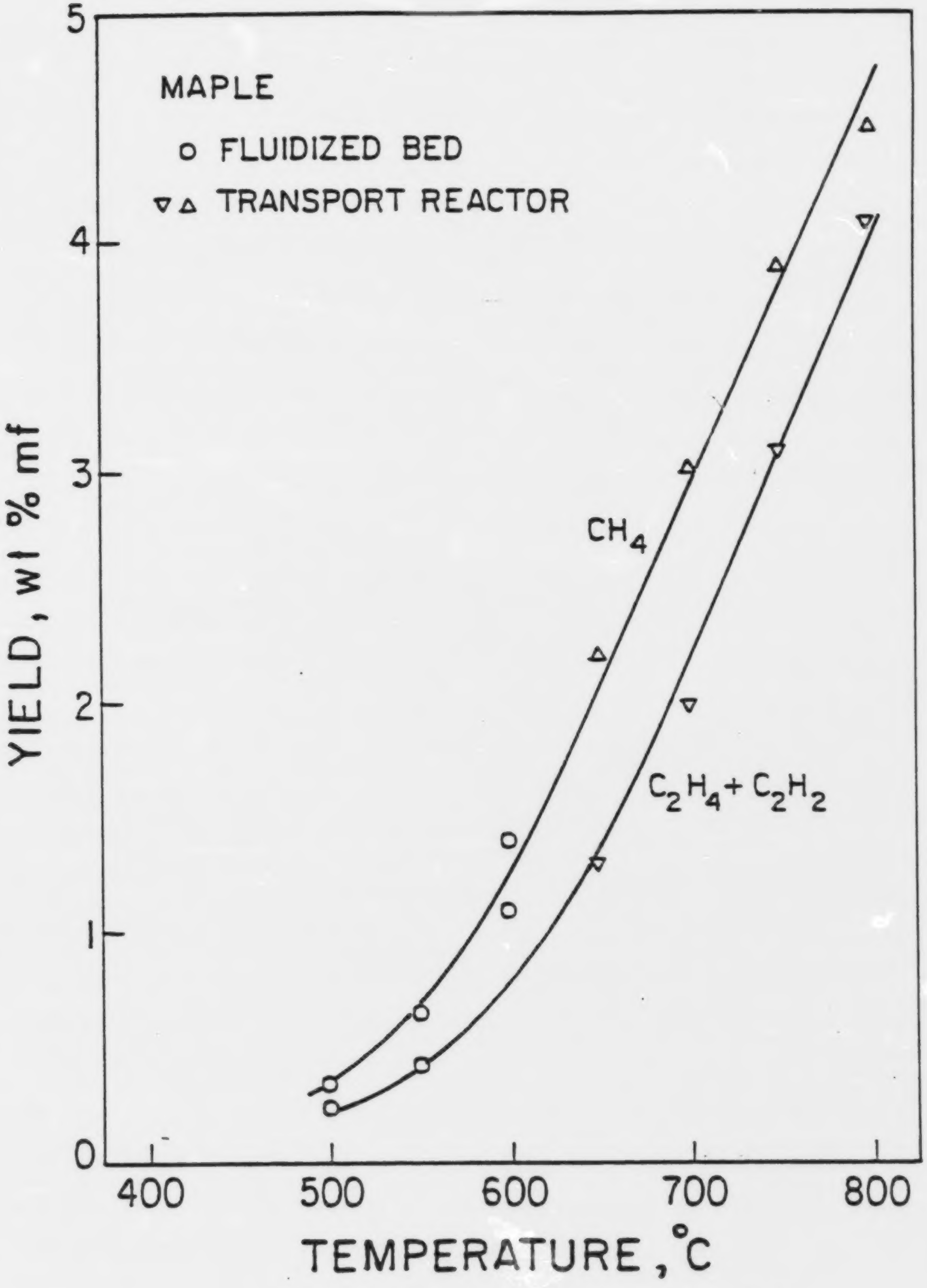

Figure 3.2.9 Yields of Hydrocarbon Gases from Maple

3.2.4 Discussion

The data for liquid yields shown in Figures 3.2.2 & 3.2.7 refer to total condensibles, that is, organic compounds plus product water formed. Product water yield tends to increase with temperature although only to a minor degree, so that the organic tar and oil yield decreases somewhat more rapidly with temperature than indicated by the decreasing liquid yield in Figures 3.2.2 or 3.2.7. The total liquid yield for the maple wood shows an optimal yield temperature at about 500°C, in agreement with other results from wood pyrolysis (Scott and Piskorz, 1984). However, this is not true of the Avicel cellulose pyrolysis, for which liquid yields continued to increase as temperature decreased to the lowest value of 450°C used in these experiments. However, other experiments indicate that the maximum liquid yield for Avicel occurs near 450°C.

The total gas yield for the Avicel cellulose is essentially the inverse of the liquid yield, with negligible char yield except at the lowest temperature. Char yields from wood decrease rapidly as the temperature increases to 500°C and then decrease very slowly to 800°C.

Comparison of the yields of individual gases with temperature shows that for CO, CH_4 and (C_2H_4 + C_2H_2) the pattern of changes in yield are very similar. It is therefore not surprising that Scott et al. (1985), Antal (1983) and Funazukuri et al. (1986) have drawn attention to this feature of cellulose or wood pyrolysis by showing that the logarithms of ratios of yields of major gaseous products such as CO/CH_4 or CO/C_2H_4 show a reasonably linear relationship over wide temperature ranges. A logarithmic plot of the CO/CH_4 and $CO/(C_2H_4 + C_2H_2)$ ratios is shown in Figure 3.2.10 for the Avicel cellulose, and confirms this previously reported behavior at least over the region of 500°-800°C.

For the Avicel cellulose the CO_2 yield increases monotonically with temperature, and therefore could also be correlated as a ratio with CO or CH_4. However, for wood a plateau exists in the CO_2 yield as temperature increases over the range of 450°-550°C. This plateau has been observed in our laboratories for fast pyrolysis with several wood feeds, and is not likely, therefore, to be experimental error. This effect has been ascribed by Piskorz et al. (1986) to the fact that CO_2 is produced as a primary product in the initial decomposition of cellulose and hemicellulose fractions by a less favored pathway, and thus reaches a limiting yield at about 450°C [Diebold (1985) calls this "prompt gas"]. As secondary decomposition reactions become of more significance at higher temperatures, the CO_2 yield increases again. The relatively high CO_2 and H_2O contents at higher temperatures suggests that some of this increased CO_2 yield may be due to the shift reaction, and while this is very likely, it is only at the very highest temperatures that the non-catalyzed rate of this reaction would contribute measurably to CO_2 yield.

In order to determine if the criterion of the ratio of heat-up time to time at reaction temperature is $\ll 1.0$, it is necessary to estimate heat transfer rates in the reactors and for the particles used. These estimates should be relevant to the pheno-

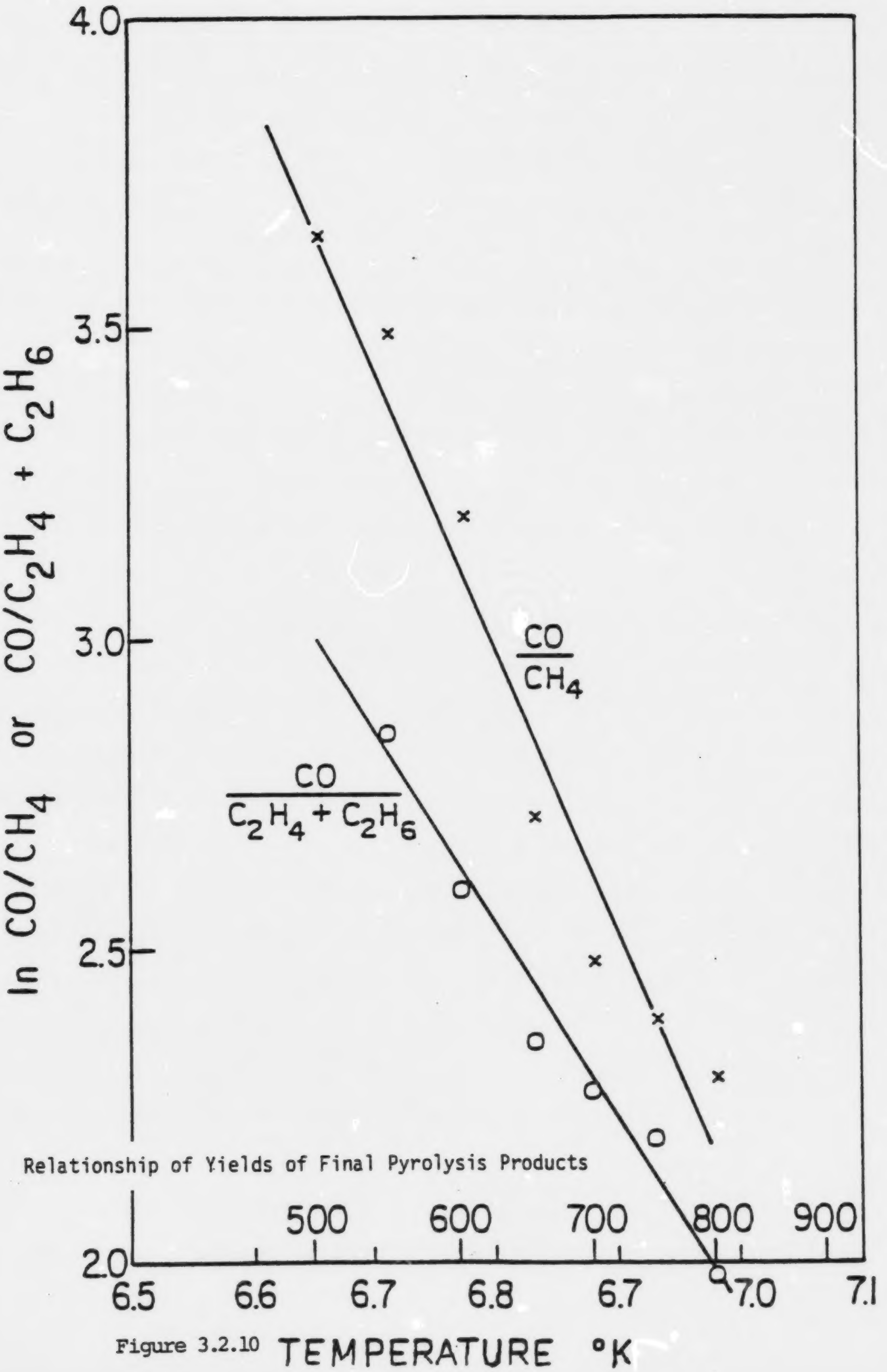

Relationship of Yields of Final Pyrolysis Products

Figure 3.2.10

mena occurring, although some controversy still exists as to the rates of initial decomposition steps. If the ideas of Kothari and Antal (1985) are accepted, then the initial depolymerization to potentially volatile compounds must be completed by a temperature of 500°C at any heat flux (note that this depolymerization step probably does not involve significant weight loss). If this is true, then above this temperature, all solid phase reactions are completed and the actual temperature of the particle is of little concern, inasmuch as any further decomposition processes must occur in the vapor phase or on solid surfaces. In this event, the time required for the centre of a particle to approach 500°C would represent the heat-up time. Lede (1985) comes to similar conclusions for pyrolysis at high heat fluxes, but sets the decomposition temperature at 466°C for wood. The most extreme case, that is, the longest heat-up time in the present work, would be for the largest particles at the lowest reactor temperatures. The center point temperature was calculated for 600 μm and 100 μm wood particles for the heating conditions of a fluidized bed (Lidén, 1985), for a reactor temperature of 500°C with sawdust feed at 20°C. The time required for the particle mid-point temperature to reach 450°C was found to be 618 ms for the 600 μm particle and 62 ms for the 100 μm particle. Inasmuch as the solid particle residence times for the larger particles were from 2 to 6 seconds in the fluidized bed, and for smaller particles in the transport reactor were at least 500 ms, the criterion of ratio of heat-up time/available reaction time <<1 is well satisfied for all the work reported here.

Another approach was taken by Lidén (1985) to estimate the importance of the heat-up period. On the basis of low temperature pyrolysis results reported in the literature, and the results obtained in our laboratory, it was assumed that if the particle temperature reached at least 450°C before more than 10% of the wood decomposed (as measured by a rate-of-weight loss kinetic expression) then excessive char production would be avoided, and the condition for high tar yields would be met, since tar decomposition would be minimized by the rapid volatilization and removal of tar components. Assuming a first order weight loss expression, this heat-up time criterion can be expressed as

$$\ln\left[\frac{1}{0.9}\right] \geq \int_{0}^{t_c} k\,[T(t)]\,dt \qquad (1)$$

where t_c is the time required for the particle centre to reach 450°C and $T(t)$ are the set of functions describing the particle centre temperature as a function of time after introduction of feed into the reactor. The value of the first order rate constant, k, used should be one which is applicable for the rate of weight loss of the biomass species used. For the purposes of evaluating the above criterion, the kinetic parameters for the rate expression describing the total decomposition of wood as given by Thurner and Mann (1981) were used, that is

$$k = 2.468\,(10^6)\,\exp - 106.5/RT \quad s^{-1} \qquad (2)$$

where the activation energy is given in kJ/mole.

Numerical integration of the right hand side of equation (1) for hardwood particles in a fluidized bed reactor at 500°C shows that for all particle sizes less than 2 mm diameter the criterion will be satisfied. It follows that for all the data presented here for the two reactors, the particles were heated throughout to at least 450°C, even at the lowest reaction temperatures, before any appreciable weight loss occurred from them. Under these conditions, then, the product distribution from either reactor for the same gas residence times could be expected to be a function of reactor temperature only, even though biomass solids were well mixed in one reactor, and in plug flow in the other.

It is a reasonable assumption that any reactor which can supply heat sufficiently rapidly to meet the criteria used here (which are essentially all very similar) will show the same product yields as a function of temperature as those found in this investigation. When the heat-up criteria are met, then product distribution depends only on secondary vapor phase reactions, and for systems approximating plug flow of the vapor, this distribution will depend only on homogeneous reaction parameters, therefore.

Recently, Lidén (1985) and Diebold (1985) using different reactor configurations have presented very similar kinetic models for the secondary decomposition of primary pyrolysis tars from biomass. The kinetic steps for which rate constants were evaluated are proposed to be parallel initial first order decompositions, one yielding volatile liquids, while the other yields char and gas, with respective rate constants k_1 and k_2. The ratio of k_1/k_2 in both models was assumed to be a constant with respect to temperature and to represent a theoretical maximum (ultimate) liquid (or tar) yield. The volatile organics were then assumed to decompose by another first order process to lower molecular weight products, because experimental results for short time pyrolysis suggest that little secondary char is formed in this step (see Figures 3.2.2 & 3.2.7). Experimental results also suggest that the primary decomposition step is largely completed before significant loss of tar yield occurs, as evidenced by a nearly minimum char yield at the maximum liquid yield, as well as low gas yields at this point. As tar yield decreases due to secondary decomposition reactions, gas yield increases proportionally. It becomes possible, then, to neglect the rate of the tar forming step and to express the change of tar yield due to secondary reactions by a simplified kinetic expression, given by both Lidén (1985) and Diebold (1985) as

$$x = \frac{x_o\,[1 - \exp(-k_3\,\Theta)]}{k_3\,\Theta} \qquad (3)$$

where x is the fractional tar yield, x_o is the theoretical "ultimate" tar yield, k_3 is the first order constant for the tar decomposition step and Θ is the reaction time for the vapor phase. The values given for the reaction parameters for tar decomposition were

Lidén $k_3 = 4.28 \times 10^6 \exp(-107500/RT)\ s^{-1}$, $x_o = 0.703$
Diebold $k_3 = 1.551 \times 10^5 \exp(-87634/RT)\ s^{-1}$, $x_o = 0.78$ or 0.76

Lidén's parameters are based on experimental data from hardwood (poplar) pyrolysis in a fluidized bed, while Diebold's values are obtained from measurements of the ablative pyrolysis of softwood followed by thermal cracking of the pyrolysis vapors.

In applying these parameter values and equation (3) to the results shown in Figure 3.2.7, these plots are based on the yields of total liquids, that is, tar + water of reaction, whereas equation (3) does not include water of reaction in the fractional yield. Therefore, a constant value for water yield (11.5%) was added to the fractional conversions calculated from equation (3). The water yield is not constant with temperature but tends to increase slightly as reaction temperature increases. Similarly, in principle the parameter, x_o, the ultimate tar yield, must also vary with temperature. However, both Lidén and Diebold have assumed this to be a constant, although over rather a more narrow temperature range than considered here, so a constant value was used.

For the prediction of the liquid yields from maple pyrolysis Diebold's values of the parameters were used with $x_o = 0.78$. However, equation (3) with Liden's parameters was found to give better results if the pre-exponential factor was given a value of $2.0 \times 10^6 s^{-1}$. rather than 4.28×10^6. The resultant predictions from equation (3) for the two models are shown in Figure 3.2.11. Prediction from both models is reasonably good, and the difference between the two is due primarily to the different values of x_o used. The low prediction of liquid yield at the highest temperature may be due to any of the assumptions made, that is, water yield is higher than assumed, or x_o changes with temperature, or to the fact that the total yield has been normalized to 100%. However, given the simplicity of the model, the fact that the parameters were determined using woods other than maple, and the wide range of temperature covered, the prediction of tar yield is remarkably good.

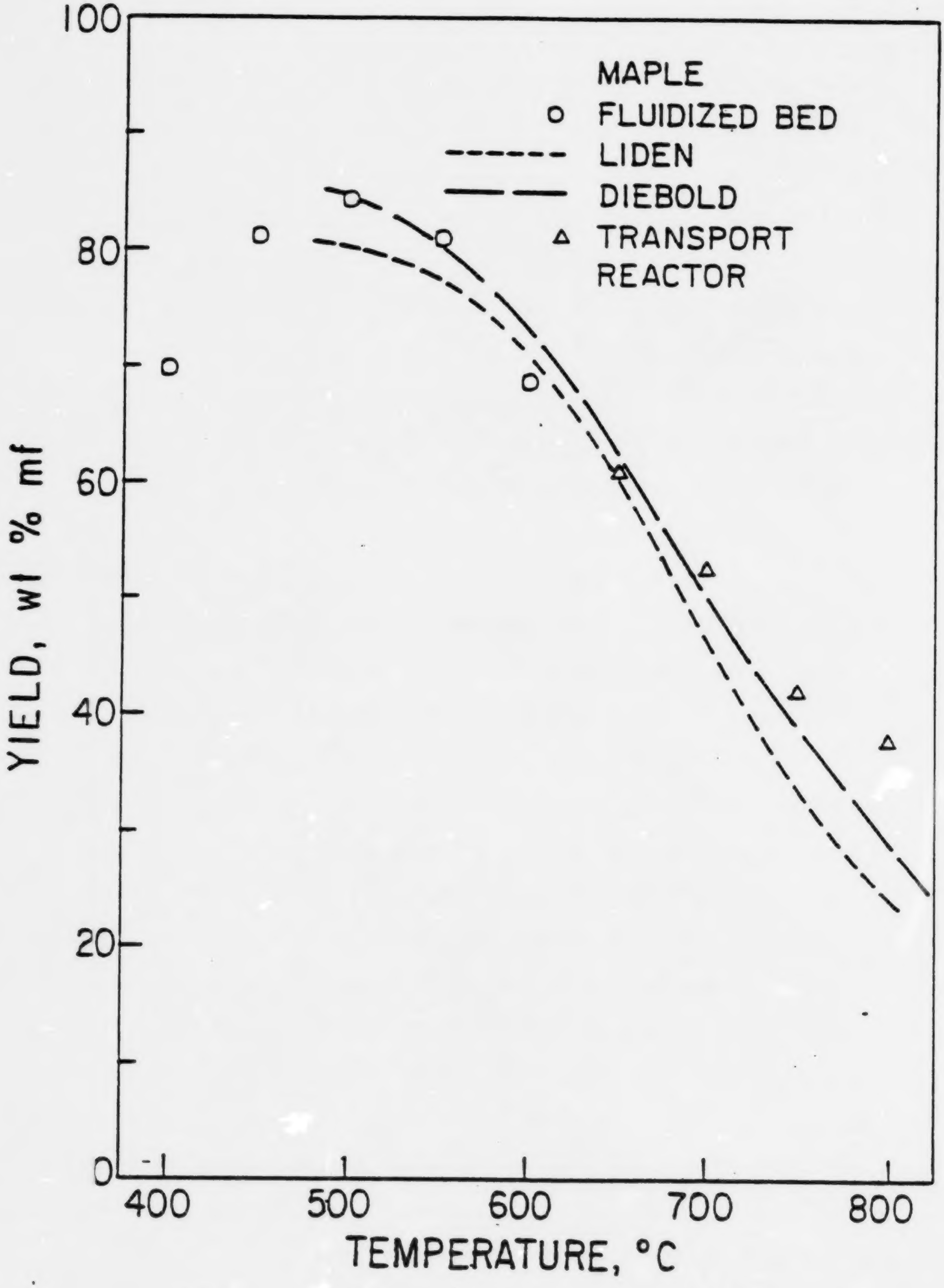

Figure 3.2.11 Prediction of Total Liquid Yields from Maple with Equation (3)

Equation (3) was also applied to the results from the pyrolysis of Avicel cellulose with prediction as shown in Figure 3.2.12. In applying equation (3) to these results, the ulimate yield, x_o, was assumed to be 100%, although the low temperature results suggest a value slightly less than this might be more appropriate. Similarly, the yield of water was neglected, although it ranges from 2%-5%. Again, Diebold's parameters were used with the suggested values, while the pre-exponential factor for Lidén's parameters was set at 3.1×10^6 s^{1}. Again, the predicted tar yields as shown in Figure 3.2.12 are in remarkably good agreement with experiment, considering the assumptions of the model, and the fact that parameters derived from wood pyrolysis are being used to predict yields from the pyrolysis of a microcrystalline cellulose. Further, no effort was made to optimize values of the parameters with the experimental data, but only to use the values of Lidén or Diebold.

In summary, equation (3) appears to give a reasonable description of the complex cracking reactions in which biomass pyrolysis tars are converted to gaseous products, at least over the temperature range of about 500°-850°C, and for short vapor phase reaction times. The simple model may apply as well as it does largely because the major vapor phase decomposition mechanism appears to be a series of successive decarbonylations, and therefore an "averaged" description of the rate process can be used with some success.

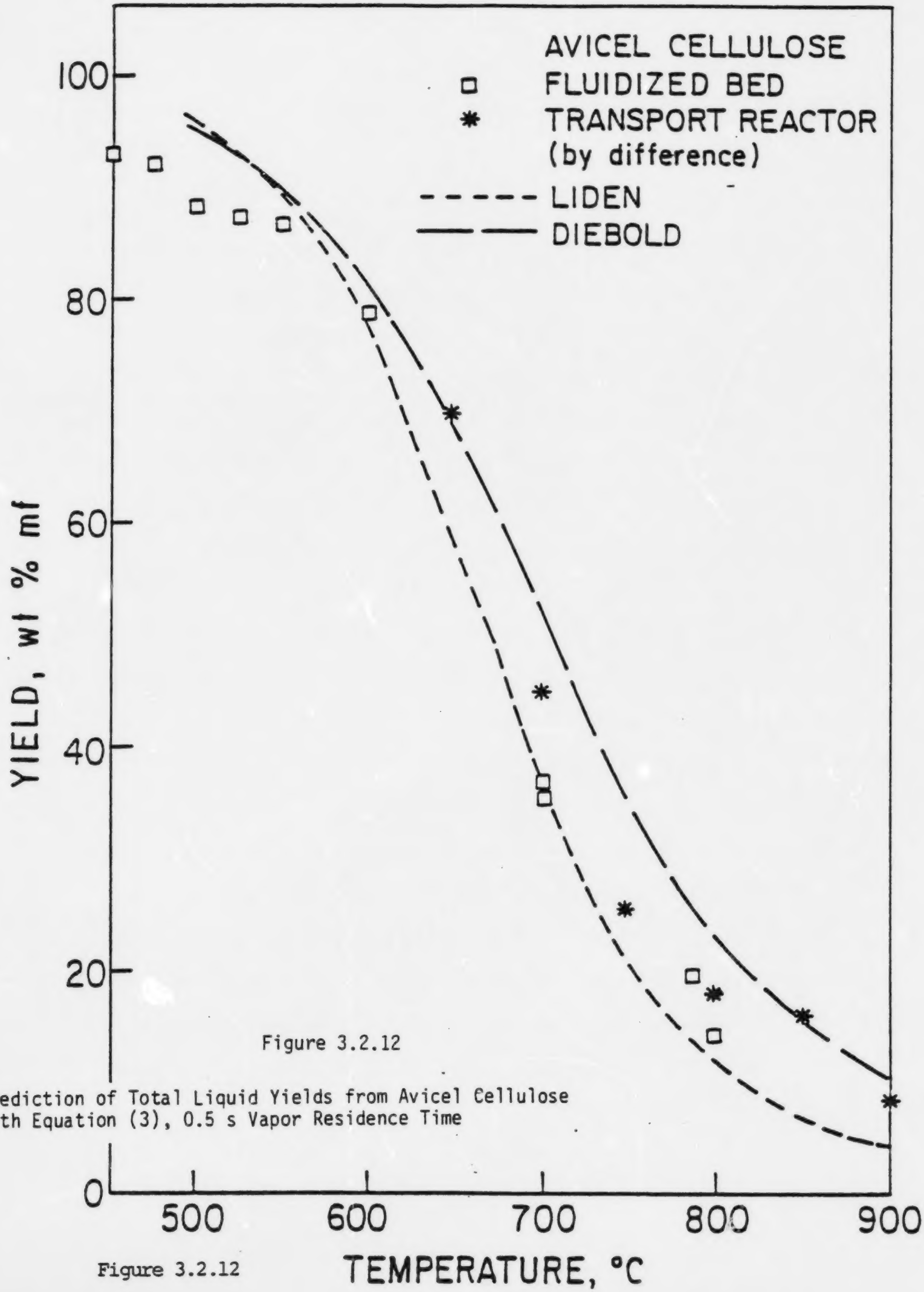

Figure 3.2.12

Prediction of Total Liquid Yields from Avicel Cellulose with Equation (3), 0.5 s Vapor Residence Time

Figure 3.2.12

3.2.5 Literature Cited

Antal, M.J.,Jr. Advances in Solar Energy 1983, 1, 61-112
Antal, M.J.,Jr. Ind.Eng.Chem.Prod.Res.Dev. 1983, 22, 366-376
Antal, M.J.,Jr. Advances in Solar Energy 1985, 3, 175-255
Antal, M.J.,Jr. Fuel 1985, 64, 1483-1486

Berruti, F. "Measuring and Modelling Lateral Solids Mixing and Residence Times in a Fluidized Bed Reactor" Ph.D. Thesis, Dept. of Chemical Engineering, University of Waterloo, December, 1985

Diebold, J. "The Cracking Kinetics of Depolymerized Biomass Vapors in a Continuous Tubular Reactor" MASc Thesis, Dept. of Chemical and Petroleum Refining Engineering, Colorado School of Mines, Golden, Colo. 1985

Funazukuri, T.; Hudgins, R.R.; Silveston, P.L. Ind.Eng.Chem.Process Des.Dev. 1986, 25, 172-181

Graham, R.G.; Bergouganou, M.A.; Overend, R.P. J.Anal.Appl.Pyrol. 1984, 6, 363-374

Kothari, V.; Antal, M.J.,Jr. Fuel 1985, 64, 1487-1494

Lede, J.; Panagopoulos, J.; Huai Zhi Li; Villermaux, J. Fuel 1985, 64, 1514-1520
Liden, A.G. "A Kinetic and Heat Transfer Modelling Study of Wood Pyrolysis in a Fluidized Bed" MASc Thesis, Dept. of Chemical Engineering, University of Waterloo, 1985

Piskorz, J.; Radlein, D.; Scott, D.S. J.Anal.Appl.Pyrol. 1986, 9, 121-137

Scott, D.S. "Flash Pyrolysis of Wood in a Fluidized Bed" Final Report, ENFOR Project C-28, November, 1981
Scott, D.S.; Piskorz, J. "The Flash Pyrolysis of Aspen-Poplar Wood" Can.J.Chem.Eng. 1982b 60, 666-674
Scott, D.S.; Piskorz, J. "Low Rate Entrainment Feeder for Fine Solids" Ind.Eng.Chem.Fundamentals, 1982a, 21, 319-322
Scott, D.S. "Characterization of Pyrolysis Oils from Continuous Flash Pyrolysis of Wood" Final Contract Report, ENFOR Project C-223, Sept. 1984a
Scott, D.S.; Piskorz, J. Can.J.Chem.Eng. 1984, 62, 404-412
Scott, D.S.; Piskorz, J.; Radlein, D. Ind.Eng.Chem.Process Des.Dev. 1985, 24, 581-588
Solomon, P.R; Serio, M.A.; Carangelo, R.M.; Markham, J.R. Fuel 1986, 65, 182-194

Thurner, R.; Mann, U. Ind.Eng.Chem.Process Des.Dev. 1981, 20, 482-488

4. MIXING AND SCALE-UP IN SHALLOW FLUIDIZED BEDS

4.1 Introduction

The Waterloo Fast Pyrolysis Process, in its present state of development, makes use of fluidized bed technology. Operating practice uses from 1.5 to 2.5 the minimum fluidization velocity, so that the fluid beds operate in the bubbling mode. Clean highly spherical Ottawa sand has normally been used as the bed solid. A major project was carried out as a Ph.D. study, to evaluate the nature of mixing of solids, particularly of different densities, in shallow fluid beds. In addition, methods were devised to measure wood particle mean residence times in a shallow fluid sand bed. Finally, this information together with a mixing and kinetic model was used to predict conversions to tar in the WFPP (Lidén, 1985, Berruti, 1985).

A sand fluidized bed reactor was chosen for the process on the basis of a number of advantageous properties including good mixing and good heat transfer between the hot sand and the injected biomass particles; the possibility of operating at specific gas superficial velocities to allow a continuous entrainment of the char particles formed during the reaction; and to achieve at the same time the desired residence times of the phases, in order to maximize the liquid yield and to reduce secondary side reactions.

A number of experiments to study the extent of solids mixing in the pyrolysis fluidized bed reactor were performed (Berruti, 1985), which demonstrated the mixing to be strongly dependent upon several parameters, including fluidizing gas velocity, particle size, particle density and local position inside the bed. The degree of axial and radial solids mixing were separately measured as well (Berruti, 1985; Berruti et. al., 1986).

This study led to a new correlation for the prediction of the radial dispersion coefficients in a shallow bubbling fluidized bed. These results were reported in the latter publication quoted above, and a copy of this publication is appended as Appendix 4-A.

An additional study of the residence time distribution (RTD) of the light biomass particles injected into the fluidized bed was undertaken in order to obtain additional information about the overall mixing behaviour of the reactor, in the presence of solid particles having widely different physical characteristics. Knowledge of the residence time of different biomass particles at various operating conditions is necessary to model the pyrolysis kinetic process and the heat transfer characteristics of the system.

A report of the results from these residence time studies is attached as Appendix 4-B. This work was presented at the Annual Meeting of the Canadian Society for Chemical Engineering, Sarnia, Ont., October, 1986.

4.2 Modelling of the Pyrolysis Reactor

The kinetic model developed by Lidén (1985) has been employed, particularly the step describing the decomposition rate of the liquid tars, to calculate the conversion behaviour around a feed point in a shallow fluidized bed. These results are reported in the final thesis of Berruti (1985).

In brief, the WFPP fluidized bed reactor acts as a self-governing device. Wood particles fed to the sand bed mix rapidly throughout the bed, and no segregation of the wood from the sand is apparent. As the wood particle decomposes, it largely retains its original shape, but the density decreases to only about 10%-20% of the original. At this point, the particle now is sufficiently light to segregate as flotsam, and is then eluted from the bed. In effect, the particle remains in the bed until it is fully decomposed before being eluted. However, the vapors formed are swept very quickly from the bed and so secondary decomposition of these vapors is minimized.

From heat transfer calculations, a particle size can be defined which is a maximum, depending on the criterion used. Liden (1985) set a requirement that the centre point temperature of the particle must reach 450°C before 10% decomposition (as defined by weight loss) occurred. If this criterion is met, then the heating-up time will be a minor fraction of the total particle residence time in the bed.

Similarly, if the rate of heat transfer relative to the wood particle feed rate is below a specified value, then "flooding" of the bed can occur, that is, there is not enough heat transfer available to decompose the amount of wood fed, so that partially reacted wood accumulates in the bed. Hence, for a given reactor and operating conditions, a maximum feed rate will exist determined by heat transfer conditions.

The statistically designed experiments which were carried out on the pilot plant reactor to determine optimal conditions were described in Appendix 3-A. Within the rather narrow operating limits which could be used in the pilot plant reactor, temperature of reaction was found to be by far the most significant variable. As shown in Chapter 3, the simple kinetic model developed (in which axial and radial mixing effects are neglected) is capable of adequately describing pilot plant yields of tar from maple wood over a temperature range from 450°C-850°C. In a larger scale reactor, the mixing effects would need to be considered, and allowed for in the model.

On the basis of the above models of kinetic and mixing behaviour, it is estimated that a shallow fluidized bed reactor could be successfully designed from present information for feed rates up to 50 dry tonnes/day, and possibly to 100 dry tonnes/day. At larger feed rates, either multiple feeds, parallel units, or some other type of fluid bed (for example, a circulating fluid bed) might be desirable.

APPENDIX 4-A

Measuring and Modelling Lateral Solids Mixing in a Three-Dimensional Batch Gas-Solid Fluidized Bed Reactor

Measuring and Modelling Lateral Solid Mixing in a Three-Dimensional Batch Gas–Solid Fluidized Bed Reactor

F. BERRUTI, D. S. SCOTT and E. RHODES

Department of Chemical Engineering, University of Waterloo, Waterloo, Ontario, Canada N2L 3G1

A 0.27 m diameter fluidized bed reactor has been designed to allow experimental measurement of the axial and radial mixing behaviour of the solids.

A unique method has been developed which permits the continuous determination of solid tracer concentration with time at different radial and axial positions within the fluidized bed.

Solids mixing has been described by a model in which vertical mixing is instantaneous and lateral mixing occurs by dispersion.

The lateral solids dispersion coefficients have been evaluated at various operating conditions from the experimental results of tracer concentration versus time. Based on the results, a modification of an existing correlation is proposed.

On a conçu un réacteur à lit fluidisé de 0.27 m de diamètre, qui permet de mesurer expérimentalement le comportement des mélanges axiaux et radiaux des solides.

On a mis au point une méthode unique qui permet la détermination continue de la concentration d'un traceur solide en fonction du temps, à différentes positions radiales et axiales à l'intérieur du lit fluidisé.

On décrit le mélange des solides au moyen d'un modèle, dans lequel le mélange vertical est instantané et le mélange latéral se fait par dispersion.

Les coefficients de dispersion latérale des solides ont été évalués dans différentes conditions opératoires, à partir des résultats expérimentaux de la concentration du traceur en fonction du temps. On propose, à partir des résultats obtenus, une modification d'une corrélation existante.

Gas fluidized bed technology is increasingly being applied to a wide range of industrial situations where good solids mixing and/or good heat transfer must be achieved. Although fluidized beds in different fields of application vary in many aspects, they may be classified roughly into two types: the first type relatively narrow and deep, with a height to diameter ratio larger than unity, and the second type relatively wide and shallow, with a $H/D < 1$. The term "shallow" is meant to refer only to low H/D ratios and is not meant to imply a bed depth so small that grid effects become a major influence. Examples of these two types of fluidized bed reactors can be found in numerous references (Davidson and Harrison, 1963, 1971; Vanecek et al., 1966; Kunii and Levenspiel, 1969).

An exhaustive review of the literature indicates that the majority of published experimental and modelling studies have been carried out using deep fluidized beds, and most of them are only concerned with variations of concentrations and temperatures along the axial direction of the beds.

An assumption often used of uniform concentrations and temperatures in the lateral (radial) direction may be valid for fluidized beds of the first type, but it is quite questionable for shallow and wide beds.

Lateral particle mixing is known to be at least an order of magnitude slower than the mixing in the vertical direction, i.e. in the direction of the bubble flow (Lewis et al. 1962): and for this reason, it is very likely that lateral concentration gradients are established in a shallow bed. According to Grace (1981), knowledge of such radial gradients is very important in assessing the mixing performance of a gas–solid fluidized bed reactor. Thus the subject of lateral solids mixing has been the object of studies performed by a number of researchers (Brötz, 1956; Gabor, 1964; Mori and Nakamura, 1965; Kunii and Levenspiel, 1969; Highley and Merrick, 1971; Hirama et al., 1975; Chang et al., 1982; Shi and Fan, 1984).

Kunii and Levenspiel (1969) proposed a correlating equation for the lateral solids dispersion coefficient, on the basis of the so-called "Bubbling Bed Model":

$$D_{sr} = \frac{3}{16} \cdot 10^{-4} \left[\frac{\delta}{1 - \delta} \right] \cdot \frac{U_{mf} \cdot d_b}{\epsilon_{mf}} \quad \ldots\ldots\ldots\ldots\ldots\ldots \quad (1)$$

but it appears that this correlation has not been well validated experimentally (Hirama et al., 1975), partly because of the difficulty of evaluating some of the parameters.

A number of other correlations, however, have been proposed in the literature to overcome these difficulties in measuring and evaluating the various parameters of Equation (1). Recently Shi and Fan (1984) obtained a semi-empirical dimensionless correlation for estimating the lateral solids dispersion coefficient, taking into account several influencing parameters:

$$\frac{D_{sr}}{(U - U_{mf})h_{mf}} = 0.46 \cdot 10^{-4} \cdot \left[\frac{(U - U_{mf})d_p \rho_f}{\mu_f} \right]^{-0.21} \times \left[\frac{h_{mf}}{d_p} \right]^{0.24} \cdot \left[\frac{\rho_s - \rho_f}{\rho_f} \right]^{-0.43} \quad \ldots\ldots\ldots\ldots\ldots\ldots \quad (2)$$

This correlation, obtained using a rectangular two-dimensional bed, appears to be the best available. Because the solid circulation pattern seems to be greatly affected by the wall effects and geometrical configuration of the reactor in general, the same correlation has to be verified experimentally in a cylindrical reactor.

The aim of this work was to test the ability of this correlation to predict lateral solids dispersion coefficients as functions of particle characteristics, properties of the

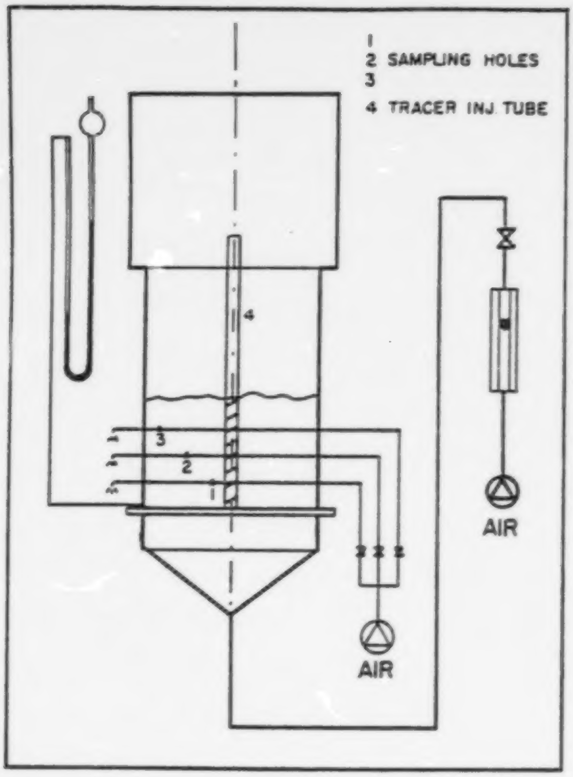

Figure 1 — Sketch of the experimental apparatus.

fluidizing medium, and operating conditions. It was also intended to investigate the possibility of modifying the known correlation by taking into account the geometric characteristics of the reactor and non-uniformities within the fluidized bed. It has generally been proposed, in fact, that solids travel down a fluidized bed close to the wall and up through the center of the bed with cross flow between the center and the wall taking place at several elevations in the bed, and that the bubble flow pattern determines the particle flow pattern (Nguyen et al., 1977; Marsheck and Gomezplata, 1965). Most of these speculations about the circulation pattern are based almost entirely on visual observations of two-dimensional beds.

The development of miniature capacitance probes has contributed to better understanding of local bubble behavior in gas−solid fluidized beds. These devices allow the investigation of radial bubble volume fraction and flow distributions (Werther and Molerus, 1973; Werther, 1974; Burgess and Calderbank, 1975; Calderbank, 1976; Wittmann et al., 1978). Even though there may exist a uniform permeability of the gas distributor plate over its entire area, an annular zone of increased bubble development has been generally observed to form initially close to the wall near the distributor. As a consequence of the rapid increase in bubble size due to coalescence, this annular zone is displaced toward the vessel center-line with increasing height above the gas distributor. The solid circulation pattern and hence the mixing process can be expected to be greatly influenced by this radially and axially non-uniform bubble distribution. Typical radial profiles of the local bubble flow have been measured by Masson and Jottrand (1978).

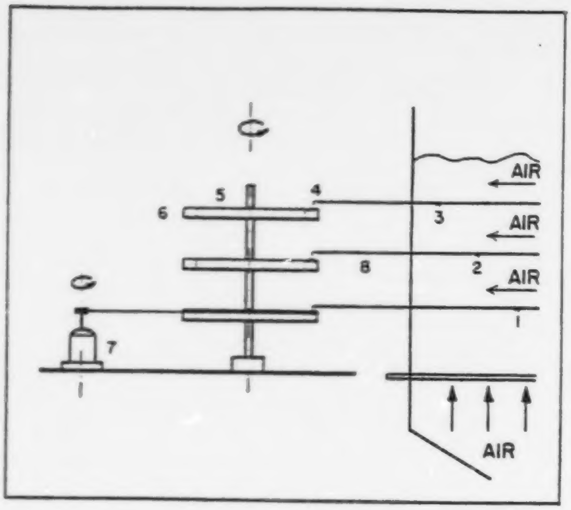

Figure 2 — Schematic representation of the sampling system. 1. Sampling hole #1; 2. Sampling hole #2; 3. Sampling hole # 3; 4. Sample outlet; 5. Rotating tray; 6. Collecting box; 7. Motor drive; 8. Sampling tubes.

Experimental methods

APPARATUS

A sketch of the experimental apparatus is given in Figure 1. The fluidized bed reactor consisted of a 0.267 m ID acrylic tube, 7 mm thick and 0.4 m long. The gas distributor plate was a stainless steel porous disc (Mott Porous 316L SS), 3.2 mm thick, with a mean pore size of 40 microns. The reactor was designed in such a way that it was possible to vary the length of the acrylic tube very easily, without changing anything else in the equipment. The fluidizing medium was air, supplied through a conical shaped bottom to achieve the best gas distribution through the porous plate. On top of the reactor an aluminum disengaging section 0.4 m long and 0.36 m in diameter was provided to prevent carry-over of fines.

Static charges, caused by the flow of dry air through the bed material (sand), led to particle accumulation on the inner part of the reactor acrylic wall. This phenomenon interfered with the visual inspection of the bed during the operation. Similar problems have been widely reported in the literature and they have usually been solved by humidifying the gas before it entered the reactor. In the present work these static charges causing particles to stick against the walls were completely eliminated by using a simple technique consisting of wrapping a copper net with a mesh size of about 15 mm around the reactor wall and connecting it to the ground. In this way static charge was reduced sufficiently so that no particles deposited on the acrylic material.

The fluidized bed reactor employed was designed to carry out tracer-type experiments. An innovative technique has been developed to withdraw continuously from the reactor during fluidization a small sample of the bed material containing the tracer. This technique is based on the principle of the low rate entrainment feeder for fine solids developed by Scott and Piskorz (1982). In practice, a sampling port consists of an horizontal entrainment tube which intersects the cylindrical body of the reactor in a specified position. This tube, 3.18 mm OD, contains a small hole 1.5−2 mm in size, drilled in the desired position with respect to the radial coordinate of the reactor. During the fluidization solid particles behave similarly to a liquid and when an air flow (0.2−2 L/min) is fed to the entrainment tube, it is possible to convey away a constant small solids flow (normally about 0.6 g/s) coming through the orifice. As a result, this system allows the continuous withdrawal of particle samples from a specified radial and axial position of the bed. The particles coming through different sampling ports (three or four) are then collected on an equal number of rotating trays in parallel, whose rotational speed can be regulated by adjusting the speed of the electrical motor drive. In this way it is possible to collect samples within a pre-set time interval and to get a tracer concentration profile as a function of the time and of the radial and axial positions inside the reactor. Fifteen small boxes (30 mm long, 10 mm wide and 15 mm high) are provided on each tray to collect discrete samples at particular times. A schematic representation of the sampling system is shown in Figure 2. The time lag in the tracer measurement due to the sample transit time was estimated to be of the order of 3 ms and was considered to be negligible in this work.

MATERIALS

The bed consisted of sand particles with an average particle diameter of 400 μm having a density of 2,470 kg/m^3. Potassium ferricyanide crystals were used as tracer material; the salt was screened to get the same particle size as the sand and the density (2,210 kg/m^3) was close enough to that of the sand, to allow a study of mixing of particles having the same physical characteristics. Characteristics of the fluidized bed and of the materials employed are listed in Table 1.

EXPERIMENTAL PROCEDURE

Each experiment performed consisted of three parts: tracer injection, tracer analysis and tracer separation from the bed particles.

The tracer injection was performed by inserting a tube (19 mm ID) filled with tracer up to a particular level, exactly in the central position of the empty reactor. The sand was then charged to reach the same level as the tracer in the central tube. The fluidization was started by opening the air valve and regulating the flowrate to the desired value, allowing both tracer and sand to fluidize for a period of time to reach a steady-state fluidization. The air flowrate through the sampling tubes was also adjusted for each channel, to get a constant particle flow out from the ports. As soon as steady conditions were reached, the tube containing the tracer was suddenly pulled out, at time zero, to allow tracer lateral (radial) dispersion. At the same time the trays started to rotate to collect continuously the samples within the previously set time interval, based on the speed of the electrical motor. When the experimental time had expired, the fluidization was interrupted, which also stopped the particle flow through the sampling ports. At that point, the series of trays were taken apart and the various samples, collected inside the small boxes, each at a paticular time, were recovered for analysis.

Each sample, consisting of tracer and sand, was then weighed and the tracer dissolved by mixing the whole sample with 15 mL of distilled water in small tubes. Five mL of the resulting solution were later analyzed by titration using an iodometric method.

TABLE 1
Characteristics of the Fluidized Bed and of the Materials Employed

For RUNS 1 to 12:	
Reactor diameter:	$D = 0.267$ m
Static bed height:	$H_{mf} = 0.19$ m
Bed material:	Ottawa sand
Average particle diameter:	$d_p = 400$ μm
Particle density:	$\rho_s = 2{,}470$ kg/m^3
Minimum fluidizing velocity:	$U_{mf} = 0.18$ m/s (exper.)
Bed void fraction @ m.f.:	$\epsilon_{mf} = 0.45$
Injection tube diameter:	$a = 19$ mm
Tracer type:	potassium ferricyanide (red crystals)
Tracer particle density:	$\rho_t = 2{,}210$ kg/m^3
Average tracer particle diam.:	$d_{pt} = 400$ μm
Fluidizing gas:	air
For RUNS 13 and 14:	
Average particle diameter (sand):	$d_p = 200$ μm
Minimum fluidizing velocity:	$U_{mf} = 0.053$ m/s (exper.)
Average tracer particle diam.:	$d_{pt} = 200$ μm

TABLE 2
Coordinates of the Sampling Ports

RUN #	PORT #	r/R	h/H_{mf}
1	1	0.225	0.289
2	2	0.420	0.552
3	3	0.750	0.816
4	1	0.225	0.552
5	2	0.420	0.552
6	3	0.547	0.552
13	4	0.682	0.552
	5	0.750	0.552
	1	0.225	0.816
7	2	0.420	0.816
8	3	0.547	0.816
9	4	0.682	0.816
	5	0.750	0.816
10	1	0.225	0.289
11	2	0.420	0.289
12	3	0.547	0.289
14	4	0.682	0.289
	5	0.750	0.289

TABLE 3
Operating Conditions

RUN	F (L/s)	U (m/s)	$U - U_{mf}$ (m/s)
1, 4, 7, 10	14.983	0.268	0.088
2, 5, 8, 11	20.334	0.364	0.184
3, 6, 9, 12	16, 889	0.302	0.122
13, 14	13.955	0.250	0.196

Experimental results

Experiments were performed with the sampling tubes positioned at different reactor levels, each tube having the hole corresponding to a different reactor radial position, as described in Table 2.

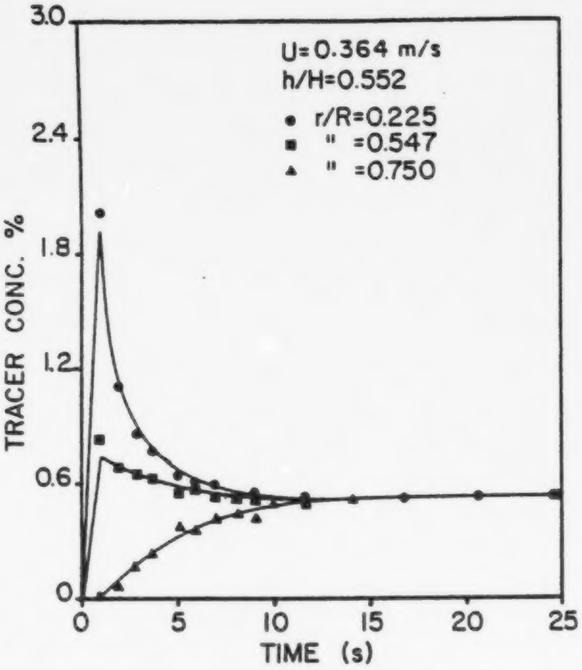

Figure 3 — Tracer concentration profiles versus time for RUN #5 ((U_{mf} = 0.18 m/s). Curves represent best model fitting.

The operating conditions of all the experiments performed are listed in Table 3. A typical set of tracer concentration profiles versus time is illustrated in Figure 3 (run #5), for three different sampling ports positioned at the same intermediate level above the gas distributor plate.

TREATMENT OF THE EXPERIMENTAL DATA

In most of the published works concerning studies of solid lateral mixing in fluidized bed reactors, the lateral movement of the particles has been described by a random walk process, which can be expressed by the diffusion (dispersion) equation:

$$\frac{\partial C_t}{\partial t} = D_{sr} \cdot \nabla^2 C_t \quad \ldots\ldots\ldots\ldots\ldots\ldots \quad (3)$$

This dispersion model has been used to characterize lateral mixing by several investigators (May, 1959; Hayakawa et al., 1964; Highley and Merrick, 1971; Hirama et al., 1975; Shi and Fan, 1984).

The governing partial differential equation of the model, in cylindrical coordinates, is:

$$\frac{\partial C_t}{\partial t} = D_{sr}\left[\frac{\partial^2 C_t}{\partial r^2} + \frac{1}{r}\frac{\partial C_t}{\partial r}\right] \quad \ldots\ldots\ldots\ldots\ldots \quad (4)$$

which assumes instantaneous axial mixing and lateral mixing occurring by dispersion. The appropriate initial and boundary conditions are:

$$\begin{array}{lll} t = 0, & 0 <= r <= a; & C_t = 100\% \\ t = 0, & a < r <= R; & C_t = 0\% \quad \ldots\ldots\ (5) \\ r = 0 \text{ and } r = R & & \partial C_t/\partial r = 0 \end{array}$$

The solution of the dispersion equation, subject to these initial and boundary conditions, is (Highley and Merrick, 1971; Carslaw and Jaeger, 1959; Crank, 1957):

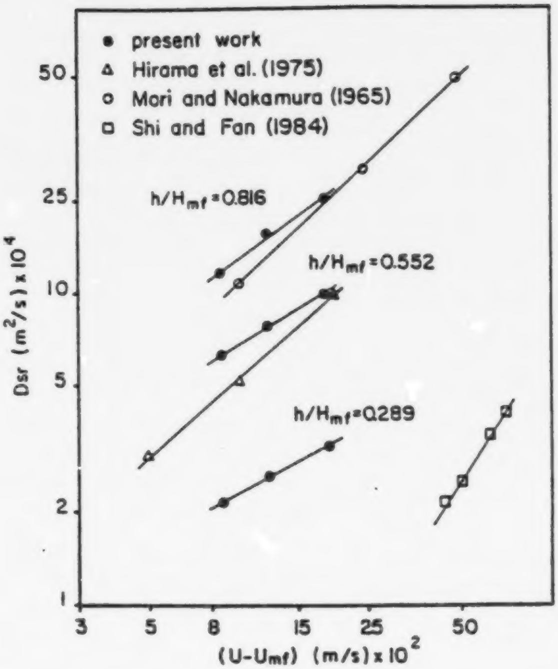

Figure 4 — Effect of the excess gas velocity on the lateral dispersion coefficient (for r/R = 0.225) at different levels above the gas distributor; values obtained by other Authors are also plotted as a comparison.

$$\frac{C_t}{C_{t\infty}} = 1 + \frac{2}{a}\sum_{i=0}^{\infty}\frac{J_1(\alpha_i a)J_0(\alpha_i r)}{\alpha_i[J_0(\alpha_i R)]^2}\exp\left[-D_{sr}\alpha_i^2 t\right] \quad \ldots\ldots \quad (6)$$

The lateral dispersion coefficient of the solid particles, D_{sr}, was determined by fitting empirically the experimental results of tracer concentration versus time with the profiles calculated at particular values of r/R, as shown in Figure 3. A sensitivity analysis demonstrated that the D_{sr} values have been evaluated within a 5% error range. Table 4 summarizes the values of the solid lateral dispersion coefficients derived from the experimental tracer concentration profiles.

Discussion

MIXING MECHANISM

As described previously, it is generally assumed that the main cause of lateral mixing of solids in gas–solid fluidized bed reactors can be attributed and correlated to the upward movement of gas bubbles through the bed. Moreover, experimental evidence shows that bubble breakage at the upper surface of the fluidized bed induces lateral particle dispersion (Davidson and Harrison, 1971) and that this phenomenon contributes substantially to the overall lateral mixing of solids (Hirama et al., 1975). The spreading of these particles over the bed surface and their subsequent motion depends upon several parameters, including the initial velocity relative to the velocity of the bubble, gravitational force, and drag force. Hence, besides bubble size and velocity, other parameters, such as particle size and density and fluid density and viscosity, play an important role.

Calderbank et al. (1967) and Gel'perin et al. (1970) observed a regular circulation pattern, or the so-called "Gulf

TABLE 4
Experimental Results

RUN #	PORT #	D_{sr} (m^2/s) × 10^4
1	1	1.89
	2	6.18
	3	2.24
2	1	3.45
	2	10.41
	3	4.88
3	1	2.70
	2	8.12
	3	3.48
4	1	6.28
	2	6.28
	3	7.32
	4	5.21
	5	2.74
5	1	9.81
	2	10.22
	3	11.46
	4	8.04
	5	3.87
6	1	7.89
	2	7.90
	3	8.94
	4	6.12
	5	3.15
7	1	11.54
	2	9.39
	3	9.18
	4	6.40
	5	2.18
8	1	19.80
	2	16.19
	3	16.64
	4	10.37
	5	5.08
9	1	15.67
	2	14.31
	3	10.44
	4	9.51
	5	3.26
10	1	2.09
	2	2.41
	3	1.96
	4	3.52
	5	3.72
11	1	3.18
	2	4.42
	3	4.46
	4	5.15
	5	5.61
12	1	2.58
	2	4.41
	3	2.11
	4	4.88
	5	5.50
13	1	18.22
	3	19.58
	5	8.46
14	1	6.87
	3	7.08
	5	7.74

Stream" behavior, which occurs naturally in fluidized beds. Merry and Davidson (1973) have suggested that uneven gas distribution through the bottom of the bed accentuates this tendency for circulation, influencing in this way the lateral solid displacement and mixing. Whitehead et al. (1970) and Whitehead (1979) have found that gross particle circulation is dependent on the bed height and gas flow rate.

The experimental results obtained in this work demonstrate not only the expected relationship between D_{sr} and the fluidizing velocity, but also the fact that the lateral dispersion coefficient changes with radial and axial positions within the fluidized bed (Table 4). Figure 4 is a logarithmic plot of D_{sr} against $(U - U_{mf})$ and shows the experimental results obtained in this work at one particular radial position ($r/R = 0.225$) and at different axial positions compared to the data obtained by other investigators. This figure shows that the lateral solids dispersion coefficient depends strongly on the level above the gas distributor plate and this dependence is shown also in Figure 5, where D_{sr} is plotted as a function of the height of the sampling tubes above the gas distributor plate, for one radial position ($r/R = 0.225$) at different fluidizing velocities.

EXISTING CORRELATION

As described previously, Shi and Fan (1984) correlated the solid lateral dispersion coefficient D_{sr} with several influencing parameters (Equation (2)):

$$D_{sr} = f[(U - U_{mf}), h_{mf}, d_p, \rho_s - \rho_f, \rho_f, \mu_f] \quad \ldots\ldots (7)$$

Figure 6 shows that Shi and Fan's empirical dimensionless correlation predicts adequately well the values of the solid dispersion coefficient only for 40−50% of the reactor radius, and only if the static bed height (h_{mf}) in the correlation (see Equation (2)) is substituted with the level of the sampling tube above the gas distributor (h). However, this modification does not take into account any decrease of the dispersion coefficient in the radial direction, which was observed to be very significant for r/R larger than about 0.5, especially at high fluidizing gas velocities and in the upper portion of the fluidized bed.

If the fact is accepted that the bubble flow is the main cause of solid lateral displacement (Nguyen et al., 1977; Marsheck and Gomezplata, 1965), and that the bubble flow does not exhibit flat velocity profiles over the reactor cross-section area due to bubble coalescence, as observed by Werther (1973), Calderbank et al. (1976), Nguyen et al. (1977), Wittmann et al. (1978), Masson and Jottrand (1978), a trend similar to that of the bubble flow rate should be expected for the lateral solids dispersion coefficient. The experimental results show qualitatively such a trend, but no correlation is yet available which is able to predict quantitatively the spatial non-uniformities of the bubble flow rate at a given axial level of the bed. Nguyen et al. (1975) and

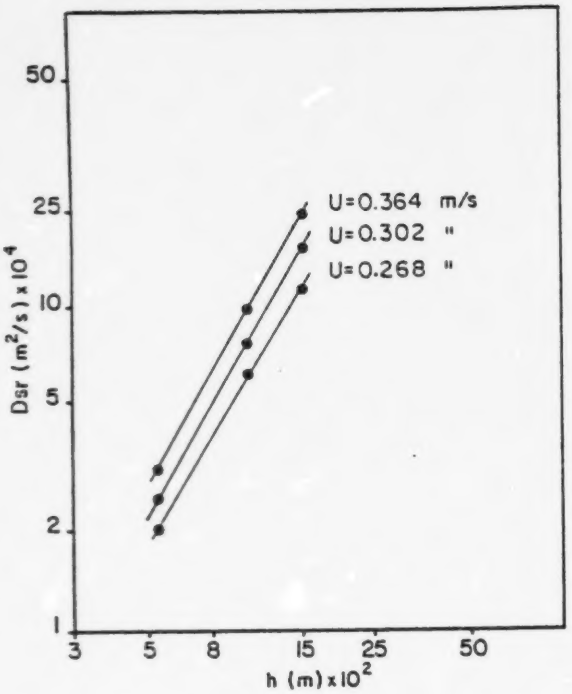

Figure 5 — Effect of the height above the gas distributor plate on the lateral dispersion coefficient (for $r/R = 0.225$) at different gas superficial velocities.

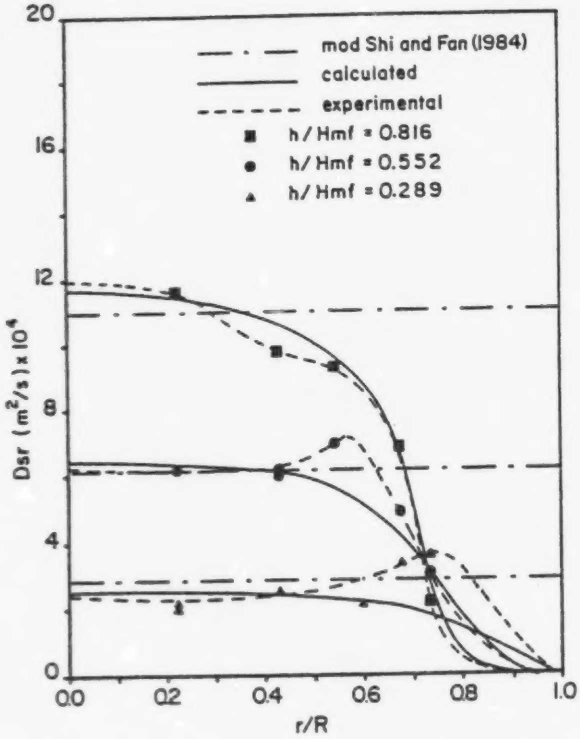

Figure 6 — Experimental lateral dispersion coefficients, $U - U_{mf} = 0.088$ m/s, $d = 400$ μm, compared to values calculated from Equation (8), and from the correlation of Shi and Fan (1984) (Equation (2)), when h_{mf} is substituted with the level of the sampling tube above the gas distributor plate (h).

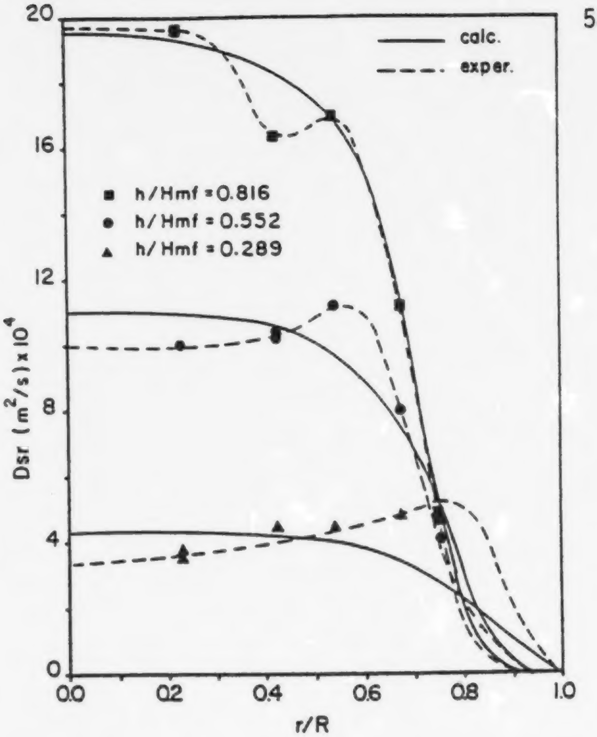

Figure 7 — Experimental lateral dispersion coefficients, $U - U_{mf} = 0.184$ m/s, $d_p = 400$ μm, compared to the values calculated from Equation (8).

Farrokhalaee and Clift (1980) developed two models for freely-bubbling beds, using computer simulations which predicted the size and spatial distribution of bubbles and of the bubble flow rate at any level above the distributor. However, further development and simplification of these simulations would be necessary before they could be used to assess completely the interaction between local bubble flow and solids circulation and mixing.

DEVELOPMENT OF A MODIFIED CORRELATION

On the basis of the above discussion, the correlation developed by Shi and Fan (1984) has been modified in order to take into account radial and axial variations of the lateral dispersion coefficient D_{sr} within a gas–solid fluidized bed reactor.

The following assumptions have been introduced:

— The excess gas velocity (strictly related to the bubble flow) is a function of the radial bed coordinate according to a 5th order parabolic expression, whose parabolic coefficient depends linearly on the axial reactor coordinate (h/H_{mf}). This assumption is based on a nonlinear regression analysis of the bubble flow profiles reported by several investigators (Werther et al., 1973; Calderbank, 1976; Wittmann et al., 1978), neglecting the maximum in the bubble flow rate observed by all of these authors. In the present experimental work a maximum in the lateral solids dispersion coefficient has been observed also occurring approximately at the same radial position as the maximum in bubble fow rate and therefore presumably linked to the same phenomena.

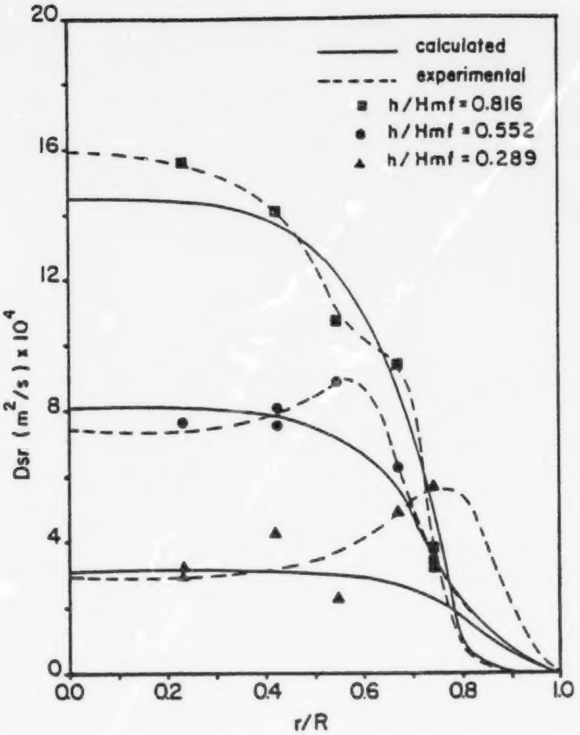

Figure 8 — Experimental lateral dispersion coefficients, $U - U_{mf} = 0.122$ m/s, $d_p = 400$ μm, compared to the values calculated from Equation (8).

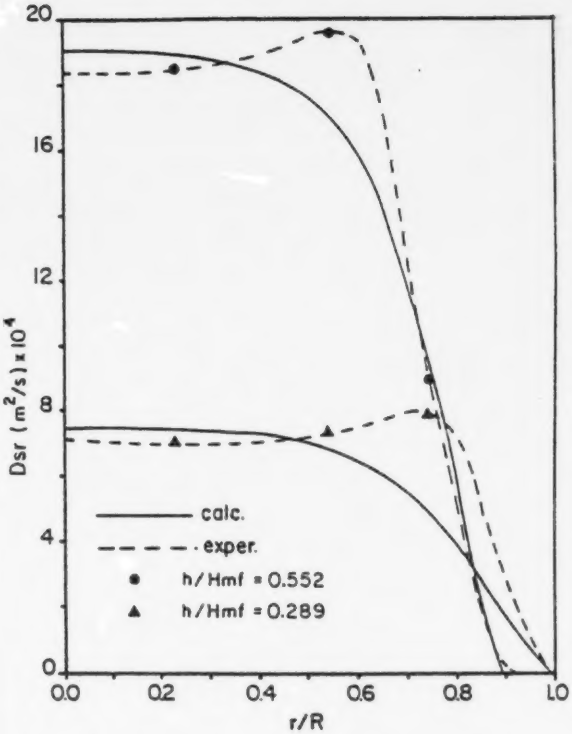

Figure 9 — Experimental lateral dispersion coefficients, $U - U_{mf} = 0.196$ m/s, $d_p = 200$ μm, compared to the values calculated from Equation (8).

— The parameter h_{mf} in the original expression is substituted with the axial bed coordinate (h), to take into account longitudinal variations of D_{sr}.

The experimental results obtained in the present work show that D_{sr} is proportional to $(U - U_{mf})^{0.70}$, $(h)^{1.65}$ and $(d_p)^{-0.64}$, which differ somewhat from those given in Equation (2). By means of dimensional analysis Equation (2) was reformulated to include these exponents on the relevant variables. A modified expression (Equation (8)) was then obtained by nonlinear regression analysis using the above exponents as initial values,

$$D_{sr} = 0.185 \cdot 10^{-4}\left[1 - \left(0.44 + 2.87\frac{h}{H_{mf}}\right)\left(\frac{r}{R}\right)^{5}\right] \times (U - U_{mf})d_p\left[\frac{(U - U_{mf})d_p\rho_f}{\mu_f}\right]^{-0.25} \cdot \left[\frac{h}{d_p}\right]^{1.45} \cdot \left[\frac{\rho_s - \rho_f}{\rho_f}\right]^{-0.43} \qquad (8)$$

The coefficient $0.185 \cdot 10^{-4}$ in Equation (8) has been evaluated according to the best fit of the experimental results.

In Figures 6, 7, 8 and 9 all the values of D_{sr} evaluated in the present work, in the different runs performed, are plotted as a function of the radial reactor coordinate, together with the curves resulting from the modified correlation of Equation (8). The agreement between the observed values of D_{sr} and the values predicted by the correlation is fairly good, with a maximum difference of less than 10% to 20% over most of the cross section. However, in the local regions where the maxima occur in the values of the solid lateral dispersion coefficients, the errors are larger because these local perturbations have been omitted in order to simplify the form of Equation (8).

It should be realized that the original correlation by Shi and Fan was based on experimental results obtained also by other investigators (Gabor, 1964; Highley and Merrick, 1971; Mori and Nakamura, 1965; Hirama et al., 1975), and therefore their choice of variables, particularly the effect of fluid properties, is well supported. The proposed correlation is valid in the range of operating conditions tested and for geometries where the H/D ratio is between 0.6 and 1, when one single general solids circulation pattern is established in the reactor. However, further verification and improvement of the correlation proposed in this work by use of a wider range of conditions and of larger diameter beds is planned for the near future.

Conclusions

From the experimental results obtained in a 0.27 m diam. fluidized bed reactor and the development of the theory of the proposed model, it appears that solids mixing in a batch fluidized gas−solid reactor can be successfully described by a process in which vertical solids mixing is assumed to be instantaneous and lateral mixing occurs by dispersion. Variations in the solid tracer concentration with time can be described by the model with reasonable accuracy.

The work described in this paper indicates that the usual assumption that solid mixing conditions are spatially uniform within a fluidized bed reactor may not always be correct.

The values of the lateral solids dispersion coefficients D_{sr}

are proportional to the local bubble velocity, as expected, and dependent on radial and axial positions within the bed.

A continuous dynamic solids sampling system has been successfully tested, resulting in a very practical method to determine tracer concentration variations with time of specified positions of the bed during the fluidization operation.

Based on the experimental results, a modified empirical dimensionless correlation based on that proposed by Shi and Fan (1984) has been developed for estimating the lateral solids dispersion coefficient. The values predicted by this modified correlation are in good agreement with the experimental results.

Acknowledgements

The research reported in this paper was supported through a Natural Sciences and Engineering Research Council of Canada grant. The authors are grateful to Mr. Jan Piskorz who provided helpful suggestions and to Prof. A. Gianetto for many interesting discussions on this work. The authors wish also to acknowledge the contribution of Mr. Peter Majerski for his technical help.

Nomenclature

a = radius of the tracer injection tube (mm)
C_t = tracer concentration (%)
$C_{t\infty}$ = tracer concentration after infinite time (%)
D = reactor diameter (m)
d_b = bubble diameter (m)
d_p = particle equivalent diameter (m)
d_{pt} = tracer particle diameter (m)
D_{sr} = lateral solid dispersion coefficient (m^2/s)
F = gas volumetric flow rate (m^3/s)
H, h_{mf}, H_{mf} = static bed height (m)
h = reactor axial coordinate (m)
H_{exp} = expanded bed height (m)
J_0, J_1 = Bessel functions
r = reactor radial coordinate (m)
R = reactor radius (m)
t = time after tracer injection (s)
U = gas superficial velocity (m/s)
U_{mf} = minimum fluidizing velocity (m/s)

Greek symbols

α_i = constant such that $\alpha_i R$ is the ith zero of the Bessel function J_1
δ = volume fraction of bubbles in the fluidized bed (---)
ϵ_{mf} = void fraction of the bed at minimum fluidization conditions (---)
μ_f = fluid viscosity ($kg/m \cdot s$)
ρ_f = fluid density (kg/m^3)
ρ_s = solid density (kg/m^3)
ρ_t = tracer particle density (kg/m^3)

References

Brötz, W., "Untersuchungen uber Transportvorganger in Durchstromtem, Gekorntem Gut", Chem. Ing. Techn., 28, 165−174 (1956).

Burgess, J. M. and P. H. Calderbank, "The Measurement of Bubble Properties in Two Phase Dispersions-III: Bubble Properties in a Freely Bubbling Fluidized Bed", Chem. Eng. Sci. 30, 1511−1518 (1975).

Calderbank, P. H., J. Pereira and M. M. Burgess, "The Physical and Mass Transfer Properties of Bubbles", in "Fluidization Technology", D. L. Keairns, Ed., Hemisphere Publ. Co., Vol. 1, 115−167 (1976).

Calderbank, P. H., F. D. Toor, and F. H. Lancaster, "Proceeding of the International Symposium on Fluidization", A. A. H. Drinkenberg, Ec., Eindhoven, Netherland University Press, 652−660 (1967).

Carslaw, H. S., and J. C. Jaeger, "Conduction of Heat in Solids", 2nd Ed., Calendon Press: Oxford (1959).

Chang, C. C., L. T. Fan and S. X. Rong, "Modeling of Shallow Fluidized Bed Reactors: I-Analytic solution of a simplified model", Can. J. Chem. Eng., 60, 272−281 (1982).

Chang, C. C., S. X. Rong and L. T. Fan, "Modeling of Shallow Fluidized Bed Reactors: II-Analytical and numerical solutions", Can. J. Chem. Eng., 60, 781−790 (1982).

Crank, J., "The Mathematics of Diffusion", 2nd ed., Clarendon Press: Oxford (1963).

Davidson, J. F. and D. Harrison, "Fluidised Particles", Cambridge University Press: New York (1963).

Davidson, J. F. and D. Harrison, "Fluidization", Academic Press: New York (1971).

Farrokhalaee, T. and R. Clift, "Mechanistic Prediction of Bubble Properties in Freely-Bubbling Fluidised Beds", in "Fluidization", J. R. Grace and J. M. Matsen, Eds., Plenum Press: New York, 135−142 (1980).

Gabor, J. D., "Lateral Solid Mixing in Fluidized-Packed Beds", AIChE J., 10, 345−350 (1964).

Gel'perin, N. I., B. M. Grakhovskii and V. M. Dement'ev, "Transverse Mixing of Particles in a Fluidized Bed with Small Ratio of the Height of the Bed to the Linear Transverse Dimension" Theor. Found. Chem. Eng., 4, 572−575 (1970).

Grace, J. R., "Fluidized Bed Reactor Modeling: an Overview", presented at the Second Chemical Congress of North America Continent, Las Vegas, Aug. 24−29 (1980), also ACS Symp. Ser., 168, 3−18 (1981).

Hayakawa, T., W. Graham and G. L. Osberg, "A Resistance Probe Method for Determining Local Solid Particle Mixing Rates in a Batch Fluidized Bed", Can. J. Chem. Eng., 42, 99−103 (June 1964).

Highley, J. and D. Merrick, "The Effect of the Spacing Between Solid Feed Points on the Performance of a Large Fluidized-Bed Reactor", AIChE Symp. Ser., Vol. 67, No. 116, 219−227 (1971).

Hirama, T., M. Ishida and T. Shirai, "The Lateral Dispersion of Solid Particles in Fluidized Beds", Kagaku Kogaku Ronbunshu, 1, 272−276 (1975).

Kunii, D. and O. Levenspiel, "Fluidization Engineering", John Wiley & Sons: New York (1969).

Lewis, W. K., E. R. Gilliland and H. Girouard, "Heat Transfer and Solid Mixing in Beds of Fluidized Solids", Chem. Eng. Prog. Symp. Ser., 58, No. 38, 87−97 (1962).

Marsheck, R. M. and A. Gomezplata, "Particle Flow Patterns in a Fluidized Bed", AIChE J., 11, 167−173 (1965).

Masson, H. and R. Jottrand, "Measurement of Local Bubbles Properties in a Fluidized Bed", in "Fluidization", J. F. Davidson and D. L. Keairns, Eds., Cambridge University Press, 1−6 (1978).

May, W. G., "Fluidized Bed Reactor Studies", Chem. Eng. Prog., 55, 49−56 (1959).

Merry, J. M. D. and J. F. Davidson, "Gulf Stream Circulation in Shallow Fluidized Beds", Trans. Instn. Chem. Engrs., 51, 361−368 (1973).

Mori, Y. and K. Nakamura, "Solid Mixing in Fluidized Bed", Kagaku Kogaku, 29, 868−875 (1965).

Nguyen, T. H., J. E. Johnsson, R. Clift and J. R. Grace, "Prediction of Bubble Distributions in Freely-Bubbling Three-Dimensional Fluidized Beds", in "Fluidization Technology", D. L. Keairns, Ed., Hemisphere Publ. Co., 205−214 (1975).

Nguyen, H. V., A. B. Whitehead and O. Potter, "Gas Backmixing, Solids Movement, and Bubble Activities in Large Scale Fluidized Beds", AIChE J., 23, 913−922 (1977).

Scott, D. S. and J. Piskorz, "Low Rate Entrainment Feeder for Fine Solids", Ind. Eng. Chem. Fundam., 21, 319−322 (1982).

Shi, Y. and L. T. Fan, "Lateral Mixing of Solids in Batch Gas−Solids Fluidized Beds", Ind. Eng. Chem. Proc. Des. Dev., 23, 337−341 (1984).

Vanecek, V., M. Markvart, M. and R. Drbohlav, "Fluidized Bed Drying", Leonard Hill: London (1966).

Werther, J. and O. Molerus, "The Local Structure of Gas Fluidized Beds: I-A statistically based measuring system", J. Multiphase Flow, **1**, 103−122 (1973).

Werther, J. and O. Molerus, "The Local Structure of Gas Fluidized Beds: II-The spatial distribution of bubbles", J. Multiphase Flow, **1**, 123−138 (1973).

Werther, J., "Influence of the Bed Diameter on the Hydrodynamics of Gas Fluidized Beds", AIChE Symp. Ser., Vol. 70, **141**, 53−62 (1974).

Whitehead, A. B., G. Gartside, and D. C. Dent, "Flow and Pressure Maldistribution at the Distributor Level of a Gas−Solid Fluidised Bed", The Chem. Eng. J., **1**, 175−185 (1970).

Whitehead, A. B., "Prediction of Bubble Size in a Gas-Fluidised Bed", Chem. Eng. Sci., **34**, 751 1979).

Wittmann, K., D. Wippern, H. Helmrich and K. Schugerl, "Behaviour of the Bubbles in a Bench Scale Fluidized Bed Reactor with Conversion of Solids in Continuous Operation at Various Temperatures", in "Fluidization", J. F. Davidson and D. L. Keairns, Eds., Cambridge University Press, 173−178 (1978).

Manuscript received February 4, 1985; revised manuscript received July 12, 1985; accepted for publication July 15, 1985.

APPENDIX 4-B

Measuring and Modelling Residence Time Distribution of Low Density Solids in a Fluidized Bed Reactor of Sand Particles

MEASURING AND MODELLING RESIDENCE TIME DISTRIBUTION OF LOW DENSITY SOLIDS IN A FLUIDIZED BED REACTOR OF SAND PARTICLES

F. Berruti, A. G. Lidén[*], D. S. Scott

Department of Chemical Engineering, University of Waterloo,
Waterloo, Ontario, Canada N2L 3G1.

[*] Department of Chemical Engineering, University of Minnesota
Minneapolis, Minn. U.S.A.

ABSTRACT

An experimental study was carried out in order to estimate the residence time distribution of low density particles injected into a fluidized bed reactor containing sand particles.

Tracer experiments were performed at room temperature, using a pilot plant pyrolysis reactor. A novel technique was used to detect and measure the flow of solid tracer particles entering and leaving the fluid bed.

Tests were carried out employing solid tracers having different physical characteristics. The experimental results demonstrated that the degree of particle entrainment was a function of fluidizing gas velocity, particle size and particle density. Solid mixing, segregation and entrainment were studied also in the fluidized bed, as functions of physical and operating parameters.

Various models were tested to characterize the nonideal solids flow patterns within the fluid bed, and a circulation model appeared to give a good description of the physical mechanism involved and to provide the best agreement with the experimental results.

The experiments described in this work were performed with the aim of estimating such residence times, in the range of the optimal operating conditions for the Waterloo flash pyrolysis process (gas residence times ranging between 0.45 and 0.60 seconds and temperatures between 450° and 560°C).

A literature survey showed that the available information on mixing and residence time distribution of low density particles in fluid beds of heavier particles is very scarce and most of the models fail to represent closely enough the real physical characteristics of the systems. Heertjes et al. (1967) studied the transport and residence time of particles in a continuously fed rectangular fluidized bed using either the ideal mixing model ~~and~~ or the piston flow model and provided a qualitative description of the phenomena involved. Verloop et al. (1968) presented a critical survey of the different models proposed in the literature for solids transport in gas fluidized beds and concluded that although many models based on combined flow systems or on a number of perfect mixers can fit the residence time distribution curve fairly well, the physical behavior of the real system is not recognized. Valenzuela and Glicksman (1983) measured the residence time of fine iron powder injected in a 2-D fluidized bed of glass particles. A percolation model was proposed for interpreting the mixing, segregation and elutriation of fines. Colakyan and Levenspiel (1984) measured the elutriation characteristics of widely different solids and proposed an empirical correlation valid for beds having very high freeboard regions.

EXPERIMENTAL APPARATUS AND METHOD

Ideally, residence time distributions of biomass feed particles would be carried out in the fluidized bed reactor used for the actual flash pyrolysis experiments employing the same materials (i.e. biomass and char particles) as tracers ~~and~~ by injecting a pulse of particles trough through the feed injection tube of the fluid bed and detecting the tracer entering and leaving the bed with an appropriate system. However, it was not possible to study the RTD of the biomass particles at reaction conditions (about 500°C). For practical reasons, the study was carried out at room temperature, using the same reactor as that employed for the pyrolysis process, and operating at the same gas residence times.

The pilot plant fluidized bed reactor is shown in Figure 1. The reactor was 0.1 m in diameter and 0.401 m long with 0.163 m of this representing the settled bed height.

The experimental set-up for the tracer-type experiments is shown in Figure 2. The equipment consisted of two Brinkmann Probe Colorimeters PC/700, whose probes were placed at the inlet and outlet of the reactor respectively.

Each probe consisted of a pair of parallel fiber optic light guides: one cable provided a light beam and the other one received the light, after it was reflected by a small concave mirror placed on each probe tip, and directed it to a detector which could read the signal and convert it into a voltage value (Figure 3). When a stream of solid particles was directed in the gap between the tip of the fiber optic guide and the mirror, the intensity of the light beam as measured by the detector was reduced due to the presence of solid obstacles along the light path. This decrease in intensity was found to be proportional to the amount of solid particles instantly present in the gap.

Preliminary experiments carried out using a bench-scale setup demonstrated that the use of wood particles (biomass) or char as tracers was impractical due to the collection on the surface of the mirror of dust and fines contained in the raw materials, resulting in a rapid decrease of the signal.

Other materials had to be selected to be used as tracers which had approximately the same physical properties as the wood and char, in order to correctly simulate the system.

Among all the materials considered, styrofoam beads (Stax Plastic Co., Toronto) and PVC particles (B.F. Goodrich Canada Inc., Waterloo) were chosen to simulate char and wood respectively. Some wood samples were subsequently used also as tracers, after an appropriate treatment to eliminate fines and dust. Each wood sample was screened to get a very narrow range of sizes, washed with deionized water, dried and fluidized with air in a small fluid bed to reduce as much as possible all the fines. The biomass treated in this way demonstrated acceptable characteristics for use as tracer, showing no detectable dust deposition on the reflecting mirror of the probes.

The physical characteristics of the tracers used in this work are listed in Table 1 where they are also compared to those of the materials used in the actual flash pyrolysis runs.

Both the colorimeters were connected to two different channels of an analog-to-digital converter of an IBM PC. An appropriate software was developed for the particular application, which allowed the collection, conversion and storage of about 200 data points per second per channel. Another computer program allowed for subsequent data plotting and printing.

The use of the above system allowed the simultaneous collection and storage of the voltage readings of both the colorimeters and thus the detection of the pulse injection of tracer (approximately a delta function) at the inlet and the continuous tracer response at the outlet of the reactor.

The tracer injection was performed in all the experiments through the feed tube of the pyrolysis reactor using the same volumetric gas rate as that used for feeding biomass particles during pyrolysis runs. Each tracer sample consisted of a weighed amount of particles (10-15 g) placed inside the feed tube about 0.12 m upstream from the inlet probe. For each experiment, the tracer injection was performed as soon as steady state conditions were reached inside the fluid bed, detected by a constant pressure drop through the reactor. When the experimental time expired, as determined by a constant "zero" reading at the outlet, the data collected were plotted and printed.

EXPERIMENTAL RESULTS

Several preliminary experiments were conducted to test the experimental apparatus, the analytical system and the reproducibility of the results obtained.

A final set of 20 experiments was performed for the purpose of determining the mean residence times of particles having different physical characteristics, and for different operating conditions.

Four gas residence times were tested within the range of the optimal conditions giving maximum organic liquid production in the flash pyrolysis runs (i.e. 0.45, 0.50, 0.55 and 0.61 s).

Typical tracer input and output signals for some of the experiments are shown in Figures 4 and 5, plotted as normalized concentrations versus time (s) after the input pulse. As shown, the tracer input signal was in all cases a narrow square wave, whereas the output tracer signals were represented by skewed curves, with a rapid sharp increase and a slow decrease, the typical response configuration of a system having a flow behaviour somewhere between a plug flow reactor and a perfectly mixed tank.

Experimental conditions used in each run performed are summarized in Table 2.

Initially, it was observed that when wood particles were used as tracer, the injected wood pulse, regardless of the gas superficial velocity employed in the reactor (within the range used in this work), did not leave the system but remained in all cases well mixed with the sand particles, although there was a sensible difference in density between the two materials (i.e. wood 450 kg/m^3, sand 2,470 kg/m^3).

On the other hand, when the other tracers used (styrofoam or PVC beads) were injected into the fluidized system, all the particles, after a certain residence time, were quantitatively eluted from the bed. Mass balances, conducted for every run, confirmed this behaviour.

Another important finding was that both particle size and particle density played important roles in determining the residence time of injected particles into a sand fluidized bed.

INTERPRETATION OF THE RESULTS

The curve that describes the concentration-time function of tracer in the exit stream of a vessel in response to an idealized instantaneous pulse injection is defined as the C-curve (Levenspiel, 1972). However, the measured concentrations can be normalized by referring them to the initial concentration of the tracer injected and by using reduced time units.

The two most useful and universally measured quantities for describing tracer response curves, are the mean residence time, which locates the center of gravity of the response, and the variance, which describes how the response is spread out in time. A given distribution of tracer residence times can be completely defined mathematically by the moments of the distribution.

The first moment about the origin, commonly called the mean or centroid of the distribution, is defined as

$$\mu = \frac{\int_0^\infty x\ f(x)\ dx}{\int_0^\infty f(x)\ dx} \tag{1}$$

which represents the mean residence time of the particles in the reactor.

The second moment about the mean, commonly called the variance, measures the spread of the distribution around the mean point and it is defined as

$$\sigma^2 = \frac{\int_0^\infty (x-\mu)^2\ f(x)\ dx}{\int_0^\infty f(x)\ dx} \tag{2}$$

The results of the moment analysis performed for all the experiments of this work which were done with solids that could be eluted from the reactor are shown in Table 3.

MODELLING

Mono-dimensional models

Many types of models can be used to characterize nonideal flow patterns within vessels. Some of them draw on the analogy between mixing in actual flow and that in diffusional processes (dispersion models). Others visualize various flow regions connected in series or parallel (combined flow models) (Verloop et al., 1968; Nauman and Buffham, 1983).

Models vary in complexity, but generally one-parameter models can adequately represent flow patterns in packed beds or tubular vessels. On the other hand, two- to six-parameter models have been proposed to represent fluidized bed reactors (Levenspiel, 1972).

The analysis of the present system was carried out by considering first the simplest mono-dimensional models, i.e. the dispersion model and the tanks-in-series model. The dispersion model is based on the following equation:

$$\frac{\partial C}{\partial \theta} = \left(\frac{D_{SA}}{U \cdot L}\right) \frac{\partial^2 C}{\partial z^2} - \frac{\partial C}{\partial z} \qquad (3)$$

where $(D_{SA}/U \cdot L)$ = "vessel dispersion number"

$\longrightarrow$ 0 for plug flow (negligible dispersion)

$\longrightarrow \infty$ for mixed flow (large dispersion).

The vessel dispersion number can be calculated from the experimental results as a function of the variance. In the presence of a large extent of dispersion, the following relationship can be used (Levenspiel, 1972):

$$\sigma_\theta^2 = \frac{\sigma^2}{\bar{t}^2} = 2\left(\frac{D_{SA}}{U \cdot L}\right) - 2\left(\frac{D_{SA}}{U \cdot L}\right)^2 \cdot \left(1 - e^{-(U \cdot L/D_{SA})}\right) \qquad (4)$$

In the case of the tanks-in-series model, the flow is considered to pass through a series of equal-size ideal stirred tanks, and the one parameter of the model is the number of tanks N in the chain. The concentration-time relationship is given by:

$$C = \frac{N \cdot (N \cdot \theta)^{N-1}}{(N-1)\,!}\, e^{-N \cdot \theta} \qquad (5)$$

N can be calculated from the experimental results both by comparison of the RTD curve given by equation (5) for various N with the experimental data, or by using the simple relationship:

$$\sigma_\theta^2 = \frac{1}{N} \qquad (6)$$

The results of both the one-parameter models (i.e. the vessel dispersion number and N) are listed in Table 4.

Multiparameter models

More complex models can be attempted to interpret the nonideal flow of the system being considered, or to achieve a representation which is more physically acceptable based on the actual flow situation present in the pyrolysis fluidized bed reactor.

To select the proper model, the actual flow patterns and the geometries of the bed must be considered first. A model with a relatively large number of parameters is flexible in fitting a wide variety of situations. However, the mathematical expressions for many-parameters models are complex and usually too cumbersome to handle. Therefore, the general aim should be the selection of a simple realistic model which fits the physical phenomena present in the real system.

Previous solids mixing experiments (Berruti, 1985) demonstrated that a gross solid circulation (gulf stream effect) can be observed in gas-solid fluidized bed reactors having a height-to-diameter ratio up to 2 or 3. However, when this ratio reaches values larger than 3, multiple solid circulation patterns are likely to be established, one on top of the other, and thus the overall solids mixing is significantly improved. The existence of such gross solids circulation in the pyrolyzer sand fluidized bed was clearly indicated by the wavy characteristic tracer response at the outlet of the reactor (Figures 4 and 5).

Weber (1953) proposed a circulation model for interpreting the fluid flow in stirred tank reactors, which was based on the concept that a portion of fluid recirculates in the vessel. This portion of recirculating fluid comprised a number, m, of passes of plug flows.

Van de Vusse (1962) proposed another type of circulation model in which there were basically three main loops circulating in the reactor: one receives the feed stream, another delivers to the outflow stream and all the other internal loops combine together to form a third loop, as shown schematically in Figure 6. A physical diagram for the circulating model consisting of three loops is also represented in Figure 6.

The response equation for such a system, as evaluated by Van de Vusse (1962) for the case of a pure impulse of tracer is given by:

$$C(t) = \frac{q}{r+q}\left(\frac{r+q}{r}\right)^{\frac{n-1}{n}} \cdot \frac{n}{\tau_C} \cdot \exp -\left(\frac{n \cdot t}{\tau_C}\right) \cdot g(at) \qquad (7)$$

where

$$a = \frac{n}{\tau_C}\left(\frac{r}{r+q}\right)^{\frac{1}{n}} \qquad (8)$$

and

$$g(at) = \frac{1}{m}\left(\sinh(at) + \sum_{k=1}^{m-1} \exp\left(at\cos\left(\frac{\pi k}{m}\right)\right)\cos\left(at\sin\left(\frac{\pi k}{m}\right) + \frac{\pi k}{m}\right)\right) \qquad (9)$$

For n = 2 m (even), equation (9) yields:

$$g(at) = \frac{1}{n}\sum_{k=0}^{n-1} \exp\left(at\left(\cos\left(\frac{2\pi k}{n}\right) + i\,\sin\left(\frac{2\pi k}{n}\right)\right) + \left(\frac{2\pi k}{n}\right)\right) \qquad (10)$$

For n = 2 m + 1 (odd), equation (9) yields:

$$g(at) = \frac{1}{2m+1}\left(\exp(at) + 2\sum_{k=1}^{m} \exp\left(at\cos\left(\frac{2\pi k}{2m+1}\right)\right)\cos\left(at\sin\left(\frac{2\pi k}{2m+1}\right) + \left(\frac{2\pi k}{2m+1}\right)\right)\right) \qquad (11)$$

In order to reduce the number of variables and to simplify the model, the circulation rate was assumed to be equal to the feed rate (i.e., all the tracer material circulates into the reactor).

The above equations were solved and the two parameters (number of circulations and circulation time) were evaluated for the various experiments by fitting the resulting mathematical expressions to the experimental results.

The model predictions compared to the experimental curves obtained with different particle sizes at different gas fluidizing velocities are shown in Figures 7, 8 and 9.

The fit which resulted from this model was gratifying and the circulation model appeared to represent closely the real physical mechanism involved in the mixing-elutriation process occurring in the pyrolysis reactor. The values of the model parameters (n and τ_c) evaluated in the present work are shown in Table 5 and plotted as functions of the particle size in Figures 10 and 11 respectively.

MIXING, SEGREGATION, ENTRAINMENT

A number of experiments have been performed in order to develop a practical criterion for determining for solids of different densities when good mixing, entrainment or segregation will occur in the fluidized bed as a function of the operating conditions and the physical characteristics of the materials used.

Styrofoam beads, cork particles, PVC beads and wood particles having different particle sizes have been employed as tracers in these experiments, where the amount of tracer particles was small (about 5% in volume or less) compared to the quantity of sand in the bed (jetsam-rich system). The physical characteristics of the materials used are given in Table 6.

Three gas superficial velocities, namely 1.3, 2.1 and 3 times the minimum fluidizing velocity of the bed sand particles (d_p = 400 μm) were tested.

The experimental results obtained during this investigation are shown in Figures 12 and 13 for different gas velocities. The effects caused by the depth of the bed (shallow versus deep bed) are also shown in Figure 12. The boundaries of each of the specific regions identified are shown as single lines, which should be understood to really represent a band, since the experimental results did not cover a continuous range of conditions. Besides, a certain degree of uncertainty in determining the exact position of the boundary is present due both to the particle size distribution of each sample and to the fact that the experimental technique was based on visual observation of the settled bed after 10 - 30 seconds of fluidization.

The final objective of these experiments was, in fact, the gross determination of the various regions, in order to be able to estimate the extent of mixing, segregation and entrainment for different operating conditions in the range used for the Waterloo flash pyrolysis.

The results obtained show that even at gas velocities slightly in excess of the minimum fluidizing velocity of the sand (i.e. $u = 1.3\ u_{mf}$) a well mixed region was present when denser or larger tracer particles were used. These findings confirm the results obtained during the experiments carried out to study the residence time distribution of wood particles in the fluidized bed. However, when particles lighter and smaller than wood were employed as tracer, segregation and entrainment were achieved.

The segregation region reduced to a narrow band with increasing gas velocity, and two distinct regions of entrainment and well mixing are then defined, as shown in Figure 13.

The experimental results obtained with a shallower bed indicate an enhanced segregation zone (limited by a discontinuous line in Figure 12), probably related to the higher frequency of bubbling and to the smaller bubble size which preferentially increases the extent of segregation by reducing the lateral solids displacement and mixing (Berruti, 1985).

DISCUSSION AND CONCLUSIONS

The experimental results obtained in the study of the residence time of low density particles in the pyrolysis fluidized bed of sand particles demonstrated that the solids entrainment from the bed was a function of fluidizing gas velocity, particle size and particle density.

Wood particles injected into the fluidized bed remained well mixed with the bed material (sand), regardless of the difference in density and of the fluidizing velocity used within the normal operating range of the Waterloo flash pyrolysis process. Lighter particles simulating the solid pyrolysis product (char) were observed to leave the reactor quantitatively after a few seconds of residence time (between 2 and 8.2 seconds depending upon their size).

These findings demonstrate the autoregulating characteristics of the fluidized bed pyrolysis system: the biomass particles are kept in the bed until a sufficient degree of weight loss has been attained to reduce the original density to the point at which entrainment can occur.

The values of solids residence times obtained in this work are in very good agreement with those evaluated by Liden et al. (1986) using a kinetic prediction model for the production of liquids from the biomass flash pyrolysis process taking place in a fluidized bed. Liden's model assumes the biomass to be decomposed according to two parallel reactions, one yielding tar, and the other char+gas. The tar is then assumed to undergo further secondary reactions giving mainly gas as a product. Such a model has been demonstrated to predict very closely the liquid organic yields obtained in the Waterloo flash pyrolysis process.

Three different models have been tested to characterize the nonideal flow pattern of the low density particles within the sand fluidized bed.

The analysis of the system was performed by considering first the simplest mono-dimensional models, i.e. the dispersion model and the tanks-in-series model. Although the numerical values of the models' parameters were reasonable, indicating in both cases a large extent of dispersion and backmixing, as can be expected in a fluidized bed, the models tested were not found satisfactory in interpreting the real physical phenomena occurring in the actual pyrolysis fluid bed reactor and its characteristics. In particular, the calculated curves did not represent closely enough the experimental results at any time, predicting much smaller values in the central part of the response and higher values in the tail.

Beek (1966), Calderbank et al. (1967), Gel'perin et al. (1970), Merry and Davidson (1973), Berruti (1985) and many other researchers have observed that regular solids circulation patterns occur naturally in fluidized bed reactors. Such circulation patterns have been confirmed in the course of this work by the observation of the oscillating nature of the tracer responses at the outlet of the reactor. For this reason, the circulation model proposed by Van de Vusse (1962) was adopted for interpreting the experimental results. This model appears to successfully describe the flow of entrainable particles through the sand fluid bed and in particular, to be more closely related to the real physical mechanism involved in the mixing-entrainment process occurring in the pyrolysis reactor. The model parameters (i.e. circulation time and number of circulations) were observed to follow certain consistent trends when plotted as functions of particle size and gas velocity.

The circulation time was found to increase with increasing particle size of the low density solid (See Figure 11.) and to decrease with increasing gas velocity, conclusions which are reasonable and physically acceptable, since bigger particles can be expected to circulate more slowly than smaller ones, whereas an increase in gas fluidizing velocity would speed up the solid circulation and mixing in the bed.

The number of circulations was observed to increase with increasing size of the low density particles, (see Figure 10) and with increasing gas velocity, because bigger particles stayed longer in the bed before being entrained by the gas stream, and a higher gas velocity promoted a better mixing between solids having different densities. Although the time required to complete one circulation through the bed would be shorter, a higher number of circulations would be required before entrainment could be attained.

There are no literature values of these model parameters available to be used as a comparison. However, in view of the good simulation achieved, further application of the circulation model to studies of residence time of low density particles in fluidized bed dryers, combustors or pyrolysis reactors would appear to have potential in explaining fluid bed behavior.

Two practical charts are proposed as shown in Figures 12 and 13 and discussed earlier, which are useful in indicating the physical characteristics (size and density) of solid particles which may be entrained from a fluid bed, may be well mixed into the vessel, or may be simply segregated through the bed material, for the operating conditions in the range used for the Waterloo fluid bed pyrolysis process.

ACKNOWLEDGEMENTS

The research reported was supported through a Natural Sciences and Engineering Research Council of Canada grant. The authors are grateful to Mr. Peter Majerski for his technical help and to Mr. Marino Battezzati for offering his

contribution in developing the computer software.

NOMENCLATURE

a = parameter defined in Equation (8)

C = normalized tracer concentration (---)

D = fluidized bed diameter (m)

D_{SA} = axial solids dispersion (m^2/s)

d_p = particle size (um)

$f(x)$ = frequency of an element of a distribution (---)

$g(at)$ = function defined in Equation (9)

h = depth of the fluidized bed (m)

L = length of dispersion path (m)

m = function of the number of circulations (---)

n = number of circulations (---)

N = number of perfect mixers in a series (---)

q = feed rate (m^3/s)

r = circulation rate (m^3/s)

t = time (s)

$\bar{t}$ = average solids residence time (s)

U = solids velocity (m/s)

u = gas velocity (m/s)

u_{mf} = minimum gas fluidizing velocity (m/s)

x = generic element of a distribution

z = dimensionless axial coordinate (---)

Greek Symbols

$\theta = t/\bar{t}$ = dimensionless time (---)

μ = mean of a distribution (s)

ρ = density (kg/m^3)

σ^2 = variance of a distribution (s^2)

σ_θ^2 = dimensionless variance of a distribution (---)

τ_C = circulation time (s)

τ_G = gas residence time (s)

Subscripts

c = char

p = particle

ps = sand particle

REFERENCES

Beek, W.J., De Ingenieur, Utrecht, 78, 109 (1966).

Berruti, F., "Measuring and Modelling Solid Mixing and Particle Residence Times in a Gas-Solid Fluidized Bed Reactor for Biomass Flash Pyrolysis", Ph.D. Dissertation, University of Waterloo, Waterloo, Ontario, Canada (1985).

Berruti, F., D.S. Scott, and E. Rhodes, "Measuring and Modelling Lateral Solid Mixing in a Three-Dimensional Batch Gas-Solid Fluidized Bed Reactor", The Can. J. Chem. Eng., 64, 48-56 (1986).

Calderbank, P.H., F.D. Toor, and F.H. Lancaster, in Proceeding of the International Symposium on Fluidization, A.A.H. Drinkenberg, Ed., Eindhoven, Netherland University Press, 652-660 (1967).

Colakyan, M., and O. Levenspiel, "Elutriation from Fluidized Beds", Powder Technology, 38, 223-232 (1984).

Gel'perin, N.I., B.M. Grakhovskii, and V.M. Dement'ev, "Transverse Mixing of Particles in a Fluidized Bed with Small Ratio of the Height of the Bed to the Linear Transverse Dimension", Theor. Found. Chem. Eng., 4, 572-575 (1970).

Heertjes, P.M., L.H. de Nie, and J. Verloop, "Transport and Residence Time of Particles in a Shallow Fluidized Bed", Proc. Int. Symp. on Fluidization, A.A.H. Drinkenberg, Ed., Eindhoven, Netherlands University Press, 477-490 (1967).

Levenspiel, O., "Chemical Reaction Engineering", 2nd Ed., J. Wiley (1972).

Lidén, A.G., F. Berruti, and D.S. Scott, "A Kinetic Model for the Production of Liquids from the Flash Pyrolysis of Biomass", Chem. Eng. Commun. (Submitted for publication), (1986).

Merry, J.M.D., and Davidson, J.F., "Gulf Stream Circulation in Shallow Fluidised Beds", Trans. Instn. Chem. Engrs., 51, 361-368 (1973).

Nauman, E.B., and B.A. Buffham, "Mixing in Continuous Flow Systems", J. Wiley Ed. (1983).

Scott, D.S., and J. Piskorz, "The Flash Pyrolysis of Aspen-Poplar Wood", The Can. J. Chem. Eng., 60, 666-674 (1982).

Scott, D.S., and J. Piskorz, "The Continuous Flash Pyrolysis of Biomass", The Can. J. Chem. Eng., 62, 404-412 (1984).

Scott, D.S., and J. Piskorz, "Liquid Product from the Continuous Flash Pyrolysis of Biomass", Ind. Eng. Chem. Proc. Des. Dev., 24 (3), 581-588 (1985).

Valenzuela, J.A., and L.R. Glicksman, "Residence Time and Dispersion of Fine Particles in a 2-D Fluidized Bed of Large Particles", Proc. Fourth Int. Conf. on Fluidization, Kashikojima, Japan, 2-8-1/2-8-7 (1983).

Van de Vusse, J.G., "A New Model for the Stirred Tank Reactor", Chem. Eng. Sci., 17, 507-521 (1962).

Verloop, J., L.H. de Nie, and P.M. Heertjes, "The Residence Time of Solids in Gas-Fluidized Beds", Powder Techn., 2, 32-42 (1968).

Weber, A.P., Chem. Eng. Progr., 49, 26-30 (1953).

TABLE 1

Physical Characteristics of Tracers used and of Materials used in Actual Pyrolysis Runs

TRACERS:

1. Styrofoam beads
d_p = 154, 450, 505, 715, 850, 920 μm
ρ_p = 82 kg/m^3

2. PVC particles
d_p = 154 μm
ρ_p = 547 kg/m^3

3. Wood particles (IEA Poplar)
d_p = 505, 715, 920 μm
ρ_p = 450 kg/m^3

BIOMASS:

IEA Poplar Wood
Maple Wood
Straw (Wheat)
Corn Stover
Bagasse
Peat Moss

average particle size: 400 to 800 μm
particle density: 300 to 600 kg/m^3
char density: 100 kg/m^3
bed material: Ottawa Silica Sand
sand particle size: 710 μm
sand particle density: 2,470 kg/m^3
minimum fluidizing velocity: 0.299 m/s (air @ 22°C)
fluidizing medium: recycled gases products (CH_4, CO, CO_2, H_2, ...)
pyrolysis temperature: 400°C to 650°C
pyrolysis pressure: 1 atm
gas residence time (reactor): 0.45 to 0.60 s

TABLE 2

Experimental Conditions for All the Runs Performed

Exp. #	τ_G (s)	d_p (μm)	ρ_p (kg/m^3)
1	0.45	154	82
2	0.45	450	82
3	0.45	850	82
4	0.50	450	82
5	0.50	715	82
6	0.50	850	82
7	0.50	920	82
8	0.55	450	82
9	0.55	715	82
10	0.55	850	82
11	0.61	450	82
12	0.61	505	82
13	0.61	850	82
14	0.45	154	547
15	0.50	154	547
16	0.55	154	547
17	0.61	154	547
18	0.50	505	450
19	0.50	715	450
20	0.50	920	450

TABLE 3

Moments Analysis

Exp. #	$\bar{\tau}_G$ (s)	d_p (μm)	ρ_p (kg/m^3)	$\mu - \bar{\tau}$ (s)	σ^2 (s^2)	σ_θ^2 (-)
1	0.45	154	82	2.02	1.9	0.46
2	0.45	450	82	3.51	5.1	0.41
3	0.45	850	82	4.18	14.3	0.82
4	0.50	450	82	4.35	7.2	0.38
5	0.50	715	82	5.16	11.4	0.43
6	0.50	850	82	6.34	15.2	0.38
7	0.50	920	82	7.91	19.3	0.31
8	0.55	450	82	4.80	6.5	0.28
9	0.55	715	82	6.33	14.2	0.35
10	0.55	850	82	7.89	15.6	0.25
11	0.61	450	82	6.49	16.1	0.38
12	0.61	505	82	7.45	18.0	0.32
13	0.61	850	82	8.22	20.5	0.30
14	0.45	154	547	4.07	12.8	0.77
15	0.50	154	547	4.88	8.2	0.37
16	0.55	154	547	5.28	15.4	0.55
17	0.61	154	547	7.11	13.7	0.27
18	0.50	505	450		—	—
19	0.50	715	450		—	—
20	0.50	920	450		—	—

TABLE 4

Vessel Dispersion Numbers and N for All the Runs Performed

Exp. #	$\bar{\tau}_G$ (s)	d_p (μm)	ρ_p (kg/m^3)	($D_{SA}/U \cdot L$) (—)	N (—)
1	0.45	154	82	0.345	2
2	0.45	450	82	0.287	2
3	0.45	850	82	1.570	1
4	0.50	450	82	0.253	2
5	0.50	715	82	0.302	2
6	0.50	850	82	0.251	2
7	0.50	920	82	0.190	3
8	0.55	450	82	0.170	3
9	0.55	715	82	0.229	3
10	0.55	850	82	0.147	4
11	0.61	450	82	0.255	3
12	0.61	505	82	0.203	3
13	0.61	850	82	0.186	3
14	0.45	154	547	1.210	1
15	0.50	154	547	0.247	3
16	0.55	154	547	0.472	2
17	0.61	154	547	0.162	4
18	0.50	505	450	—	-
19	0.50	715	450	—	-
20	0.50	920	450	—	-

TABLE 5

Van de Vusse Model Parameters

Exp. #	τ_G (s)	d_p (μm)	ρ_p (kg/m^3)	τ_C (s)	n (—)
1	0.45	154	82	0.8	7
2	0.45	450	82	1.5	14
3	0.45	850	82	1.9	18
4	0.50	450	82	1.8	10
5	0.50	715	82	2.4	13
6	0.50	850	82	2.8	13
7	0.50	920	82	3.4	15
8	0.55	450	82	2.3	8
9	0.55	715	82	3.2	10
10	0.55	850	82	4.0	12
11	0.61	450	82	2.5	7
12	0.61	505	82	3.2	6
13	0.61	850	82	4.5	10
14	0.45	154	547	1.8	12
15	0.50	154	547	2.3	9
16	0.55	154	547	2.7	8
17	0.61	154	547	3.1	7
18	0.50	505	450	—	—
19	0.50	715	450	—	—
20	0.50	920	450	—	—

TABLE 6

Physical Characteristics of Tracers used for Mixing - Segregation - Entrainment Experiments

Bed material:	Ottawa Silica Sand
Average particle size:	400 um
Particle density:	2,470 kg/m^3
Minimum fluidizing velocity:	0.18 m/s (air @ 20°C)

TRACERS:

- Styrofoam beads	d_p = 450 to 850 μm
	ρ_p = 82 kg/m^3
- Cork particles	d_p = 200 to 1100 μm
	ρ_p = 240 kg/m^3
- PVC particles	d_p = 154 μm
	ρ_p = 547 kg/m^3
- IEA Poplar Wood	d_p = 230 to 1140 μm
	ρ_p = 450 kg/m^3

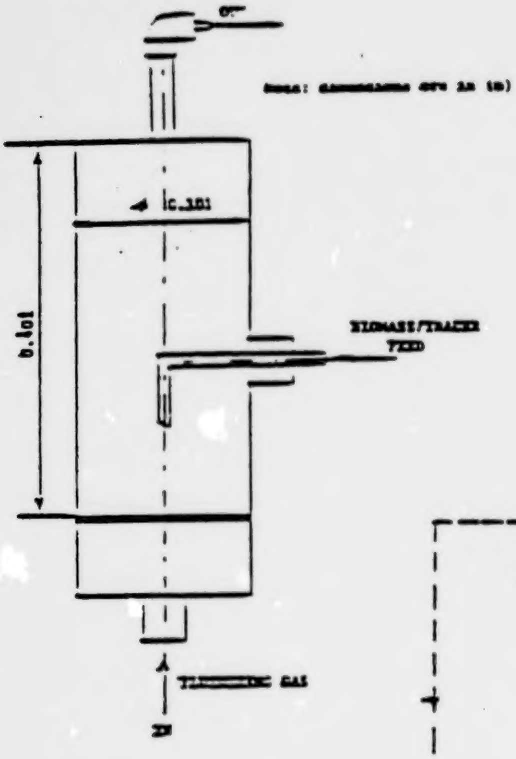
0.101
0.401
BIOMASS/TRACER FEED
GAS
IN

FIGURE 1 - Pilot Plant Fluidized Bed Reactor used for Tracer Experiments

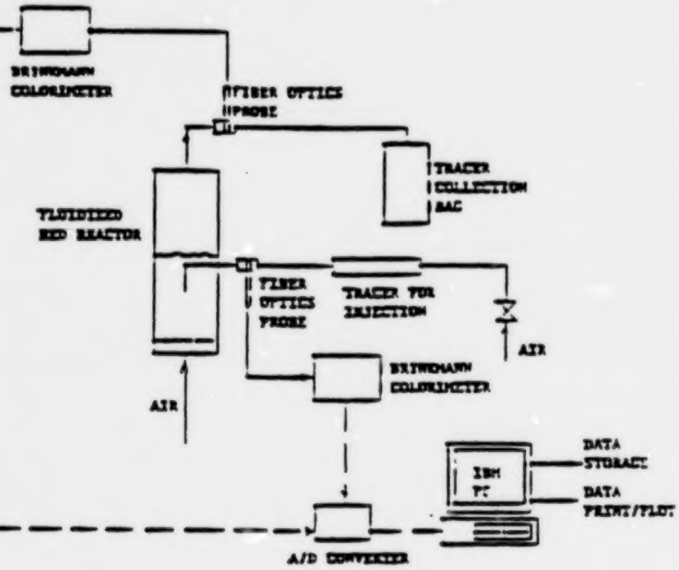
BRINKMANN COLORIMETER
FIBER OPTICS PROBE
TRACER COLLECTION BAG
FLUIDIZED BED REACTOR
FIBER OPTICS PROBE
TRACER FOR INJECTION
AIR
BRINKMANN COLORIMETER
AIR
IBM PC
DATA STORAGE
DATA PRINT/PLOT
A/D CONVERTER

FIGURE 2 - Experimental Set-up for Tracer Experiments

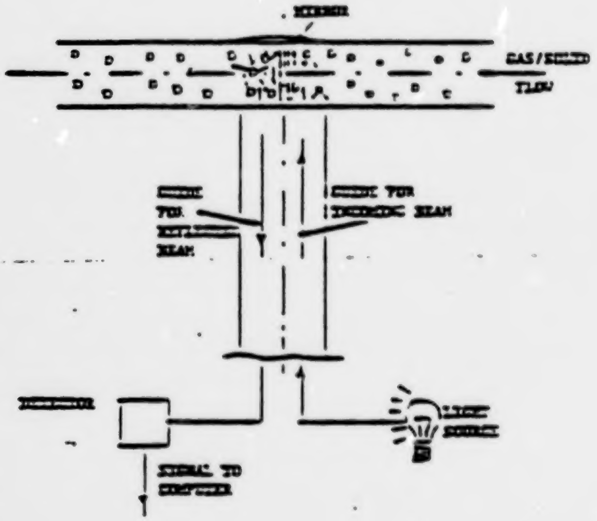
MIRROR
GAS/SOLID FLOW
GUIDE FOR INCOMING BEAM
LIGHT SOURCE
SIGNAL TO COMPUTER

FIGURE 3 - Brinkmann Probe (Schematic)

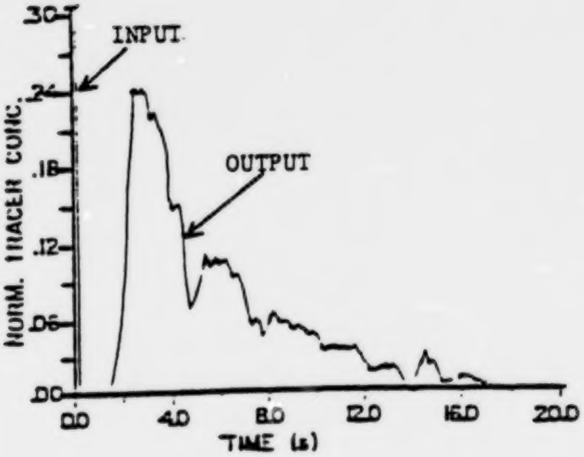

FIGURE 4 - Typical tracer input and output signals (Exp. #7)

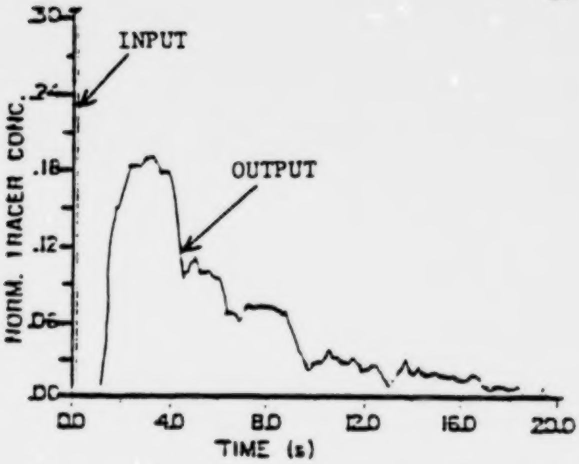

FIGURE 5 - Typical tracer input and output signals (Exp. #9)

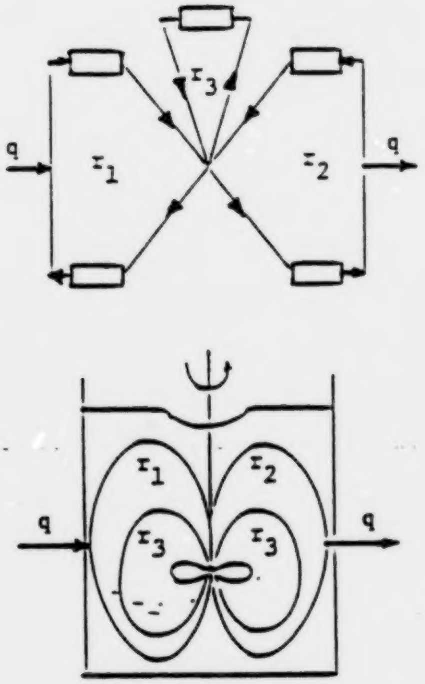
r_3
q
r_1
r_2
q
r_1
r_2
q
r_3
r_3
q

FIGURE 6 - Van de Vusse (1962) Model and Physical Diagram

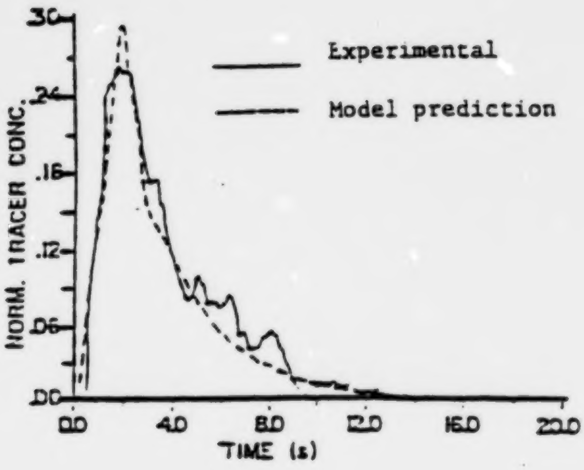

FIGURE 7 - Van de Vusse's Model Prediction and Experimental Response for Exp. # 4

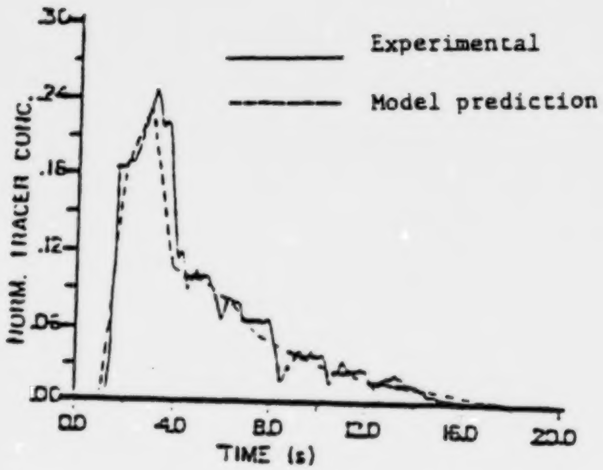

FIGURE 8 - Van de Vusse's Model Prediction and Experimental Response for Exp. # 6

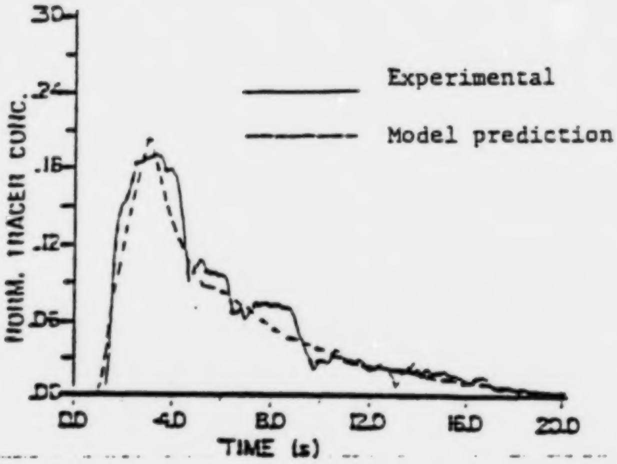

FIGURE 9 - Van de Vusse's Model Prediction and Experimental Response for Exp. # 9

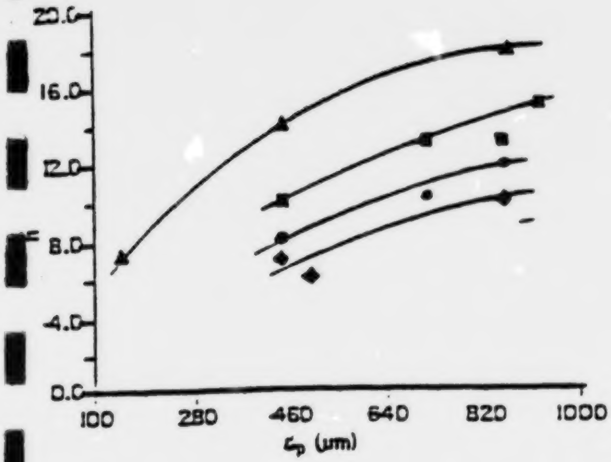

FIGURE 10 - Effect of the particle size on the number of circulations (n) for different gas residence times:

▲ τ_G = 0.45 s
■ τ_G = 0.50 s
● τ_G = 0.55 s
◆ τ_G = 0.61 s

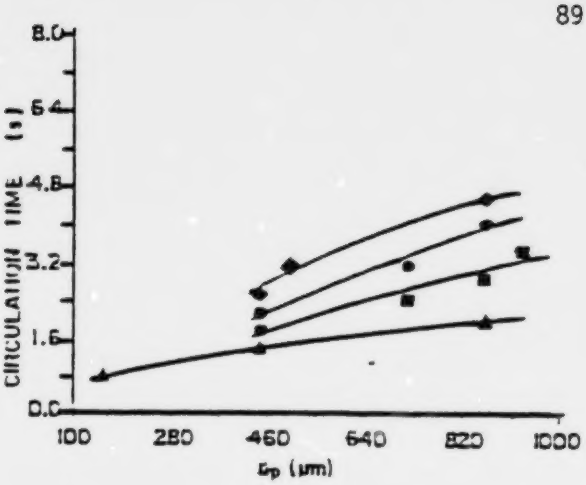

FIGURE 11 - Effect of the particle size on the circulation time (τ_C) for different gas residence times. Symbols are the same as in Figure 10.

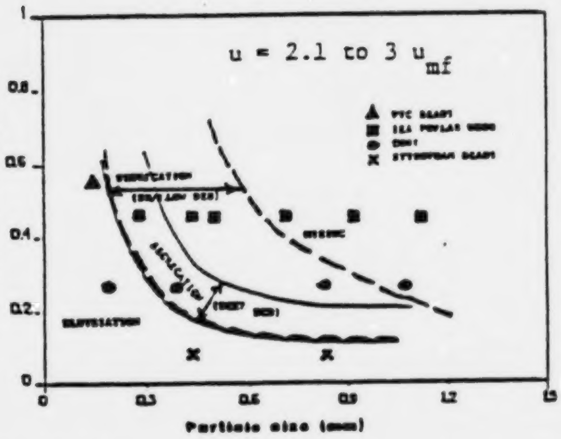

FIGURE 12 - Mixing-Segregation-Entrainment Experimental Results
(Shallow bed: h/D = 0.5) ———
(Deep bed: h/D = 1.2) ______

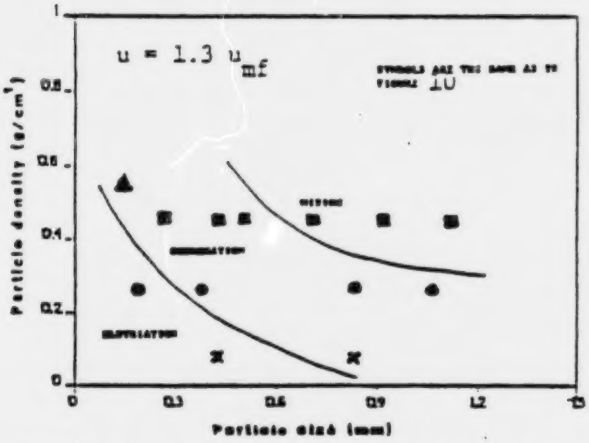

FIGURE 13 - Mixing-Segregation-Entrainment Experimental Results

5. ADDITIONAL ASPECTS OF THE WATERLOO FAST PYROLYSIS PROCESS

5.1 Effect of Moisture Content of the Feed

The effect of moisture content in the feed on the yields of the various products was determined from a number of runs carried out on air-dried eastern maple, and one run using green maple wood. The wood samples were from a mature maple tree (91 years old estimated) cut in Waterloo county in 1983. The material was taken from a cross section of the main trunk 36 cm in diameter, and was either air dried after grinding or stored in plastic bags in a cold room until used as green feed.

No operating problems were encountered with the high moisture content feed, although there exists a maximum moisture content which a screw feeder can successfully handle. For this reason, a feed rate slightly lower than normal was used with the greenest wood.

Results of a number of pilot plant runs with maple done over a three year period over a temperature range of 508°-535°C are shown in Table 5-1. Moisture content variation from 3.8% to 25.2% showed no significant trend in results which could be ascribed to the moisture content. The major effect of higher moisture content in the feed was to dilute the product oil. At the highest moisture content (25.2%), this additional water was sufficient to cause phase separation.

At the temperature and residence times employed, and in the absence of catalysts, water would not be expected to react to any extent with any of the pyrolysis products, and the results of Table 5-1 support this conclusion. Therefore, the water is an inert material as far as the pyrolysis process is concerned. However, because of the high heat requirement to vaporize excess water in the feed, the presence of a high moisture content would reduce the maximum feed rate possible, and probably also require a somewhat smaller maximum particle size. It is clear, therefore, that a reasonably dry feed (5 to 10% moisture) is desirable for the WFPP.

5.2 Pyrolysis of Softwood, Comparison of Liquid Product from Different Feeds

Three runs were carried out using a clean eastern spruce feed material obtained from sawmill sawdust and mill scrap. For the sake of completeness, the results obtained with softwood are compared with three other feeds; maple, poplar wood and whole-tree poplar.

In previously reported tests, yields have been classified as gases, organic liquids, char and product water. Mass balances were generally close to 95% or better. Elemental analyses were also reported for many runs, but identification of individual compounds was done only for non-condensable gases and for some volatile organics such as methanol, acetaldehyde, furan, etc. However, more detailed analyses of liquid products have recently been carried out, and some of these preliminary results which are of particular significance are reported here.

All experimental results given were obtained at conditions of close to optimal feed rate, particle size and

Table 5.1.1

Pilot Plant Pyrolysis Yields from Eastern Red Maple
Ash 0.40% mf; C 48.5 , H 6.1 mf ,

	1983	1983	1985	1985	1986
Particle Size μm	-590	-590	-1000	-590	-1000
Moisture w/w%	3.8	3.8	25.2	5.9	9.5
Run #	14	9	61	63	81
Temp °C	532	531	535	508	515
App.Res.Time, sec	0.69	0.73	0.46	0.47	0.44
Feed Rate, kg/hr	2.16	2.12	1.10	1.98	1.32
Yield, w/w%, mf					
Organic Liquid	67.25	69.54	65.88	67.89	65.01
Water	7.4	7.8	12.65	9.80	9.96
Char	9.02	9.37	8.98	13.75	12.11
H_2	0.045	0.037	0.02	0.01	0.02
CO	6.96	5.78	5.41	4.12	4.83
CO_2	4.02	3.67	3.80	4.89	5.36
CH_4	0.75	0.61	0.58	0.36	0.57
C_2H_4	0.24	0.21	0.24	0.16	0.21
C_2H_6	0.038	0.036	0.08	0.04	0.07
C_3			0.09	0.07	0.10
C_4+			0.14	0.14	0.41
Total Gas	12.05	10.35	10.36	9.80	11.57
Overall Recovery	95.72	97.06	97.9	100.77	98.66

residence time for maximum liquid yield at the stated temperatures, as determined by over 200 bench scale runs and 90 pilot scale runs.

Table 5.2.1 shows the experimental yields of products from selected runs for four different woods whose properties are given in Table 5.2.2.

High organic liquid yields are characteristic of all four materials when undergoing fast pyrolysis in our process. The total liquid yield, including water of reaction, varies from 70% to 80% of the dry biomass fed, all of which can be directly used as a substitute fuel oil if desired. The liquids are single-phase, homogeneous fluids, which pour readily, and which contain from 15% to 25% water depending on the feed material and its moisture content.

These liquids are quite stable at room temperature. The water content, in a period of twelve months, was found to increase slightly presumably due to the slow processes of condensation-polymerization going on even at room temperature. At higher temperatures, 120°C and above, the oils become increasingly unstable and decompose with evolution of gas, and finally charification of a polymeric residue. All the pyrolysis vapors produce an oil mist following rapid quenching, but their polar character allows the easy utilization of electrostatic precipitation in the recovery system of a pyrolysis process.

Preliminary small scale combustion tests carried out with the pyrolysis oil as produced (20% water content) showed that it burns readily in a furnace with a

Table 5.2.1

Pyrolysis Yields from Different Woods

	Brockville Poplar			White Spruce			Red Maple			IEA Poplar		
Run #	51	58	50	42	43	45	14	63	81	27	59	A-2*
Temperature, °C	497	504	555	485	500	520	532	508	515	500	504	497
Moisture content, wt%	*	5.2	*	*	7.0	*	3.8	5.9	9.5	6.2	4.6	3.3
Particle Top Size, μm	*	1000	*	*	1000	*	590	590	1000	590	1000	590
Apparent Residence Time, sec	0.64	0.47	0.57	0.70	0.65	0.62	0.69	0.47	0.44	0.55	0.48	0.46
Feed Rate, kg/hr	2.24	2.10	4.12	2.07	1.91	1.58	2.16	1.98	1.32	2.24	1.85	0.05
Yields, wt% of m.f. wood												
Organic liquid	62.9	62.9	59.0	63.1	66.5	66.1	67.3	67.9	65.0	65.8	66.2	65.7
Water	10.3	9.7	10.2	10.7	11.6	11.1	7.4	9.8	10.0	9.3	10.7	12.2
Char	14.4	16.5	10.6	16.3	12.2	12.3	9.0	13.7	12.1	12.1	11.8	7.7
Gas:												
H_2	0.02	0.02	0.07	0.04	0.02	0.01	0.04	0.01	0.02	0.02	0.01	--
CO	4.95	4.71	8.40	4.16	3.82	4.01	6.96	4.12	4.83	5.32	4.44	5.34
CO_2	6.14	5.89	7.06	3.38	3.37	2.69	4.02	4.89	5.36	6.30	5.75	4.78
CH_4	0.45	0.44	0.97	0.34	0.38	0.43	0.75	0.36	0.57	0.48	0.37	0.41
C_2H_4	0.22	0.19	0.40	0.16	0.17	0.16	0.24	0.16	0.21	0.20	0.13	0.19
C_2H_6	0.06	0.05	0.11	0.02	0.03	0.05		0.04	0.07	0.04	0.05	--
C_3	0.06	0.07	0.10					0.07	0.10		0.08	0.09
C_4	0.13	0.16	0.28	0.03	0.04	0.06	0.04	0.14	0.41	0.09	0.19	3.10
Total Gas	12.0	11.5	17.4	8.1	7.8	7.4	12.1	9.8	11.6	12.4	11.0	10.8
Overall recovery wt%, m.f.	99.7	100.5	97.2	97.8	97.7	96.7	95.7	101.2	98.7	99.7	99.8	96.4

* Bench Scale Unit

Table 5.2.2

Properties of Feed Materials

	Whole Tree Poplar	White Spruce	Red Maple	IEA Poplar Wood
Source	Brockville Plantation, Whole Tree Except Leaves and Roots Ontario MNR Clone C-147	Eastern Canada Clean Wood Sawmill Sawdust and Mill Scrap		Clean Wood only Ontario MNR Clone D-38
Moisture, wt%	5.2	7.0	3.8 - 25.2	4.6
Ash, % mf	1.19	0.50	0.40	0.46
Elemental Analysis, %				
C	49.06	49.63	48.5	49.45
H	6.23	6.36	6.1	6.05
O	43.6	43.1	--	44.4
N	1.08	0.2	--	0.07

Table 5.2.3

Properties of Pyrolitic Liquids

	Brockville Poplar			White Spruce			Red Maple	IEA Poplar
Run #	51	58	50	42	43	45	63	59
Yields, wt% of wood as fed	74.1	73.3	70.5	75.2	79.2	78.5	77.9	77.6
Water content, wt%	19.8	18.7	21.7	21.9	22.4	21.8	18.0	18.6
pH	2.6	2.4	2.8	2.1	2.1	2.3	2.4	2.4
Density, g/cc	1.19	1.20	1.18	1.22	1.22	1.22	1.19	1.23
Elemental analysis, wt%, m.f.								
Carbon	54.1	54.7	55.6	53.5	54.0	56.6	54.7	53.6
Hydrogen	7.1	6.9	6.9	6.6	6.8	6.9	6.4	7.0

Table 5.2.4

Analysis of Liquid Products

	Brockville Poplar	White Spruce	Red Maple	IEA Poplar
Run #			63	A-2
Temperature	504	500	508	504
Yields, wt% of feed, m.f.				
organic liquid	62.9	61.5	67.9	69.8
1. oligosaccharides				0.70
2. cellobiosan	1.11	2.49	1.62	1.30
3. glucose	0.55	0.99	0.64	0.41
4. fructose	1.34	2.27	1.51	1.32
5. glyoxal	1.42	2.47	1.75	2.18
6. methylglyoxal	}	}		0.66
7. levoglucosan	2.52	3.96	2.84	3.04
8. 1,6 anhydroglucofuranose	—	—	—	2.43
9. hydroxyacetaldehyde	6.47	7.67	7.55	10.03
10. formic acid	5.40	7.15	6.35	3.09
11. formaldehyde	—	—	—	1.16
12. acetic acid	6.30	3.86	5.81	5.43
13. ethylene glycol	0.87	0.89	0.63	1.05
14. acetol	1.70	1.24	1.15	1.40
15. acetaldehyde	—	—	—	0.02
16. methanol				
Water-solubles-total above	27.7	33.0	29.9	34.2
Pyrolytic lignin	24.8	20.6	20.9	16.2
Amount not accounted for (losses, water soluble phenols, furans etc.)	10.5	7.9	17.1	18.3

conventional pressure atomizing burner, providing the combustion box is preheated. If an air atomizing nozzle is used with a pilot flame, no preheating of the combustion chamber is necessary. Larger scale tests for extended periods have not yet been done, but preliminary work shows that the pyrolysis oil has potential as a substitute fuel oil.

Some properties of "wet" liquids as produced are given in Table 5.2.3. The elemental analyses of the pyrolytic liquids as given in Table 5.2.3 are very similar to those of the starting materials - wood. One could probably fairly accurately describe these liquids, therefore, by the term "liquid wood". Two major characteristics of these liquids are high oxygen content and high density (much higher than wood). Another specific property is a limited water solubility. In the case of pyrolytic sirups produced by the Waterloo process, water is dissolved in the organic phase. The addition of more water to the level of about 60% by weight causes a phase separation and this behaviour has been utilized in our work for analytical purposes, in that both fractions were analyzed separately after dilution of the original oil product.

The details of the HPLC technique developed for analysis of the water soluble fraction are given below:

Column : Aminex HPX-87H, high performance cation exchange resin in hydrogen form 300 x 7.8 mm from Biorad

Eluant : H_3PO_4 0.007 N

Flow Rate : 0.80 ml/min., isocatic

Temperature : 65°C

Detector : Waters R 401 Differential Refractometer

Internal Standard : n-propanol

The quantitative data obtained by the HPLC technique are presented in Table 5.2.4.

To obtain relative response factors and retention times, the pure compounds were fed and then eluted, although some of them, such as cellobiosan and 1,6 anhydro-β-D-glucofuranose, had to be synthesized in-house. Confirmation of compound identification was obtained by GC-MS (Hewlett-Packard 5970 Mass Selective Detector coupled to 5890A Gas Chromatograph). For GC-MS analysis, sugars and anhydrosugars were first trimethylsilylated to the corresponding ethers. Small amounts of simple phenols and of furanoid compounds were also detected by GC-MS in the water soluble fraction. These components were not quantified by HPLC.

Comparison of the yields given in Table 5.2.1, Table 5.2.3 and Table 5.2.4 shows some differences between the products obtained from softwoods and those from hardwoods. Yields of major product categories such as tar, char and gas are essentially the same, although the spruce appeared to produce a little less gas, particularly CO_2, and a little more water. Liquid product overall properties were nearly the same for softwoods and hardwoods, although the liquor from softwood was slightly more acidic (pH of 2.1 vs. 2.4 for poplar).

The detailed list of liquid components shown in Table 5.2.4 shows other minor differences. Acetic acid yield from spruce is notably lower, with an increase in formic acid. Other differences in composition are probably not meaningful.

The yields of the water insoluble fraction are given also in Table 5.2.4. This fraction separated as a dark brown viscous liquid which solidified during drying into a hard, black, easily powdered material. From the NMR spectra (see Chapter 6) it is evident that this material is aromatic in character, and is clearly derived from the lignin fraction of the wood.

In summary, four different woods under conditions of fast pyrolysis yielded very similar liquid products. Analyses show that this product is a complex mixture of chemicals.

The pyrolytic "wet" tar-sirup can be readily separated into two principal fractions by water extraction. The water-insoluble fraction is derived from lignin while the water-soluble fraction is carbohydrate in origin. Analytical results indicate large amounts of low molecular weight (<100) lactones and aldehydes, and a significant fraction of these are multifunctional in nature. Four major classes of chemicals can be differentiated,

1. sugars and anhydrosugars
2. carbonyl and hydroxycarbonyl compounds
3. acids - formic, acetic
4. "pyrolytic" lignin.

Results in Table 5.2.4 show that 81% to 92% of the content of the pyrolysis oils produced in this work from wood has been quantitatively identified.

Detailed analysis of pyrolytic oils is needed in order to allow possible mechanistic or kinetic models to be formulated which can explain the various observed aspects of fast biomass thermal degradation. A knowledge of chemical composition of these oils may also assist in the eventual future utilization, upgrading or separation of these compounds as higher value products.

5.3 Genotoxicity Testing of Pyrolysis Oils

A subcontract was placed in January, 1985 with the Carcinogen Testing Laboratory of the British Columbia Cancer Foundation to carry out mutagenicity assays (salmonella - Ames tests) as well as some preliminary chromasone aberration assays. Two samples of whole pyrolysis oil were supplied as produced, one from Run 43 with a spruce wood feedstock and one from Run 51 with a poplar wood feedstock.

The report of the study is attached as Appendix 5.3-A. We are not competent to comment on the conclusions. It is of interest, however, that only in high dilutions did the pyrolysis oil show any biological activity, since at higher concentrations it is toxic to the organisms used. In one salmonella strain no mutagenic activity resulted at any dosage level for either sample, but another strain showed some response in a narrow dosage range. Both oil samples also showed some chromosome damaging activity in the chromosome aberration assay, but again only over a very limited and very dilute dosage range. Apparently, in all tests, the effects were only marginally above the statistically significant threshold.

Our conclusion would be that the oil as produced in concentrated form is not biologically hazardous. However, some precautions might be advisable for those habitually handling dilute solutions, although at present it is not known what the relative hazards of external vs. internal exposure may be.

5.4 Alternative Product Recovery Methods for the WFPP

In the present pilot plant unit, liquid product is condensed in two surface condensers in series, each having vertical tubes equipped with clean-out plugs at the top and individual bottom drains. For biomass, the first condenser is usually kept about 20°C, and the second condenser at 0°C-4°C. A heavy tar fog usually forms in the first condenser which can represent from 10% to 50% of the liquid product (normally about 20%). The second cold condenser recovers a largely aqueous product, and residual mist is removed in filters. The two liquid products are combined to give the final oil product.

In the course of our pilot plant studies a number of alternative schemes were conceptualized for product recovery. It would be highly desirable for such a scheme to also allow for heat recovery. Normally, hot oil quenching and scrubbing would be a first choice, as is done in coal pyrolysis systems, using product oil as a scrubbing fluid. However, in the case of biomass liquids, the thermal sensitivity is such that the maximum usable temperature would be 100° to 120°C, and even this level would not be advisable for any extended time period. Cold liquid scrubbing would be satisfactory but would not allow for heat recovery at any reasonable level of quality.

One potentially feasible scheme is to use a surface condenser to form a tar fog at a fairly high temperature and then to immediately collect this fog in an electrostatic precipitator. The clean product gas would then be cooled to about 0°C to give a largely aqueous product which would be used (with or without additional solvent and/or water) to backwash the condenser and precipitator to remove any heavy deposits. Because of the highly polar nature of the tar fog it is very readily collected at high efficiency by electrostatic precipitation. Only low voltages are needed and no ionizing corona discharge. A small cylindrical type has been designed and is now in regular use in the bench scale unit as the principal collector for liquid product. A larger plate type unit was also constructed based on a commercial unit. Additional cooling coils were added in an inlet section to promote fog formation. It was found that the normal commercial plate spacing is too small for the concentrated highly conductive fog formed, and arcing occurred readily. With a wider plate spacing, satisfactory operation was achieved. However, the problem of washing the plates after a run to obtain 100% product recovery for material balances was such that this unit was not practical for obtaining good yield data. Hence, no systematic testing was done.

It is probable that multiple cylindrical electrostatic precipitators would be preferable for a larger unit. Tar fog removal is close to 100%, so that cleanup filtration can be easily installed with a good life time. Further, the cylindrical configuration gives simpler washing than does the plate type, and can be more readily combined with a heat exchange function.

One possible configuration for a large scale unit would then be for the hot product gases to first contact a cooling coil with or without added cold quench gas or water spray. This step would allow some recovery of heat, possibly for wood drying. A tar fog would form at this point, and the product gas stream containing the fog would go to cylindrical electrostatic precipitators which would be water cooled. The precipitators would be followed by a cold condenser to recover water and light organics. Finally, a dry filtration unit would precede the recirculating compressor. The hot condenser and precipitator bank would consist of two units in parallel, so that one could be flushed with aqueous product from the cold condenser while the second was on-stream.

Some extended runs in the pilot plant or a small demo plant would be necessary to test these concepts.

APPENDIX 5 -A

Genotoxicity Testing of Pyrolysis Oils

FINAL REPORT

Study Title:	Genotoxicity Testing of Extract No. 43 (Pyrolysis Oil from Softwood) and Extract No. 51 (Pyrolysis Oil from Hardwood)	
Experiment No.:	Salmonella Mutagenicity Assay (VS-52, VS-53) Chromosome Aberration Assay Using Chinese Hamster Ovary Cells in Culture (VX-87, VX-89)	
Test Articles:	1. Extract No. 43 (Pyrolysis Oil from Softwood: Spruce 2. Extract No. 51 (Pyrolysis Oil from Hardwood: Poplar	
Report Prepared For:	Dr D.S. Scott Department of Chemical Engineering Faculty of Engineering University of Waterloo Waterloo, Ontario N2L 3G1	
Study Performed and Report Prepared By:	Carcinogen Testing Laboratory British Columbia Cancer Foundation 601 West 10th Avenue Vancouver, B.C. V5Z 1L3	
Study Started:	23 January 1985	
Study Completed:	18 April 1985	
Study Director:	R.H.C. San, Ph.D	
Study Personnel:	V.M. Anthony, B.Sc.	V.M. Anthony

TABLE OF CONTENTS

Page

List of Tables i

1. Objective 1

2. Materials and Methods 1

2.1 Test Articles 1

2.2 Salmonella Mutagenicity Test 1

  2.2.1 Metabolic activation 2

  2.2.2 Test procedure 2

  2.2.3 Data interpretation 3

2.3 Chromosome Aberration Assay 3

  2.3.1 Cell line 3

  2.3.2 Test procedure 4

  2.3.3 Preparation of metabolic activation system (S9) 4

  2.3.4 Analysis and interpretation 5

3. Results and Discussion 5

4. Conclusion 7

References 8

Tabulation of Test Results

LIST OF TABLES

Table

1 Salmonella Mutagenicity Assay Results on Extract No. 43 (Pyrolysis Oil from Softwood)

2 Salmonella Mutagenicity Assay Results on Extract No. 51 (Pyrolysis Oil from Hardwood)

3 Summary of Chromosome Aberration Assay Results on Extract No. 43 (Pyrolysis Oil from Softwood)

4 Chromosome Aberration Assay Results on Extract No. 43 (Preliminary Run)

5 Chromosome Aberration Assay Results on Extract No. 43 (Confirmatory Run)

6 Summary of Chromosome Aberration Assay Results on Extract No. 51 (Pyrolysis Oil from Hardwood)

7 Chromosome Aberration Assay Results on Extract No. 51 (Preliminary Run)

8 Chromosome Aberration Assay Results on Extract No. 51 (Confirmatory Run)

1. OBJECTIVE

The objective of this study is to employ the Salmonella mutagenicity assay and the chromosome aberration assay (using Chinese hamster ovary cells in culture) as short-term tests to assess the potential of extract no. 43 (pyrolysis oil from softwood) and extract no. 51 (pyrolysis oil from hardwood) to cause genetic damage.

2. MATERIALS AND METHODS

2.1 Test Articles

The two pyrolysis oils from wood used in this study were prepared by the Department of Chemical Engineering, Faculty of Engineering, University of Waterloo, Waterloo, Ontario:

Extract from run no. 43, feed stock temperature 500°C, from spruce (softwood)

Extract from run no. 51, feed stock temperature 497°C, from Brockville poplar (hardwood)

Both extracts were stored at ambient temperature until time of assay.

Extract no. 43 was very viscous at room temperature and had to be warmed to 30°C for approximately 10 minutes prior to transferring with a pipette for dilutions.

Both extracts were quite acidic (pH 2.5-3.0). However, no attempt was made to adjust the pH to 7.0 lest that procedure should lead to changes in the chemical components.

2.2 Salmonella Mutagenicity Test

In this assay, the induction of reverse mutations of histidine-requiring bacteria to histidine independence is used as an indicator of genetic damage. This in turn indicates the presence of mutagenic activity in the material being tested. The bacteria are exposed to the test substance and plated on minimal agar which does not support the growth of histidine-requiring mutants. Reverse mutation to histidine independence is evidenced by the appearance of bacterial colonies on minimal agar after 48-72 hours.

Different bacterial strains respond to different types of changes in the genetic material. To ensure the detection of a broad spectrum of chemical mutagens, two strains of Salmonella typhimurium (TA98 and TA100) were used in this study. Strain TA98 is mutable by frameshift mutagens, while TA100 is mutable by base-pair substitution (McCann et al., 1975).

Both tester strains were obtained from the Department of Biochemistry, University of California, Berkeley. Stock cultures were stored at -80°C for short-term use and routinely evaluated for the following microbial characteristics: growth, dependence on histidine, sensitivity to crystal violet and ultraviolet light, resistance to ampicillin, and spontaneous mutation rate.

The following positive controls were used in each assay: sodium azide (NaAz, 5 μg/plate) for TA100, and 2-nitrofluorene (2NF, 5 μg/plate) for TA98.

Retention of microbial characteristics of the tester strains and the consistent response to positive control mutagens constitute the basis for determining the acceptability of the test data.

2.2.1 *Metabolic activation.* While some mutagens are direct-acting, certain chemicals require metabolic activation into mutagenic intermediates.

To ensure the detection of metabolism-requiring mutagens, each sample was also tested in the presence of an exogenous rat liver microsome preparation. Rats were exposed to arochlor 1254 to stimulate enzyme activity. The supernatant from homogenized liver following centrifugation at 9000 x g (hence S9) was used. The standard procedure for the preparation and use of S9 as described by Ames et al. (1975) was followed. Benzo(a)pyrene (10 μg/plate) and 2-anthramine (2.5 μg/plate) were used as positive controls for the S9 preparation.

2.2.2 *Test procedure.* The standard plate incorporation test procedure as described by Ames et al. (1975) was followed (Standard Operating Procedure No. 201). Overnight cultures of the two bacterial strains were prepared from frozen master stocks. Following overnight incubation, the optical density was measured to determine if there was bacterial growth.

An aliquot of the extract was transferred by pipette and dissolved in dimethyl sulfoxide (DMSO) to prepare the working stock. Subsequent dilutions were prepared in DMSO for the lower dose levels.

The incubation mixture consisted of the following components added to each tube in the following order: 0.1 ml of the appropriate working stock of the extract (except for the 1:2 dilution where 0.6 ml working stock was added), 0.1 ml bacteria, 0.3 ml S9 mix or PBS, and 2.0 ml top agar. Each dose level of the extract was tested in triplicate plates.

The different components in the tube were mixed by vortexing and then spread onto a prelabelled minimal agar plate. After swirling and allowing the agar to solidify, the plates were incubated in an inverted position at 37°C for 48-72 hours before scoring. The colonies were counted using an Artek 880 automatic colony counter.

The volume of S9 mix in the incubation mixture was 0.3 ml as compared to 0.5 ml in the procedure described by Ames et al. (1975). However, the S9 mix was prepared so that the final concentrations of S9 and the cofactors expressed on a per plate basis were maintained at the same level as described in the Ames paper: 50 ul S9, 4.0 umoles $MgCl_2$, 16.5 umoles KCl, 2.5 umoles G6P, 2.0 umoles NADP, and 50 umoles phosphate buffer (Standard Operating Procedure No. 105).

2.2.3 Data interpretation. In general, a twofold increase in colony count in a treated culture above that in the untreated control plus a further dose-related increase in colony count is taken as a positive indication of mutagenic activity.

2.3 Chromosome Aberration Assay

Chromosomes are carriers of the genetic material. Damage to chromosomes, e.g., chromatid breaks and chromatid exchanges, can be readily quantified and used as a sensitive indicator of genetic damage. Survey of a broad spectrum of structurally different chemicals indicated a good correlation between the carcinogenicity/mutagenicity of a chemical and its capacity to induce chromosome aberrations (Stich et al., 1974; Weinstein et al., 1977; Hsu and Au, 1979; Ishidate and Yoshikawa, 1980).

The chromosome-damaging effect of a chemical (or mixture) can be measured in growing mammalian cell cultures. The use of the same cell line offers several advantages, including (i) fewer culture to culture variations with respect to cell cycle time and plating efficiency, and (ii) the possibility of freezing and storing cells for repeated assays and future reference. Of the various cell lines available, the Chinese hamster ovary (CHO) cell line is probably the most suitable for routine testing because of its availability, short generation time (12-14 hours) and low chromosome number (20-22 as compared to 46 in humans or 40 in the mouse).

2.3.1 Cell line. The Chinese hamster ovary (CHO) cell line (wild type) used in this study was originally from Dr Lorne Whorton, University of Toronto. The modal number of chromosomes in this cell line is 21.

2.3.2 Test procedure. This cytogenetic assay was conducted in the presence as well as in the absence of metabolic activation system (S9 mix) using standard operating procedures (Standard Operating Procedure No. 305) of the testing laboratory.

CHO cells were seeded onto 22 x 22 mm glass coverslips (Clay Adams) in 35 mm plastic petri dishes (Falcon) at 5×10^4 cells per dish, and fed 2.0 ml Eagle's minimal essential medium (MEM) supplemented with 7.5% fetal bovine serum (FBS) and antibiotics (penicillin G, 200 U/ml; streptomycin, 40 ug/ml; kanamycin, 100 ug/ml; fungizone, 2.5 ug/ml). The cultures were maintained at 37°C in an incubator fed with 5% carbon dioxide and 95% air. In order to obtain well-spread cells for analysis, the cultures were used when they reached 50-70% confluency. At an initial seeding density of 5×10^4 cells per dish, this occurred at approximately 40-48 hours post-seeding.

Working stock solutions were prepared by dissolving an aliquot of the extracts in dimethyl sulfoxide. Working stocks at lower dose levels were prepared by dilution in DMSO. Dosing solutions of the extract for addition to the cell cultures were prepared by diluting the DMSO working stocks 100-fold with serum-free MEM, such that the final solvent (DMSO) concentration was maintained at 1%. One ml of the dosing solutions was added to each cell culture. Each dose level was tested in triplicate cultures. Following exposure at 37°C for 3 hours, the cell cultures were washed three times with 1 ml serum-free MEM, refed 2 ml MEM supplemented with 7.5% FBS, and incubated overnight at 37°C. At 16 hours post-treatment, the cells were arrested at metaphase by the addition of 0.2 ml colchicine (BDH Chemicals) stock solution at 100 ug/ml to 2.0 ml culture medium to give a final concentration of 10 ug/ml for 3-4 hours. For cytological preparations, the coverslip cultures were pretreated for 20 minutes in 1% sodium citrate solution, fixed in methanol/acetic acid (3:1) for 10 minutes, air-dried, stained in 2% aceto-orcein, dehydrated through immersion in methanol, butanol, butanol/xylene (1:1), two changes of xylene, and mounted with Permount.

The mutagen, N-methyl-N'-nitro-N-nitrosoguanidine (MNNG), was used as a reference substance in the assay.

2.3.3 Preparation of metabolic activation system (S9). The standard procedure for the preparation of S9 as described by Ames et al. (1975) was followed.

When the test was conducted in the presence of metabolic activation, dilutions of the test article were prepared in S9 mix. The final concentrations of S9 and the cofactors per ml of the incubation mixture were: 50 µl S9, 1.1 µmoles $MgCl_2$, 7.3 µmoles KCl, 1.11 µmoles G6P, 0.89 µmoles NADP, and 0.98 µmoles HEPES buffer (Standard Operating Procedure No. 104). The mycotoxin, aflatoxin B_1 (AFB_1), was included in the assay as a positive control for the S9 mix.

2.3.4 Analysis and interpretation. For each dose level tested, a minimum of 100 well-spread metaphase plates (when available) were analyzed in each of three replicate cultures. The dose levels selected for scoring ranged from the highest tested scorable dose level to one which produced baseline values. The preparations were coded before being scored to prevent bias during scoring. Chromosome damage was scored and classified according to the system of Savage (1975). The number of metaphases with chromosome aberrations was expressed as a percentage of the total number analyzed. A frequency of 0-2% of metaphases with chromosome aberrations (including gaps) was considered to be within the limits observable in untreated control cultures.

3. RESULTS AND DISCUSSION

The Salmonella mutagenicity assay results on the two extracts are presented in Tables 1 and 2. Both extracts were tested over a dose range of 1:10 to 1:5000 dilution in the preliminary run. Extract no. 43 (pyrolysis oil from softwood) was toxic to TA98 at all except the lowest dose level tested, as evidenced by the absence of any revertant colonies or a colony count less than that in the solvent control (Table 1). Extract no. 43 also elicited toxicity in TA100 at dose levels higher than 1:2500 dilution. An increase in colony count above baseline (solvent) values was noted at the 1:2500 dilution, irrespective of whether the S9 mix was present or not. This is suggestive of some mutagenic activity. However, a minimum of a twofold increase in colony count above background (solvent control) plus a further dose-related increase in colony count are generally considered as the requirement for positive indication of mutagenic activity.

In the confirmatory run, extract no. 43 did not elicit any mutagenic or toxic activity in TA98 over the dose range tested (1:1250 to 1:5000 dilution). In TA100, a twofold plus a further dose-related increase in revertant colony count above baseline levels was observed in the absence as well as in the presence of S9. This is indicative of the presence of both direct-acting and metabolism-requiring mutagenic component(s) in the extract. The negative and positive controls were within the acceptable limits of the historical values.

Extract no. 51 (pyrolysis oil from hardwood) elicited toxicity in TA98 in the absence of S9 over a dose range of 1:10 to 1:2500 dilution (Table 2). The addition of S9 eliminated the toxicity at the lower dose levels (1:1250 and 1:2500 dilution). No mutagenic activity was detected in TA98. The extract was toxic to TA100 (with or without S9) over the dose range of 1:10 to 1:500 dilution. In the absence of S9, a less than twofold increase in revertant colony count was observed at 1:2500 and 1:5000 dilution. The addition of S9 revealed a dose-related increase in colony count over a dose range of 1:1250 to 1:5000 dilution.

In the confirmatory run, extract no. 51 was tested over a dose range of 1:750 to 1:5000 dilution (Table 2). This extract was toxic but not mutagenic to TA98, thus confirming the preliminary findings. In TA100 in the absence of S9, an increase in colony count above baseline levels was observed at 1:5000 dilution. The next higher dilution (1:2500) elicited a greater than twofold increase in colony count. All higher dose levels were toxic. In the presence of S9, a twofold plus a further dose-related increase in colony count was observed, indicating that extract no. 51 was mutagenic to TA100.

The results of the chromosome aberration assay on extract no. 43 (pyrolysis oil from softwood) are summarized in Table 3 and detailed in Tables 4 and 5. In the preliminary run, the extract was toxic to the Chinese hamster ovary cell cultures in the absence of S9 over a dose range of 1:200 to 1:5000 dilution (Table 3). At 1:10,000 dilution, 13.6% of the metaphases showed chromosome aberrations. The aberrations were predominantly chromatid exchanges (translocations), providing definitive indication that extract no. 43 possesses chromosome-damaging activity (Table 4). However, no dose-response profile was observed since the next lower dose level (1:20,000 dilution) already showed baseline values of chromosome aberrations. In the presence of S9, extract no. 43 elicited toxicity at dose levels ranging from 1:200 to 1:2000 dilution. At lower dose levels, no substantial increase in chromosome aberrations above baseline values was observed.

In the confirmatory assay, extract no. 43 was tested over a dose range from 1:2000 to 1:20,000 dilution, including narrow dose levels (Table 3). Toxicity was observed in the absence of S9 at dose levels ranging from 1:2000 to 1:5000 dilution, confirming the preliminary findings. From 1:10,000 to 1:6000 dilution, the extract elicited a dose-related increase in the frequency of metaphases with chromosome aberrations, from baseline level at 1:10,000 dilution to 44.4% at 1:6000 dilution. In the presence of S9, a dose-related increase in chromosome-damaging activity was observed over a very narrow dose range.

The results of the chromosome aberration assay on extract no. 51 (pyrolysis oil from hardwood) are summarized in Table 6 and detailed in Tables 7 and 8. In the absence of S9, this extract was toxic to CHO cells at a dose level of 1:10,000 (or higher). Chromosome-damaging activity was observed at 1:20,000 dilution, where 20.3% of the metaphases showed predominantly chromatid exchanges (translocations). However, the next lower dose level indicated only baseline values of chromosome aberrations (Table 6). In the presence of S9, extract no. 51 was toxic over the dose range from 1:200 to 1:2000 dilution. Chromosome-damaging activity was demonstrable at only one dose level (1:5000 dilution), where 51.2% of the metaphases showed predominantly chromatid exchanges (Table 7).

In the confirmatory run, extract no. 51 was tested over a dose range from 1:5000 to 1:50,000 dilution (Table 6). Toxicity was observed from 1:5000 to 1:12,000 dilution. Lower dose levels elicited a dose-related increase in chromosome-damaging activity. The lower frequency (21.4%) of metaphases with aberrant chromosomes at 1:14,000 dilution compared to that at the next lower dose level (42.3%) is indicative of toxicity. In the presence of S9, chromosome-damaging activity was observed at the highest dose level tested (1:5000 dilution). Lower dose levels elicited only baseline values. The observations confirmed the preliminary findings that this extract was effective over a very limited dose range.

4. CONCLUSION

In this study, two extracts (no. 43, pyrolysis oil from softwood; no. 51, pyrolysis oil from hardwood) were tested for the potential to cause genetic damage. Two short-term assays were used: the Salmonella mutagenicity assay and the chromosome aberration assay (using Chinese hamster ovary cells in culture).

In the Salmonella mutagenicity assay, both extracts were toxic but not mutagenic to strain TA98, irrespective of whether a metabolic activation system (S9) was included in the incubation mixture or not. Both extracts elicited mutagenic activity in strain TA100 in the absence as well as in the presence of metabolic activation.

In the chromosome aberration assay, both extracts elicited chromosome-damaging activity in Chinese hamster ovary cell cultures in the absence as well as in the presence of metabolic activation. However, both extracts were active over a very limited dose range.

The observations in this study indicate that both extracts contain direct-acting as well as metabolism-requiring genotoxic component(s).

REFERENCES

Ames, B.N., McCann, J. and Yamasaki, E. Methods for detecting carcinogens and mutagens with the Salmonella/mammalian-microsome mutagenicity test. Mutation Res. 31: 347-364 (1975).

Hsu, T.C. and Au, W. Effects of chemical mutagens on chromosomes, in: Effects of Drugs on the Cell Nucleus, Academic Press, New York, pp. 315-332 (1979).

Ishidate, M., Jr and Yoshikawa, K. Chromosome aberration tests with Chinese hamster cells in vitro with and without metabolic activation - a comparative study on mutagens and carcinogens. Arch. Toxicol., Suppl. 4: 41-44 (1980).

McCann, J., Spingarn, N.E., Kobori, J. and Ames, B.N. The detection of carcinogens as mutagens: bacterial tester strains with R factor plasmids. Proc. Natl. Acad. Sci. USA 72: 979-983 (1975).

Savage, J.R.K. Classification and relationships of induced chromosomal structural changes. J. Med. Genet. 12: 103-122 (1975).

Stich, H.F., Kieser, D., Laishes, B.A. and San, R.H.C. The use of DNA repair in the identification of carcinogens, precarcinogens, and target tissue, in: Canadian Cancer Conference (Proc. 10th Canadian Cancer Conference), P.G. Scholefield (ed.), University of Toronto Press, Toronto, pp. 83-110 (1974).

Weinstein, D., Katz, M.L. and Kazmer, S. Chromosomal effects of carcinogens and non-carcinogens on WI-38 after short term exposures with and without metabolic activation. Mutation Res. 46: 297-304 (1977).

Table 1
Salmonella Mutagenicity Assay on Extract No. 43 (Pyrolysis Oil from Softwood)

			Number of Histidine-Independent Revertants per Plate[a]										
			Preliminary Run (VS-52)							Confirmatory Run (VS-53)			
Tester Strain			TA98		TA100					TA98		TA100	
Metabolic Activation[b]			-S9	+S9	-S9	+S9				-S9	+S9	-S9	+S9
Final Dilution of Extract	Final Concentration of Extract[f] mg/ml[g]	mg/plate					Final Dilution of Extract	Final Concentration of Extract mg/ml	mg/plate				
1:10	113.0[h]	339.0	T[c]	T	T	T	1:1250	1.03	2.57	60	64	280	274
1:50	22.6	56.5	T	T	T	T	1:1500	0.86	2.14	59	55	287	230
1:250	4.52	11.3	T	T	T	T	1:1750	0.73	1.83	50	40	264	213
1:500	2.26	5.65	T	T	T	46[d]	1:2000	0.64	1.61	48	56	200	183
1:1250	0.90	2.26	T	3[d]	104[d]	40[d]	1:2500	0.51	1.28	56	50	190	186
1:2500	0.45	1.13	4[d]	25[d]	196	153	1:3750	0.34	0.86	38	36	197	169
1:5000	0.23	0.57	29	46	102	125	1:5000	0.26	0.64	43	56	136	129
Negative Control[e]													
		per plate											
Solvent (DMSO)		100 µl	38	37	125	103				40	52	122	125
Positive Controls[e]													
NaAz		5 µg	-[c]	-	1163	-				-	-	1718	-
2NF		5 µg	1741	-	-	-				702	-	-	-
B(a)P		10 µg	34	692	100	838				42	608	107	1164
2ANTH		2.5 µg	36	426	124	984				32	543	116	950

---

[a] For positive indication of mutagenic activity, a twofold increase in colony count above background (solvent control) plus a further dose-related increase in colony count is required.

[b] Assayed with or without the addition of rat liver microsomal preparation (S9).

[c] T, toxic (no colonies seen); -, not tested.

[d] Colony count less than that at lower dose levels is indicative of some toxicity.

[e] DMSO, dimethylsulfoxide; NaAz, sodium azide; 2NF, 2-nitrofluorene; B(a)P, benzo(a)pyrene; 2ANTH, 2-anthramine.

[f] Based on weight of extract aliquoted.

[g] Based on total volume of 2.5 ml reaction mixture poured into plate (except for 1:10 dilution).

[h] Based on total volume of 3.0 ml reaction mixture poured into plate.

Table 2
Salmonella Mutagenicity Assay on Extract No. 51 (Pyrolysis Oil from Hardwood)

			Number of Histidine-Independent Revertants per Plate[a]										
			Preliminary Run (VS-52)							Confirmatory Run (VS-5			
Tester Strain			TA98		TA100					TA98		TA100	
Metabolic Activation[b]			-S9	+S9	-S9	+S9				-S9	+S9	-S9	+S9
Final Dilution of Extract	Final Concentration of Extract[f] mg/ml[g]	Final Concentration of Extract[f] mg/plate					Final Dilution of Extract	Final Concentration of Extract mg/ml	Final Concentration of Extract mg/plate				
1:10	115.2[h]	345.6	T[c]	T	T	T	1:750	1.64	4.11	T	34[d]	T	468
1:50	23.0	57.6	T	T	T	T	1:1000	1.23	3.08	T	50	T	419
1:250	4.61	11.5	T	T	T	T	1:1250	0.99	2.47	11[d]	50	53[d]	237
1:500	2.30	5.76	T	T	T	T	1:1500	0.82	2.06	30[d]	48	58[d]	233
1:1250	0.92	2.30	T	53	51[d]	242	1:1750	0.70	1.76	54	59	151[d]	253
1:2500	0.46	1.15	18[d]	47	190	165	1:2000	0.62	1.54	52	48	160[d]	202
1:5000	0.23	0.58	56	43	180	135	1:2500	0.49	1.23	49	53	261	174
							1:5000	0.25	0.62	41	43	163	165
Negative Control[e]													
		per plate											
Solvent (DMSO)		100 ul	38	37	125	103				40	52	122	125
Positive Controls[e]													
NaAz		5 ug	-[c]	-	1163	-				-	-	1718	-
2NF		5 ug	1741	-	-	-				702	-	-	-
B(a)P		10 ug	34	692	100	838				42	608	107	1164
2ANTH		2.5 ug	36	426	124	984				32	543	116	950

---

[a] For positive indication of mutagenic activity, a twofold increase in colony count above background (solvent control) plus a further dose-related increase in colony count is required.

[b] Assayed with or without the addition of rat liver microsomal preparation (S9).

[c] T, toxic (no colonies seen); -, not tested.

[d] Colony count less than that at lower dose levels is indicative of some toxicity.

[e] DMSO, dimethylsulfoxide; NaAz, sodium azide; 2NF, 2-nitrofluorene; B(a)P, benzo(a)pyrene; 2ANTH, 2-anthramine.

[f] Based on weight of extract aliquoted.

[g] Based on total volume of 2.5 ml reaction mixture poured into plate (except for 1:10 dilution).

[h] Based on total volume of 3.0 ml reaction mixture poured into plate.

Table 3
Summary of Chromosome Aberration Assay on Extract No. 43 (Pyrolysis Oil from Softwood) Using Chinese Hamster Ovary Cells in Culture

		Percent Metaphases with Chromosome Aberrations[a]					
		Preliminary Run				Confirmatory Run	
Reference (Experiment No.)		VX-87				VX-89	
Metabolic Activation		-S9	+S9			-S9	+S9
Final Dilution of Extract	Final Concentration[b] (mg/ml)			Final Dilution of Extract	Final Concentration (mg/ml)		
1:200	5.82	T[c]	T	1:2000	0.54	NT[c]	MI[c]
1:500	2.33	T	T	1:2500	0.43	NT	36.5
				1:3000	0.36	NT	4.0
1:1000	1.16	T	T	1:3500	0.31	NT	2.0
				1:4000	0.27	NT	0.7
1:2000	0.58	T	MI	1:4500	0.24	NT	-[c]
				1:5000	0.22	NT	-
1:5000	0.23	MI	2.3	1:6000	0.18	44.4(MI)	NT
				1:7000	0.16	19.6	NT
1:10,000	0.12	13.6	0.3	1:8000	0.14	2.3	NT
				1:9000	0.12	2.6	NT
1:20,000	0.06	1.0	0	1:10,000	0.11	0.7	-
				1:12,000	0.09	-	NT
1:50,000	0.02	0	-	1:15,000	0.07	-	NT
				1:20,000	0.05	-	NT
Negative Controls							
MEM		0.3	0.3			0	0.3
Solvent(1% DMSO)		0	0.3			0	0.3
Positive Controls							
MNNG, 7.5 x 10^{-5}M		74.0	NT			64.2	NT
AFB_1, 5 x 10^{-6}M		0	82.0			0.3	86.7

---

[a] Each data point based on analysis of 100 metaphases in each of 3 replicate slides unless otherwise specified in parentheses (number aberrant/number analyzed).

[b] Based on weight of extract aliquoted.

[c] -, not analyzed (since higher concentrations show baseline level of chromosome aberrations).
NT, not tested.
T, toxic effects; cells changed morphology and/or detached from coverglass.
MI, mitotic inhibition; fewer than 40 scorable metaphases on each slide.

Table 4

Chromosome Aberration Test on Extract No. 43 (Pyrolysis Oil from Softwood) Using Chinese Hamster Ovary Cells in Culture (Preliminary Run)[a]

Final Dilution of Extract	Final Concentration (mg/ml)	Chromosome Damage by Types[b] Chromatid			Chromosome						Number of Metaphases Analyzed	Metaphases with any Chromosome Damage
		Gap	Break	Exch.	Gap	Break	Exch.	Frag.	Dicen.	Ring		
Without metabolic activation (-S9)												
1:200	5.82	ND[c]	ND	ND	ND	ND	ND	ND	ND	ND	ND	T[c]
1:500	2.33	ND	ND	ND	ND	ND	ND	ND	ND	ND	ND	T
1:1000	1.16	ND	ND	ND	ND	ND	ND	ND	ND	ND	ND	T
1:2000	0.58	ND	ND	ND	ND	ND	ND	ND	ND	ND	ND	T
1:5000	0.23	ND	ND	ND	ND	ND	ND	ND	ND	ND	ND	MI[c]
1:10,000	0.12	13	2	78	0	0	0	0	0	0	286	39(13.6%)
1:20,000	0.06	2	0	2	0	0	0	0	0	0	300	3(1.0%)
1:50,000	0.02	0	0	0	0	0	0	0	0	0	300	0(0%)
Negative Controls												
MEM		0	0	0	0	0	1	0	0	0	300	1(0.3%)
Solvent(1% DMSO)		0	0	0	0	0	0	0	0	0	300	0(0%)
Positive Control												
MNNG, 7.5x10^{-5} M		d	d	d	d	d	d	d	d	d	300	222(74.0%)
With metabolic activation (+S9)												
1:200	5.82	ND	ND	ND	ND	ND	ND	ND	ND	ND	ND	T
1:500	2.33	ND	ND	ND	ND	ND	ND	ND	ND	ND	ND	T
1:1000	1.16	ND	ND	ND	ND	ND	ND	ND	ND	ND	ND	T
1:2000	0.58	0	0	5	ND	ND	ND	ND	ND	ND	2(MI)	MI
1:5000	0.23	7	0	0	0	0	0	0	0	0	300	7(2.3%)
1:10,000	0.12	1	0	0	0	0	0	0	0	0	300	1(0.3%)
1:20,000	0.06	0	0	0	0	0	0	0	0	0	300	0(0%)
1:50,000	0.02	-[c]	-	-	-	-	-	-	-	-	-	-
Negative Controls												
MEM		1	0	0	0	0	0	0	0	0	300	1(0.3%)
Solvent(1% DMSO)		1	0	0	0	0	0	0	0	0	300	1(0.3%)
Positive Control												
AFB$_1$,	-S9	0	0	0	0	0	0	0	0	0	300	0(0%)
5x10^{-6} M:	+S9	d	d	d	d	d	d	d	d	d	300	246(82.0%)

---

[a] Reference: Experiment No. VX-87.

[b] Each data point based on analysis of 100 metaphases in each of 3 replicate slides unless otherwise specified. Exch.=exchange; Frag.=fragment; Dicen.= dicentric.

[c] ND, no data; T, toxic effects: cells changed morphology and/or detached from coverglass; MI, mitotic inhibition: fewer than 40 scorable metaphases on each slide; -, not analyzed, since higher concentrations show baseline level of chromosome damage.

[d] Because of the high frequency of multiple aberrations per cell, the aberrations were not individually recorded.

Table 5
Chromosome Aberration Test on Extract No. 43 (Pyrolysis Oil from Softwood) Using Chinese Hamster Ovary Cells in Culture (Confirmatory Run)[a]

Final Dilution of Extract	Final Concentration (mg/ml)	Chromosome Damage by Types[b] Chromatid Gap	Chromatid Break	Chromatid Exch.	Chromosome Gap	Chromosome Break	Chromosome Exch.	Chromosome Frag.	Chromosome Dicen.	Chromosome Ring	Number of Metaphases Analyzed	Metaphases with any Chromosome Damage
Without metabolic activation (-S9)												
1:6000	0.18	0	0	42	0	0	0	0	0	0	9(MI)[c]	4(44.4%)
1:7000	0.16	7	1	41	0	1	0	0	0	0	92(MI)	18(19.6%)
1:8000	0.14	6	0	1	0	0	0	0	0	0	300	7(2.3%)
1:9000	0.12	3	0	8	0	1	1	0	0	0	300	8(2.6%)
1:10,000	0.11	1	0	1	0	0	0	0	0	0	300	2(0.7%)
1:12,000	0.09	-[c]	-	-	-	-	-	-	-	-	-	-
1:15,000	0.07	-	-	-	-	-	-	-	-	-	-	-
1:20,000	0.05	-	-	-	-	-	-	-	-	-	-	-
Negative Controls												
MEM		0	0	0	0	0	0	0	0	0	300	0(0%)
Solvent(1% DMSO)		0	0	0	0	0	0	0	0	0	300	0(0%)
Positive Control												
MNNG, 7.5x10^{-4} M		d	d	d	d	d	d	d	d	d	296	190(64.2%)
With metabolic activation (+S9)												
1:2000	0.54	ND[c]	ND	ND	ND	ND	ND	ND	ND	ND	ND	MI
1:2500	0.43	7	1	318	0	0	0	0	0	0	203	74(36.5%)
1:3000	0.36	5	1	14	0	0	0	0	0	0	300	12(4.0%)
1:3500	0.31	3	0	3	0	0	0	0	0	0	300	6(2.0%)
1:4000	0.27	1	1	0	0	0	0	0	0	0	300	2(0.7%)
1:4500	0.24	-	-	-	-	-	-	-	-	-	-	-
1:5000	0.22	-	-	-	-	-	-	-	-	-	-	-
1:10,000	0.11	-	-	-	-	-	-	-	-	-	-	-
Negative Controls												
MEM		1	0	0	0	0	0	0	0	0	300	1(0.3%)
Solvent(1% DMSO)		1	0	0	0	0	0	0	0	0	300	1(0.3%)
Positive Control												
AFB$_1$,	-S9	1	0	0	0	0	0	0	0	0	300	1(0.3%)
5x10^{-6}M:	+S9	d	d	d	d	d	d	d	d	d	300	260(86.7%)

---

[a] Reference: Experiment No. VX-89.

[b] Each data point based on analysis of 100 metaphases in each of 3 replicate slides unless otherwise specified. Exch.=exchange; Frag.=fragment; Dicen.=dicentric.

[c] ND, no data; MI, mitotic inhibition: fewer than 40 scorable metaphases on each slide; -, not analyzed, since higher concentrations show baseline level of chromosome damage.

[d] Because of the high frequency of multiple aberrations per cell, the aberrations were not individually recorded.

Table 6
Summary of Chromosome Aberration Assay on Extract No. 51 (Pyrolysis Oil from Hardwood) Using Chinese Hamster Ovary Cells in Culture

		Percent Metaphases with Chromosome Aberrations[a]					
		Preliminary Run				Confirmatory Run	
Reference (Experiment No.)		VX-87				VX-89	
Metabolic Activation		-S9	+S9			-S9	+S9
Final Dilution of Extract	Final Concentration[b] (mg/ml)			Final Dilution of Extract	Final Concentration (mg/ml)		
1:200	6.05	T[c]	T	1:5000	0.28	NT[c]	36.4(MI)[c]
1:500	2.42	T	T	1:6000	0.23	NT	1.3
				1:7000	0.20	NT	0
1:1000	1.21	T	T	1:8000	0.18	NT	0
				1:9000	0.16	NT	-[c]
1:2000	0.61	T	T	1:10,000	0.14	NT	-
				1:12,000	0.12	MI	NT
1:5000	0.24	T	51.2(MI)	1:14,000	0.10	21.4(MI)	NT
				1:16,000	0.09	42.3(MI)	NT
1:10,000	0.12	MI	0	1:18,000	0.08	11.1	NT
				1:20,000	0.07	3.0	NT
1:20,000	0.06	20.3	0.3	1:30,000	0.05	0.3	NT
				1:40,000	0.04	-	NT
1:50,000	0.02	1.0	-	1:50,000	0.03	-	NT
Negative Controls							
MEM		0.3	0.3			0	0.3
Solvent (1% DMSO)		0	0.3			0	0.3
Positive Controls							
MNNG, 7.5 x 10^{-5} M		74.0	NT			64.2	NT
AFB$_1$, 5 x 10^{-6} M		0	82.0			0.3	86.7

---

[a] Each data point based on analysis of 100 metaphases in each of 3 replicate slides unless otherwise specified in parentheses (number aberrant/number analyzed).

[b] Based on weight of extract aliquoted.

[c] -, not analyzed (since higher concentrations show baseline level of chromosome aberrations).
NT, not tested.
T, toxic effects; cells changed morphology and/or detached from coverglass.
MI, mitotic inhibition; fewer than 40 scorable metaphases on each slide.

Table 7
Chromosome Aberration Test on Extract No. 51 (Pyrolysis Oil from Hardwood) Using Chinese Hamster Ovary Cells in Culture (Preliminary Run)[a]

Final Dilution of Extract	Final Concentration (mg/ml)	Chromosome Damage by Types[b]									Number of Metaphases Analyzed	Metaphases with any Chromosome Damage
		Chromatid			Chromosome							
		Gap	Break	Exch.	Gap	Break	Exch.	Frag.	Dicen.	Ring		
Without metabolic activation (-S9)												
1:200	6.05	ND[c]	ND	ND	ND	ND	ND	ND	ND	ND	ND	T[c]
1:500	2.42	ND	ND	ND	ND	ND	ND	ND	ND	ND	ND	T
1:1000	1.21	ND	ND	ND	ND	ND	ND	ND	ND	ND	ND	T
1:2000	0.61	ND	ND	ND	ND	ND	ND	ND	ND	ND	ND	T
1:5000	0.24	ND	ND	ND	ND	ND	ND	ND	ND	ND	ND	T
1:10,000	0.12	ND	ND	ND	ND	ND	ND	ND	ND	ND	2(MI)[c]	MI
1:20,000	0.06	21	1	85	0	0	0	0	0	0	217	44(20.3%)
1:50,000	0.02	2	0	1	0	0	0	0	0	0	300	3(1.0%)
Negative Controls												
MEM		0	0	0	0	1	0	0	0	0	300	1(0.3%)
Solvent(1% DMSO)		0	0	0	0	0	0	0	0	0	300	0(0%)
Positive Control												
MNNG, $7.5x10^{-5}$ M		d	d	d	d	d	d	d	d	d	300	222(74.0%)
With metabolic activation (+S9)												
1:200	6.05	ND	ND	ND	ND	ND	ND	ND	ND	ND	ND	T
1:500	2.42	ND	ND	ND	ND	ND	ND	ND	ND	ND	ND	T
1:1000	1.21	ND	ND	ND	ND	ND	ND	ND	ND	ND	ND	T
1:2000	0.61	ND	ND	ND	ND	ND	ND	ND	ND	ND	ND	T
1:5000	0.24	4	0	107	0	0	0	0	0	0	43(MI)	22(51.2%)
1:10,000	0.12	0	0	0	0	0	0	0	0	0	300	0(0%)
1:20,000	0.06	1	0	0	0	0	0	0	0	0	300	1(0.3%)
1:50,000	0.02	–[c]	–	–	–	–	–	–	–	–	–	–
Negative Controls												
MEM		1	0	0	0	0	0	0	0	0	300	1(0.3%)
Solvent(1% DMSO)		1	0	0	0	0	0	0	0	0	300	1(0.3%)
Positive Control												
AFB_1,	-S9	0	0	0	0	0	0	0	0	0	300	0(0%)
$5x10^{-6}$M:	+S9	d	d	d	d	d	d	d	d	d	300	246(82.0%)

[a] Reference: Experiment No. VX-87.

[b] Each data point based on analysis of 100 metaphases in each of 3 replicate slides unless otherwise specified. Exch.=exchange; Frag.=fragment; Dicen.=dicentric.

[c] ND, no data; T, toxic effects: cells changed morphology and/or detached from coverglass; MI, mitotic inhibition: fewer than 40 scorable metaphases on each slide; –, not analyzed since higher concentrations show baseline level of chromosome damage.

[d] Because of the high frequency of multiple aberrations per cell, the aberrations were not individually recorded.

Table 8

Chromosome Aberration Test on Extract No. 51 (Pyrolysis Oil from Hardwood) Using Chinese Hamster Ovary Cells in Culture (Confirmatory Run)[a]

Final Dilution of Extract	Final Concentration (mg/ml)	Chromosome Damage by Types[b]									Number of Metaphases Analyzed	Metaphases with any Chromosome Damage
		Chromatid			Chromosome							
		Gap	Break	Exch.	Gap	Break	Exch.	Frag.	Dicen.	Ring		
Without metabolic activation (-S9)												
1:12,000	0.12	ND[c]	ND	ND	ND	ND	ND	ND	ND	ND	ND	MI[c]
1:14,000	0.10	0	0	19	0	0	0	0	0	0	14(MI)	3(21.4%)
1:16,000	0.09	4	0	20	0	0	0	0	0	0	26(MI)	11(42.3%)
1:18,000	0.08	9	1	30	0	0	0	0	0	0	153	17(11.1%)
1:20,000	0.07	5	1	13	0	0	0	0	0	0	300	9(3.0%)
1:30,000	0.05	0	0	1	0	0	0	0	0	0	300	1(0.3%)
1:40,000	0.04	-[c]	-	-	-	-	-	-	-	-	-	-
1:50,000	0.03	-	-	-	-	-	-	-	-	-	-	-
Negative Controls												
MEM		0	0	0	0	0	0	0	0	0	300	0(0%)
Solvent(1% DMSO)		0	0	0	0	0	0	0	0	0	300	0(0%)
Positive Control												
MNNG, 7.5×10^{-4} M		d	d	d	d	d	d	d	d	d	296	190(64.2%)
With metabolic activation (+S9)												
1:5000	0.28	3	1	106	0	0	0	0	0	0	44(MI)	16(36.4%)
1:6000	0.23	1	0	3	0	0	0	0	0	0	300	4(1.3%)
1:7000	0.20	0	0	0	0	0	0	0	0	0	300	0(0%)
1:8000	0.18	0	0	0	0	0	0	0	0	0	300	0(0%)
1:9000	0.16	-	-	-	-	-	-	-	-	-	-	-
1:10,000	0.14	-	-	-	-	-	-	-	-	-	-	-
Negative Controls												
MEM		1	0	0	0	0	0	0	0	0	300	1(0.3%)
Solvent(1% DMSO)		1	0	0	0	0	0	0	0	0	300	1(0.3%)
Positive Control												
AFB$_1$,	-S9	1	0	0	0	0	0	0	0	0	300	1(0.3%)
5×10^{-6}M:	+S9	d	d	d	d	d	d	d	d	d	300	260(86.7%)

[a] Reference: Experiment No. VX-89.

[b] Each data point based on analysis of 100 metaphases in each of 3 replicate slides unless otherwise specified. Exch.=exchange; Frag.=fragment; Dicen.=dicentric.

[c] ND, no data; MI, mitotic inhibition: fewer than 40 scorable metaphases on each slide; –, not analyzed, since higher concentrations show baseline level of chromosome damage.

[d] Because of the high frequency of multiple aberrations per cell, the aberrations were not individually recorded.

6. CHARACTERISTICS OF PYROLYSIS PRODUCT OILS

6.1 Introduction

A good deal of effort has been expended to characterize the liquid products from the WFPP. The yields of individual components found have been given in Chapter 3 and 5 for a number of materials and operating conditions. At the present time, from 80% to 90% of all the material in the liquid product has been uniquely identified.

These analytical results (obtained by GC-MS and HPLC) have been the basis for additional studies in order to offer some speculations on the mechanisms of the fast pyrolysis process. In particular, the large yields of hydroxyacetaldehyde - up to 15% by weight of the organic fraction of the oil from poplar wood - seemed to offer some possibilities for mechanistic speculation.

The kinetic model which appears to give the simplest overall description of the results obtained is that used by a number of workers e.g. Broido (1976) or Shafizadeh (1982) and Lidén (1985)(see Chapter 3). The first step to form activated cellulose does not necessarily imply weight loss. The two parallel decomposition steps are supported by the experimental evidence that some gas, notably CO_2, is formed in a relatively constant amount in the early stages of pyrolysis, together with char. Both this "prompt" char and gas are greatly reduced in amount if pure cellulose is used. Therefore, most of the primary char and much of the gas arises from the hemicellulose fraction of the wood, and a lesser amount from the lignin or the cellulose. The ratio of the rates of the two parallel decomposition steps will depend on both temperature and the wood fraction. The decomposition step of volatiles to tar and gases has been discussed in Chapter 3 (Lidén, 1985) and in the paper by Scott et al. (1986). Very little secondary char is formed in this step in the WFPP, contrary to slow pyrolysis models which have been presented by others. For cellulose, the decomposition to volatiles occurs at a much faster rate than the parallel char formation step, at optimal conditions.

As a consequence of these findings, a mechanistic model for the rapid decomposition of cellulose was proposed, modified from that of Shafizadeh and Lai (1972). This work was published in the Journal of Analytical and Applied Pyrolysis 9 (1986) 121-137 (copy attached as Appendix 6-A). More recent work in our laboratory would lead to some modifications of the speculations given in that publication, but the model is still essentially a useful one, at least qualitatively.

The general method of analysis of a pyrolysis oil may be of interest. Exact analytical details are given in the attached publications. Table 6.1.1 shows the sample preparation scheme that was used, with the liquid product for a spruce wood feed (Run 43) as an example. The results in Table 6.1.1 show that over 88% of the liquid product has been characterized. Recent results suggest that a substantial part of the apparently unidentified remainder is

Table 6.1.1

Characterization of Liquid Product
Run 43, Eastern Spruce Feedstock

Data:	Total yield of liquid product	79.2% by weight, as fed
	Feed moisture content	6.97%
	Water content of liquid product	22.4% (Karl Fischer)

20 product (4.48 g. H_2O, 15.52 g. organics)

↓ 61.7 g. H_2O

Phase Separation

Insoluble "Lignin"

↓

4.84 g. (by difference)

↓

24.2% of liquid product

↓

19.2% of wood as fed

↓

20.6% of wood mf

Solution 75.4 g. with 86.1% H_2O (K.F.)

↓

Water lost = 1.46 g. (by water balance)

Corrected Solution 76.86 g.

↓ Charcoal adsorption

HPLC Analysis

	wt % of wood
Cellobiosan	2.49
Glucose	0.99
Fructose	2.27
Glyoxal	2.47
Levogl.+methyl glyoxal	3.96
Hydroxyacetaldehyde	7.67
Formic acid	7.15
Acetic acid	3.86
Ethylene glycol	0.89
Acetol	1.24
	32.99

Final Balance - % of Liquid Product	
"Lignin"	24.2
Water	22.4
Organics identified	41.7
	88.3

in fact removed as adsorbate in the charcoal purification step, and represent low molecular weight soluble phenolics and some carbonyl compounds.

6.2 On the Presence of Anhydrodisaccharides in WFPP Pyrolysis Oils

After obtaining the HPLC and GC-MS units through a grant from NSERC in April, 1984, work was carried out on the detailed analysis of the "carbohydrate" or water-soluble portion of the water extract, using the scheme shown in Table 6.1.1. Initially, an ion exchange acid removal step was also employed but this was found to be unnecessary as well as not as selective as desired.

In the course of these analyses, a large unidentified peak was found in the disaccharide region of the chromatogram. Because of the amount of this component, a detailed study was carried out to identify it and to explain its presence using a sirup produced from pure cellulose, for simplicity. The results have been prepared for publication and will appear shortly in the Journal of Analytical and Applied Pyrolysis. A copy of this manuscript is attached as Appendix 6-B, which gives full details of the work.

In our opinion, this identification of cellobiosan as a primary product of fast pyrolysis of cellulose may be a significant contribution to the possible understanding of the rapid thermal decomposition of cellulose.

6.3 Lignin Derived Product from the Fast Pyrolysis of Poplar Wood

As shown in Table 6.1.1, water extraction causes the precipitation of an insoluble brown solid from the pyrolysis oils. This solid can be recovered easily, and its NMR analysis indicates that it is very similar in its functionalities to steam exploded lignin. Testing of the material as an ingredient of plywood glue has been proposed, and will be carried out in future work.

The results of the characterization of this lignin product have been prepared for publication, and will appear soon in the Journal of Analytical and Applied Pyrolysis. A copy of the article is attached as Appendix 6-C.

At the present time, it is likely that this fraction can be marketed in suitable form as an alternative lignin material for existing lignin markets.

6.4 Yields of Individual Components of Cellulose Pyrolysis Oils as a Function of Temperature

The variation of the composition of pyrolysis tars with temperature was of considerable interest, given the significant yields of many potentially useful compounds in the oils. Because some preliminary insight into the mechanism of fast pyrolysis of cellulose had been gained in this work, the oils obtained from the pyrolysis of a pure cellulose (Avicel PH-102) were analyzed for a number of the major components. The overall yields from this cellulose are given in Chapter 3.2.

Liquid products from the pyrolysis tests were obtained over a temperature range of 375°-700°C. These liquids were analyzed for specific chemical components using methods described elsewhere [Piskorz et al. 1986)](Appendix 6-A). Results for nine of the more significant components obtained in a water extract of the tars are shown in Figures 6.4.1-6.4.4. All of these results were obtained using the fluid bed pyrolysis system of the University of Waterloo. It is apparent that at a constant reaction time, well defined and fairly narrow optimal temperature ranges exist corresponding to the maximum yields for each component.

The yields of individual components shown in Figures 6.4.1-6.4.4 suggest strongly that a series of sequential decomposition steps is occurring. However, it is not clear from these results what the precursor for any particular compound may be, or what system of parallel or sequential reactions can satisfactorily explain the nature of the variation of yield with temperature. More extensive analyses of these data are now underway.

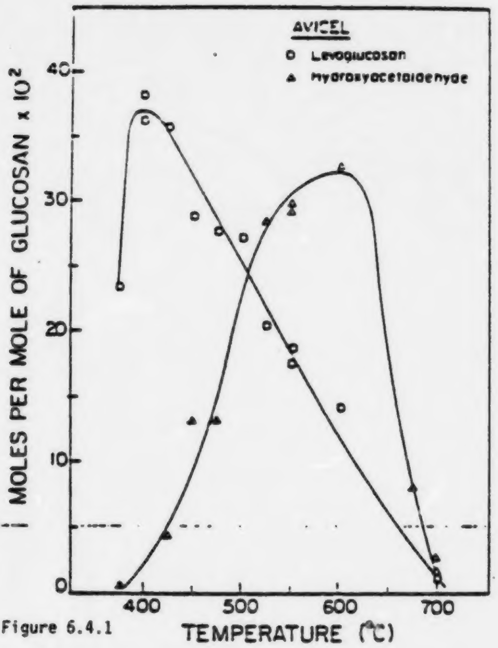

Figure 6.4.1

Yields of Levoglucosan and Hydroxyacetaldehyde, 500 ms, Fluidized Bed

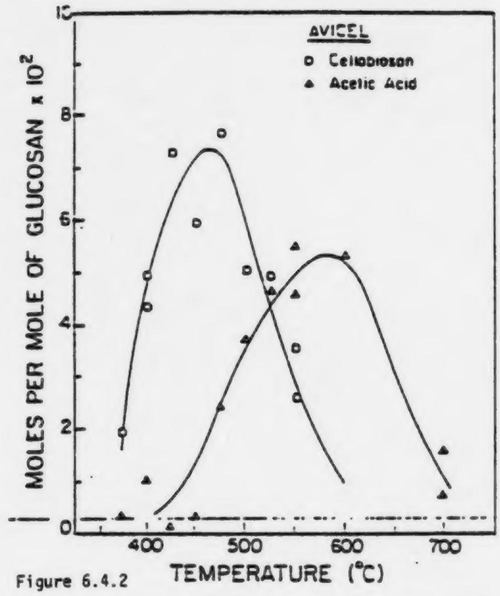

Figure 6.4.2

Yields of Cellobiosan and Acetic Acid, 500 ms, Fluidized Bed

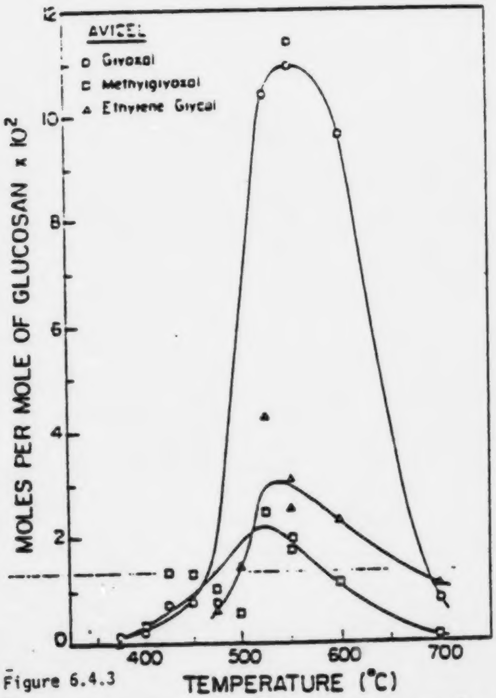

Figure 6.4.3

Yields of Glyoxal, Methylglyoxal and Ethylene Glycol, 500 ms, Fluidized Bed

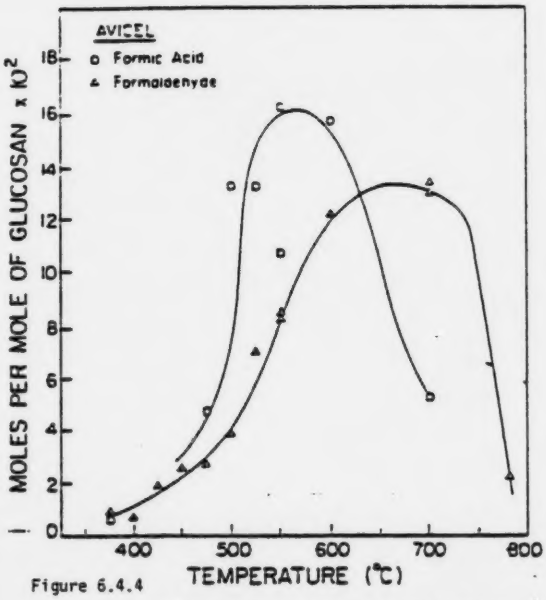

Figure 6.4.4

Yields of Formic Acid and Formaldehyde, 500 ms, Fluidized Bed

APPENDIX 6-A

On the Mechanism of the Rapid Pyrolysis of Cellulose

Journal of Analytical and Applied Pyrolysis, 9 (1986) 121–137 121
Elsevier Science Publishers B.V., Amsterdam – Printed in The Netherlands

ON THE MECHANISM OF THE RAPID PYROLYSIS OF CELLULOSE

JAN PISKORZ, DESMOND RADLEIN* and DONALD S. SCOTT *

Department of Chemical Engineering, University of Waterloo, Waterloo, Ontario, N2L 3G1 (Canada)

(Received November 1st, 1984; accepted August 6th, 1985)

SUMMARY

Experimental yields and liquid product analyses obtained from the fast pyrolysis of biomass and cellulose in a fluidized bed reactor have been used to demonstrate that the decomposition of cellulose to liquid products proceeds to a major degree by a single mechanism. At temperatures over about 450°C and at vapor residence times of one second or less, it is proposed that the monomer unit of cellulose decomposes preferentially to a two-carbon and a four-carbon fragment, with the two-carbon fragment rearranging to give a yield of hydroxyacetaldehyde (glycolaldehyde) which is 75% or more of that theoretically probable. The most likely route for decomposition or rearrangement of the four-carbon moiety is suggested. The formation of carbonyl or hydroxycarbonyl compounds with two to four carbon atoms is favored. Experimental results from the fast pyrolysis of poplar wood indicate that the cellulose decomposition in wood follows the same path as that of pure cellulose in the production of liquid products.

INTRODUCTION

Biomass flash pyrolysis methods at atmospheric pressure have been developed by Diebold and co-workers at SERI [1] who developed an "ablative" pyrolysis method, primarily to produce olefinic gases from wood, and by Kuester [2] who employed a fluidized bed reactor followed by secondary catalytic reactors to produce liquid fuels. In neither of these processes was the production of liquids directly from the pyrolysis step a primary objective. As a result, little detailed analysis of the oil product was attempted. Studies of very fast pyrolysis have been carried out by Antal [3] using a solar furnace to achieve high heating rates, but no detailed oil analyses were reported.

---

* Present address: Department of Chemistry, University of the West Indies, Kingston, Jamaica.

0165-2370/86/$03.50 © 1986 Elsevier Science Publishers B.V.

Knight et al. [4], using an entrained flow reactor, have described some of the physical and fuel quality characteristics of pyrolysis oil, as have Pober and Bauer [5] using the Occidental process which employed hot circulating char as a heat carrier. Again, few details of the chemical nature of the pyrolytic oils produced were reported, which is in general true of other reports of flash pyrolysis processes.

In recent years, a fast pyrolysis process has been developed in our laboratory designed to give a maximum yield of organic liquids from lignocellulosic materials by as economical a method as possible. Fast pyrolysis requires a reactor capable of high rates of heat transfer, and a fluidized bed was chosen for this reason, as well as for its high potential throughput rate. A bench scale atmospheric pressure fluidized bed unit using sand as the fluidized solid with a throughput of about 15–30 g/h of biomass gives very high yields of organic liquids from hardwoods and softwoods—55–65% by weight—at temperatures from 450 to 550°C in an inert nitrogen atmosphere with an apparent vapor residence time of approximately 0.5 s [6]. More recently, a continuous fluidized bed pyrolysis unit has been operated with a feed rate of 2–3 kg/h of biomass. This unit has essentially duplicated or exceeded the yields obtained in the bench scale unit [7]. Typical results obtained in the small scale pilot unit are given in Table 1, together with the elemental analysis of the poplar wood used as feed, and of the tar and char produced. Yields of some low molecular weight individual compounds as determined by gas chromatography are also given. More extensive results are given in the reports by Scott and Piskorz [7,8].

In the early stages of the work, little detailed analysis, apart from elemental analyses, was carried out on the pyrolysis oil produced, in part because of inadequate analytical facilities. In more recent studies, some pyrolysis tests were carried out in the University of Waterloo fast pyrolysis unit on a clean hybrid poplar wood as part of a program of evaluation of thermochemical liquefaction processes initiated by the International Energy Agency [9]. Samples of the pyrolysis oil produced were analyzed for individual components by gas chromatography–mass spectrometry techniques by the Pacific Northwest Laboratories of Battelle Institute [10]. Simultaneously, workers at the Université de Sherbrooke, where a vacuum pyrolysis process is under development, carried out specific analyses for carboxylic acids, phenols, monosaccharides and several low molecular weight carbonyl compounds on one of our similar pyrolytic oil samples [11]. A comparison of results from these two sources, for those components present in the largest amounts, is shown in Table 2.

Methods of quantitative determination of functional groups in the pyrolytic oil were also tested in our laboratories by Nicolaides [12]. A summary of these results is shown in Table 3. The values given for functional group analyses for carboxylic acids and for phenols check reasonably well (±20%) with the sum of the individual compounds listed by Ménard et al. [11]. The

TABLE 1

Pyrolysis of hybrid poplar wood

Ash, 0.44%; C, 48.39%; H, 5.89%; N, 0.07%; O, 45.2% mf.

	Run No.		
	59	27	29
Moisture content, %	4.6	6.3	6.3
Size, μm	-1000	-595	-595
Temperature, °C	504	500	500
Apparent residence time of vapor, s	0.48	0.55	0.55
Feed rate, kg/h	1.85	2.24	1.97
Yields, % mf wood			
Organic liquids	66.24	65.76	71.15
Water	10.75	9.3	6.6
Char	11.78	12.15	11.20
Gas	11.03	12.45	12.07
Overall recovery	99.8	99.7	101.0
Gas yields, % mf wood			
H_2	0.01	0.02	
CO	4.44	5.32	5.39
CO_2	5.75	6.30	5.86
CH_4	0.37	0.48	
C_2H_4	0.13	0.20	
C_2H_6	0.05	0.04	
C_3	0.08	0.085	
Light organics	0.19		
Individual tar components, % mf wood		Run 27/29 composite *	
Methanol	1.10	0.82	
Acetic acid	4.33	4.7	
Hydroxyacetaldehyde	8.86	7.6 (8.0) **	
Acetol	2.92	2.2 (3.3)	
Furfural	0.53	N.D. ***	
Methylfurfural	0.22	N.D.	
Char, % C mf	69.5	66.5	
% H mf	3.89	4.43	
Ash	3.6	3.2	
Tar, % C mf	53.6	55.2	
% H mf	6.97	6.10	

* Results from Elliott [10].

** Authors' results in parentheses, same sample after 16 months storage.

*** N.D. = not determined.

aliphatic hydroxy (ROH) analyses in Table 3, however, are not in agreement with the amount of aliphatic hydroxy present which would be deduced from the values in Table 2. Use of the analyses given in Table 2 indicates that the ROH reported in Table 3 should be at least four times as much. A phthalic

TABLE 2

Some components of poplar pyrolysis oils

Compound	% by weight, mf	
	Sherbrooke *	PNL **
Glycolic acid	0.60	–
Formic acid	1.76	1.18
Acetic acid	5.49	7.04
Propionic acid	1.25	–
Methanol	–	1.22
Acetone	–	–
Acetaldehyde	–	0.16
1-Hydroxypropanone	4.1	3.22
Hydroxyacetaldehyde	–	11.37
Phenol	0.53	0.20
Ethyl-2-phenol	1.64	–
p-Methoxyphenol (guaiacol)	0.32	0.14
Hydroxypropanal	1.80	1.40
2-Furanone	–	0.61
Cyclopentanone	–	0.90
Syringol	0.50	0.17
Cresols	0.27	0.10
Levoglucosan	1.46	–
α-D-Glucose	0.59	–

* Ménard [11]; Run 32 Composite.

** Elliott [10]; Run 27/29 Composite.

TABLE 3

Combined liquor/tar data

Run No.	13	22	33	31	32	35
Feedstock	Maple	Wheat straw	Poplar-aspen	Poplar-aspen	Poplar-aspen	Peat moss
Temperature, °C	482	500	450	500	550	520
	mol of functional groups/kg of liquid derived from organic matter in feed					
1. $-CO_2H$	1.8	1.3	1.9	1.5	1.5	1.1
2. Carbonyl	5.0	5.0	5.7	6.5	6.0	2.8
3. ROH *	0.81	1.3	0.71	0.82	0.70	1.2
4. ArOH	2.5	2.8	2.6	2.6	2.5	1.7
5. Methoxyl	1.8	0.99	1.5	1.4	1.1	0.68
H_2O (wt.%)	12	5.8	8.2	6.1	9.2	5.9
	% of organic oxygen accounted for					
	65	57	65	66	64	51
	% of total oxygen accounted for					
	73	62	71	69	70	56

* Low results.

acid esterification method [13] was used for the ROH determinations of Table 2. and apparently led to low results for pyrolysis oil. although satisfactory results were obtained with low molecular weight model compounds although not with carbohydrates [12]. If Table 3 is corrected for these low values then for the poplar aspen runs 31. 32 and 33 about 75% of the organic oxygen is accounted for. The balance is assumed to exist largely as ether linkages. of various kinds. and possibly some additional –OH groupings on cellulose fragments. Although the oil from Run 27/29 analyzed by Elliott is from a clean. mature poplar wood rather than young trees. pyrolysis was carried out at the same conditions as those of Run 32. so the product compositions should be similar.

The results in Table 3 indicate that a large amount of relatively low molecular weight (< 100) ketones and aldehydes must be present in the pyrolysis oil. and that a significant fraction of these must be multifunctional in nature.

It is apparent that the pyrolysis oil produced in our fast pyrolysis process is. like most pyrolytic oils from cellulosic biomass, a complex mixture of chemicals, many of them quite highly oxygenated. A large number of publications have appeared describing investigations of the mechanism of pyrolysis of cellulose, and proposing reaction schemes for both primary and subsequent decomposition steps. Antal et al. [14] have summarized this work briefly up to 1980. Some agreement exists among several workers (for example. Kilzer and Broido [15]. Broido [16] and Arseneau [17]) that the decomposition can be represented by two competing reactions: the first a dehydration of cellulose to yield an anhydrocellulose and the second a depolymerization of cellulose to yield primarily levoglucosan, as well as other anhydromonosaccharides. The first of these reactions (dehydration) is important at low temperatures and slow heating rates, but the second becomes the major decomposition pathway at higher temperatures, short times and high heating rates [1,16]. A number of other earlier workers had also reported levoglucosan as a significant intermediate product in the decomposition of cellulose [18–24]. Several experimental studies of the thermal decomposition of levoglucosan have also been reported [17,25–28]. Earlier work employed temperatures and heating rates which were low compared to flash pyrolysis conditions. Some of the later investigations, however, were carried out under the rapid pyrolysis conditions of analytical mass spectrometry [27,28].

The publications of Shafizadeh and co-workers, particularly, are notable for both the quality and quantity of the contributions made over a twenty year period in the area of cellulose and wood pyrolysis. Shafizadeh and co-workers [29,30], based on the early work of others. as well as their own investigations. have proposed the simple model shown in Fig. 1, in which a primary step is assumed to be the formation of an "active cellulose" followed by the formation of either char and gases by one decomposition

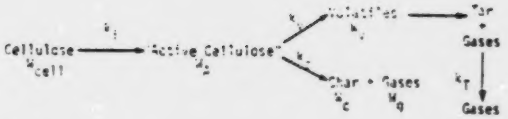

where

$$\frac{-d(W_{cell})}{dt} = k_i[W_{cell}]$$

$$\frac{d(W_A)}{dt} = k_i[W_{cell}] - (k_v + k_c)[W_A]$$

$$\frac{d(W_c)}{dt} = 0.35k_c[W_A]$$

$$k_i = 1.7 \times 10^{21} e^{-(58{,}000/RT)}\ \mathrm{min}^{-1}$$

$$k_v = 1.9 \times 10^{16} e^{-(47{,}300/RT)}\ \mathrm{min}^{-1}$$

$$k_c = 7.9 \times 10^{11} e^{-(36{,}000/RT)}\ \mathrm{min}^{-1}$$

$$k_T = 3.4 \times 10^{9}\ e^{-(25{,}000/RT)}\ \mathrm{min}^{-1}$$

Fig. 1. Kinetic model for pyrolysis of pure cellulose under vacuum [30] (k_T value for tar decomposition from this work).

route, or of primary volatiles by another route. These primary volatiles are postulated to be anhydrosugars (transglycolation products) of which levoglucosan (1,6-anhydro-β-D-glucopyranose) appears to be the major product from cellulose. A great deal of careful work studying pyrolysis oils produced at low temperatures under high vacuum has confirmed that levoglucosan can be obtained from various celluloses in yields from 20 to 60% by weight [31]. However, from wood or other lignocellulosic materials, yields of levoglucosan under similar pyrolysis conditions were less than 5% by weight, and only 1–2% under conditions of fast pyrolysis. Nonetheless, it is now commonly accepted that the formation of anhydrosugars is the first step in the formation of volatile compounds from the pyrolysis of cellulose or similar carbohydrate polymers. Whether or not this conclusion is valid for conditions of fast pyrolysis is not clear, but present evidence indicates that the two primary parallel decomposition steps in cellulose pyrolysis will be operative at both low and high heating rates, but that their relative importance will shift under fast pyrolysis conditions, to favor the formation of volatiles, particularly liquids, at lower temperatures (below 600°C).

Perhaps the most unusual result noticeable in the compounds listed in Table 1 is the abundance of hydroxyacetaldehyde (glycolaldehyde) and acetol (1-hydroxy-2-propanone). A survey of the literature reveals that these compounds have only occasionally been reported by others as pyrolysis products, and have received very little attention in the sense of being a major decomposition product. In 1966, Byrne et al. [22], during studies of pyrolysis of cellulose treated with flame retardants, reported hydroxyacetaldehyde as one major component of a group of highly oxygenated products, along with glyoxal, pyruvaldehyde and 5-hydroxymethylfurfural. They proposed, as one of several, a reaction scheme in which cellulose formed anhydrosugars by random cleavage of the glucosidic linkages followed by ring opening at the ring glucosidic linkage to form two-carbon and four-carbon fragments with the two-carbon moiety rearranging to glycolaldehyde. Other compounds were postulated to form from various rearrangements of the four-carbon fragments.

In 1969, Lipska and Wodley [33] reported acetol (1-hydroxy-2-propanone) as a major degradation product of isothermal cellulose pyrolysis at 315°C, as well as identifying significant amounts of other two-, three- and four-carbon carbonyl compounds, as well as furan derivatives. In an early paper (1972) on the mechanism of cellulose pyrolysis, Shafizadeh and Lai [26] studied the thermal decomposition of levoglucosan containing labelled ^{14}C at the 1-, 2- and 6-positions. They concluded that, under their conditions of slow pyrolysis, certain reaction pathways were more favored than others, for example, CO_2 was produced primarily from C-1 and C-2 positions, while the production of CO was much more non-specific. Glyoxal, assumed to be derived from hydroxyacetaldehyde, was produced mainly from C-1 and C-2 positions while pyruvaldehyde and 1-hydroxy-2-propanone were less specific. The reaction scheme proposed to account for the formation of hydroxyacetaldehyde and 1-hydroxy-2-propanone is shown in Fig. 2 and is very similar to that proposed by Byrne et al. [22]. This same scheme was again proposed in 1982 by Shafizadeh [30] as one of two which could furnish a plausible route to explain the formation of various volatile products under conditions of fast pyrolysis at higher temperatures in which fission, dehydration, disproportionation, decarboxylation and decarbonylation reactions are all possible. While Shafizadeh suggested that the low molecular weight fission or disproportionation products containing two or three carbon atoms arose from secondary reactions of the tar or reaction of H_2O and CO_2 with char, the production of these products by direct conversion of cellulose molecules was not ruled out.

In an investigation of the formation of ketene from the pyrolysis of carbohydrates, Kang et al. [34] proposed a mechanism in which ketene is formed from hydroxyacetaldehyde by dehydration. Subsequent rehydration leads to the formation of acetic acid. Pyrolysis tests with various carbohydrates and with hydroxyacetaldehyde led them to recommend that hydroxyacetaldehyde be considered the precursor of ketene as well as some of the acetic acid formed.

Schulten et al. [35,36] investigated the vacuum Curie-point pyrolysis of a number of carbohydrates using high resolution field ionization mass spectrometry. On the basis of their results, they assumed the primary decomposition pathway to be through the formation of levoglucosan or other anhydrosugars and then proposed decomposition routes for the levoglucosan intermediate via dehydration, retroaldolization and decarbonylation to

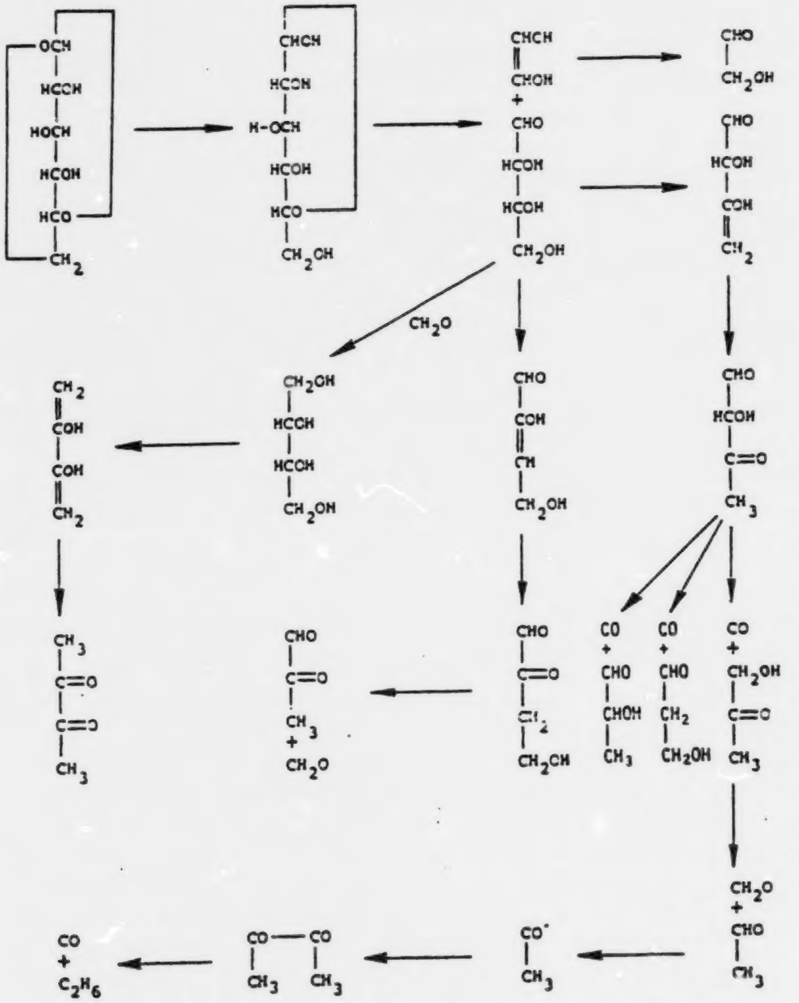

Fig. 2. Proposed mechanism for the rapid thermal decomposition of cellulose, after Byrne et al. [22] and Shafizadeh and Lai [26].

account for the production of various C_2, C_3 and C_4 compounds. Hydroxyacetaldehyde was postulated to be formed by both hydration/dehydration reactions and by retroaldolization, and hydroxypropanals by dehydration/decarbonylation reactions in a similar way to that illustrated in Fig. 2. While the proportions of pyrolysis products varied for different carbohydrates, much the same products resulted from the fast pyrolysis of various polysaccharides, especially those products in the lower molecular weight range. The same conclusion has been reported for amylose pyrolysis [23].

Evans et al. [28] used a flash pyrolysis–mass spectrometric technique (low energy electron ionization) to study the primary and secondary decomposition products of various biomass materials and their components. Both cellulose and levoglucosan were pyrolyzed at various residence times, and gave very similar cracking patterns. Light gases appeared to derive primarily from cellulose and not from other biomass components, e.g. lignin or hemicellulose. Levoglucosan was stated to be the major primary intermediate observed from cellulose. In the low mass spectral region, large and relatively stable peaks were obtained at mass 60 for both untreated cellulose and levoglucosan.

In a recent publication, Beaumont and Schwob [37] using an entrained flow pyrolysis reactor and sawdust feed have reported significant yields of hydroxypropanone and acetic acid as well as smaller yields of furaldehyde and 1-hydroxy-2-butenone. The effect of additions of acidic and basic catalysts on these yields was also reported.

Recent results from our fast pyrolysis work in fluidized beds have led us to believe that the reaction scheme outlined in Fig. 2 in which hydroxyacetaldehyde is a major pyrolysis product is a strongly favored decomposition route, and can account for many of the products found in oils obtained from flash pyrolysis processes.

EXPERIMENTAL AND RESULTS

In early gas chromatographic analyses of pyrolysis oils from wood using Fluorad FC-431 on Chromosorb W HP columns, single large peaks were obtained at retention times corresponding to acetic acid and propionic acid, and the corresponding apparent yields were reported as such. When the presence of hydroxyacetaldehyde, acetol and hydroxypropanals in these oils was pointed out by the work of Elliott [10] and Ménard et al. [11], alternative chromatographic techniques were developed using a Porapak Q column, and a 185°C initial temperature for 3 min, followed by a 25°C/min ramp to a final temperature of 225°C. With nitrogen carrier gas and a flame ionization detector a good resolution of these hydroxycarbonyl compounds was achieved. In order to give a confirmation of the reported significant yields of these compounds, 50 g of wood pyrolysis liquid tar product (about 20% water) was extracted by the addition of 200 ml of water until two layers formed. The aqueous phase, which contained about 40% of the tar, was removed and filtered to give a clear yellow solution containing many components, including phenolic and furan compounds. This filtrate after treating with an anion-exchange resin to remove carboxylic acids was treated with 10–20 g of activated charcoal to remove the aromatic or unsaturated compounds and then filtered to yield a clear decolorized solution. This solution was concentrated by vacuum evaporation to a gummy syrup containing 30% hydroxyacetaldehyde and 10% acetol, corresponding to 10% and 3.3% respectively of the original pyrolysis oil, in agreement with the results reported by Elliott [10]. The syrup also contained significant amounts of acetic acid as well as higher molecular weight compounds of unknown composition.

The yield of organic liquids in the flash pyrolysis process developed at the University of Waterloo is of the order of 66% of the moisture free wood. The hydroxyacetaldehyde yield (using Elliott's analysis) is therefore 7.6% of the dry wood fed. The cellulose content of the hybrid poplar–aspen wood used as the feed for the pyrolysis process is 39–43%, so that the yield of hydroxyacetaldehyde is then 17.4–19.2% of the cellulose. Assuming that only one mole of hydroxyacetaldehyde can be formed per mole of glucose monomer as postulated by the scheme shown in Fig. 2, the theoretical maximum yield of hydroxyacetaldehyde would be 37%. In fact, therefore, approximately 50% of the theoretical yield is obtained. This would appear to be a possible confirmation of the occurrence of a fairly specific primary ring cleavage to yield two-carbon and four-carbon fragments, in the manner suggested in Fig. 2, that is, to form hydroxyacetaldehyde by cleavage of a ring glucosidic bond and the C-2–C-3 bond. Because of the hemicellulose and lignin content of the wood, it is not possible from product analysis to determine what the additional decomposition modes of the cellulose might be.

In order to gain some further insights, pyrolysis tests were conducted using a commercial cellulose (S & S cellulose powder purified for thin-layer chromatography, ash 0.22%, Runs 1, 2 and 3). The results of these tests are summarized in Table 4. It is apparent that hydroxyacetaldehyde is produced from the pure cellulose in essentially the same yield as that obtained from the cellulose in wood, suggesting that this favored decomposition route for the cellulose is not altered in its primary stages by the presence of the other wood components. However, the 1-hydroxy-2-propanone was recovered in lower yield than expected. (The yield from the poplar wood based on cellulose would be about 5.0%.) Other possible decomposition products suggested by the schemes shown in Fig. 2 have not yet been quantitatively recovered.

Table 4 also gives the result of a cellulose pyrolysis run using a different microcrystalline cellulose. Pyrolysis conditions were the same as those in Run 1 using the S & S cellulose, except for a slightly shorter vapor residence time. Major differences exist in the product distribution for the two celluloses. While the total volatiles yield is only a little greater in Run 5 than in Run 1, a much larger fraction is organic liquid (90% vs. 73%), and much less is gas or water (5.1% vs. 14.2% and 4.6% vs. 8.0%, respectively). Similarly, the char yield is higher for the S & S cellulose, 4.2% vs. 1.0% for the Baker cellulose. The high gas yield for the S & S cellulose is due to increased production of CO and CO_2. Even more striking is the yield of major

TABLE 4

Fast pyrolysis of cellulose (bench scale)

Nitrogen atmosphere: 4.0% moisture; 0.04% ash, 1 atm pressure abs.

	Run No.				
	3 *	1 *		2 *	5 **
Temperature, °C	450	500		550	500
Approx. residence time of vapor, s	0.56	0.53		0.54	0.48
Yields, % of maf feed					
Gas	8.49	13.04	(14.2) ***	17.89	5.1
Tar + (C_4 +)	67.53	67.81	(73.6)	58.58	90.1
H_2O	8.06	7.35	(8.0)	10.17	4.6
Char	8.53	3.84	(4.2)	6.70	1.0
Overall recovery	92.61	92.04	(100.0)	93.34	100.8
H_2	0.0	0.0	(0.0)	0.06	0.14
CO	3.68	6.04	(7.0)	9.23	2.69
CO_2	4.61	5.40	(5.9)	7.47	1.53
CH_4	0.07	0.21	(0.23)	0.41	0.20
C_2H_4	0.04	0.15	(0.16)	0.27	0.14
C_2H_4	0.03	0.07	(0.08)	0.11	0.02
C_3	0.05	0.13	(0.14)	0.31	0.35
Light organics	0.49	1.31	(1.4)	2.45	N.D.
Hydroxyacetaldehyde	17.1	17.5	(19.0)	15.8	7.6
1-Hydroxy-2-propanone (acetol)	2.8	3.2	(3.5)	4.1	0.7
Hydroxyacetaldehyde/org. liquid	0.25	0.26		0.27	0.084
Acetol/org. liquid	0.041	0.047		0.069	0.008
Methanol	N.D.	0.04	(0.04)	0.16	5.2
Acetic acid	0.23	0.30	(0.33)	0.51	
Furfural + furfural alcohol	0.20	0.23	(0.25)	0.39	
Levoglucosan	1.9	2.1		1.3	25.2

* S & S powdered cellulose, 99.9%, −250 μm, ash 0.22%.

** Baker TLC microcrystalline cellulose, ash 0.04%.

*** Normalized values in parentheses.

components of the tar. Hydroxyacetaldehyde yield from Baker cellulose is only half of that from the S & S cellulose, while the levoglucosan yield is 25.2% of the cellulose fed for the Baker cellulose vs. 2.1% from the S & S cellulose at the same temperature. Quantitatively similar results were reported by Shafizadeh et al. [31] in comparing levoglucosan yields from Baker and Whatman celluloses under vacuum with fairly rapid heating to 400°C. Acid washing of the Whatman cellulose followed by rinsing, all at room temperature, was found to increase the yields of levoglucosan to essentially the same level as those from the Baker cellulose. Inasmuch as the celluloses listed in Table 4 have somewhat different ash contents, the different product distribution may be due to the well-known effect of inorganic cations in reducing tar yields by promoting the parallel char formation step *. Both celluloses show very nearly the same fraction of the weight of the cellulose fed (about 50%) appearing as levoglucosan or its equivalent as hydroxyacetaldehyde. Whatever the reason for the inconsistent primary pyrolysis behavior of different celluloses—Shafizadeh et al. [31] could offer no definite explanation in their work—it is likely that the levoglucosan formation step occurs more readily in the Baker cellulose, given the 95% yield of volatiles. The Baker cellulose apparently shows a much slower decomposition rate of levoglucosan, and the product may contain an oligosaccharide fraction. The tar from this cellulose was much denser (specific gravity 1.6) and much more viscous than that from wood or S & S cellulose **. Shafizadeh and Lu [32] showed that a significant uncatalysed polymerization of levoglucosan is possible when it is heated under nitrogen even at relatively low temperatures for a period of time.

DISCUSSION

Various schemes have been proposed for the pyrolytic decomposition of cellulose. The simple one proposing two parallel paths to char and gases or to volatiles given in Fig. 1, is based on the results of a good deal of earlier work, as discussed previously. More complex schemes involving many reaction paths have been proposed by others, e.g. by the workers at SERI [1]. However, we will consider only the simple representation of Fig. 1, and apply it to the data available for cellulose pyrolysis at 500°C, but add to it a pathway as shown for decomposition of tar to gas, inasmuch as extensive results for the fast pyrolysis of cellulose indicate that little char results from secondary tar decomposition, e.g. see Table 4 or Fig. 4.

According to this model and the scheme proposed in Fig. 2, the initial thermal decomposition of cellulose proceeds by disruption of the cellulose polymer chain, primarily at the glucosidic bond between glucose monomeric units, to form various anhydrosugar derivatives, the most prevalent being levoglucosan. While the mechanism of Fig. 2 apparently assumes the hydration of a levoglucosan unit and its subsequent decomposition, it may be possible for the proposed mechanism to occur also by direct cleavage and rearrangement of the levoglucosan structure without the initial hydration–dehydration step proposed in Fig. 2.

---

* However, the short reaction time characteristic of flash pyrolysis minimizes this effect, and below about 1% ash content there appears to be little significance to ash content among different biomass materials [38].

** Recent tests with Avicel microcrystalline cellulose have shown behavior similar to that of the Baker cellulose, again in agreement with Shafizadeh et al. [31].

Evaluation of the first-order rate constants using the values proposed by Shafizadeh [30]. together with values for the first-order decomposition of tars deduced from our own fast pyrolysis data (k_T) [7] gives the following values at 500°C: $k_i = 8.7 \cdot 10^4$ min^{-1}. $k_v = 981$ min^{-1}. $k_c = 61$ min^{-1}, $k_T = 32$ min^{-1}.

The path to form volatiles. presumably anhydrosugars and their decomposition products. is clearly strongly favored at 500°C and higher temperatures over the char forming reaction. and this favorable ratio of the parallel routes to form liquids rather than char is supported approximately by the ratio of products formed as shown in Table 4. While tar cracking to gases is also occurring, it is not a major process at 500°C and for short reaction times.

The expected maximum possible yield of hydroxyacetaldehyde at 500°C from cellulose pyrolysis can be estimated as follows. Assume that the levoglucosan content represents cellulose following the favored route but which has not decomposed further. From extensive work done by Funazukuri [39] using the same apparatus in our laboratory and the same S & S cellulose, the levoglucosan yield can be determined from the plot shown in Fig. 3. The char yield is assumed to arise from the alternative primary decomposition path shown and not from secondary tar decomposition. Results from wood pyrolysis [6] show no increase in char yield at higher temperatures, but do show gas yields increasing in direct proportion to the decrease in liquid yield. On examination, the char product from our flash pyrolysis process has much the same particle shape and size as the biomass feed, although it is only about 10% or less of the original mass, thus suggesting a primary product. Char yield can be estimated from Table 4 or from other more extensive results (shown in Fig. 4) obtained in our fluidized bed reactor by both Funazukuri [39] and by Scott and Piskorz [6]. Similarly, the yield of furan compounds is not likely to occur by the mechanism of Fig. 2, but by an alternative liquid-forming process, for example, similar to the alternative mechanism proposed by Shafizadeh and Lai for furan ring formation [26]. The acetic acid formed can also be assumed to arise almost entirely from the hydroxyacetaldehyde, perhaps by a dehydration–hydration sequence through ketene as proposed by Kang et al. [34]. Further, the mechanism of Fig. 2 does not provide for CO_2 formation, and the results of Shafizadeh and Lai [26] suggest that in the absence of catalysts both hydroxyacetaldehyde and CO_2 arise mainly from the C-1 and C-2 positions. Therefore, CO_2 yield can be assumed to represent also cellulose which does not participate in the decomposition scheme of Fig. 2. This conclusion is supported also by the fact that CO_2 yield reaches a maximum value from both wood and cellulose at about 525°C under fast pyrolysis conditions indicating that it is not a product of secondary tar decomposition. This is in contrast to the yield of CO which increases steadily and rapidly as temperature increases [6,7,39].

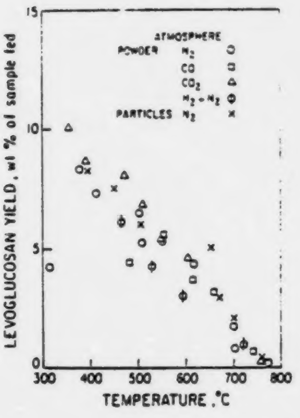

Fig. 3. Yield of levoglycosan from cellulose (4% moisture) in fast pyrolysis in a fluidized bed at atmospheric pressure; from Funazukuri [39].

The net cellulose which does decompose by the proposed scheme can then be estimated by subtracting the levoglucosan yield, the cellulose equivalent of the carbon in the char (92.8% carbon), the cellulose equivalent of the CO_2, and the cellulose equivalent of the furans. On the basis of 6.4% levoglucosan yield, 8% char, 5.9% CO_2 and 0.25% furans, the net cellulose reacting to give liquid products would be 66.8% of that fed. The maximum yield of hydroxyacetaldehyde assuming decomposition of anhydrosugars according to Fig. 2 is 37% of this or 24.7%. The normalized yield of hydroxyacetaldehyde is 19% or 77% of the maximum which might be expected. Similar conversions can also be predicted at 450°C and 550°C from the cellulose pyrolysis data given in Table 1.

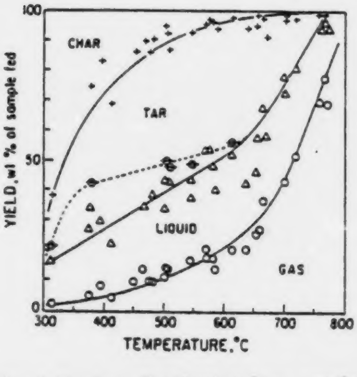

Fig. 4. Product distribution from pyrolysis of cellulose particles in a fluidized bed (nitrogen, atmospheric pressure, 4% moisture). ○, gas; △, gas + volatile liquid; ⊖, gas + volatile liquid + levoglucosan; +, gas + volatile liquid + tar [39].

It is possible to conclude from these results that the decomposition of cellulose to liquid products at short reaction times and high temperatures (say above 450°C) does not proceed in a random chaotic fashion but instead follows a highly preferred route very similar to that shown in Fig. 2. in which hydroxyacetaldehyde is a primary decomposition product of monomer cleavage. Because no other C_2 or C_3 product appears in the same yield as hydroxyacetaldehyde, it is likely that the hydroxyacetaldehyde is an intermediate produced early in the decomposition process.

Examination of bond energies in the monomer as reported by Frankiewicz [40] suggests that equal bond energies can be assigned to all the C–C or C–O bonds in the ring structure. Reported interatomic distances for β-D-glucose, however [41], show slightly greater lengths for the C-2 to C-3 bond and for the C-1 to O-ring linkage than for other similar bonds. Madorsky et al. [18,20] have also pointed out that the C–O bonds are thermally less stable than C–C bonds. These small differences lend support to the hypothesis that initial ring cleavage of the cellulose monomer tends to occur most frequently at these two locations, yielding a two-carbon fragment and a four-carbon fragment, the two-carbon fragment rearranging to a relatively stable product, hydroxyacetaldehyde, while the four-carbon fragment can undergo a number of rearrangement, dehydration, decarbonylation, scission and condensation reactions to yield a variety of lower molecular weight products, among which carbonyl and hydroxycarbonyl compounds are the most stable.

In the scheme shown in Fig. 2, the rearrangements indicated in the right hand sequence should be the most likely to occur on energy grounds, according to Benson's rules [42]. Of the other postulated reaction products, 1-hydroxypropanone (acetol) should be favored over the alternative possibility of hydroxypropanals. Both these compounds were reported by Elliott [10], with the 1-hydroxypropanone amount being about three times that of the hydroxypropanals, as would be predicted from the energetics of the mechanism shown in Fig. 2.

Finally, the estimate of theoretical yields of hydroxyacetaldehyde was based on the assumption of complete cleavage of the cellulose chain to monomeric forms. Obviously, this is unlikely to be the case, particularly as some higher molecular weight material is always observed to be present in the liquid product [28]. It follows, therefore, that the potential maximum yield of hydroxyacetaldehyde must be less than 37%, and the evidence for the preferred decomposition mechanism of the monomer ring becomes even more convincing.

It is also a matter of considerable interest that the cellulose in wood appears to follow the same monomeric decomposition mechanism, although the lower yield of anhydrosugars obtained in the fast pyrolysis of wood as compared to some pure celluloses suggests that the initial cleavage of the ring may be more readily attained in the case of wood. A number of analyses of various pyrolysis oils produced from poplar wood have all shown hydroxyacetaldehyde yields which are comparable to those reported here (see for example Table 1). Further, oil which had been stored for a lengthy period showed little change in hydroxyacetaldehyde content, indicating the stability of this material in solution. This is shown by the gas chromatographic analyses given in Table 1 which were both done at the same time, but the oil from Run 27/29 had been stored at room temperature for 16 months, while that from Run 59 was fresh.

ACKNOWLEDGEMENTS

The authors are pleased to acknowledge the financial support from the ENFOR Program of the Canadian Forestry Service, Environment Canada, from the National Research Council of Canada, and from the Natural Sciences and Engineering Research Council of Canada which made this work possible. The advice and encouragement of Dr. Ralph P. Overend of the National Research Council of Canada are also gratefully acknowledged.

REFERENCES

1 J. Diebold, Workshop Summary, Proc. Specialists Workshop on Fast Pyrolysis of Biomass, Copper Mountain, CO, October 19–22, 1980, Solar Energy Research Institute SERI/CP-622-1096, Golden, CO, 1980.
2 J.L. Kuester, in Biomass as a Non-Fossil Fuel Source, Proc. ACS Symposium, Honolulu, HI, April, 1979.
3 M. Antel, Adv. Solar Energy, 1 (1982) 61.
4 J.A. Knight, D.R. Hurst and L.W. Elston, in D.A. Tillman, K.V. Sarkanen and L.L. Anderson (Editors), Fuels and Energy from Renewable Resources, Academic Press, New York, 1977, p. 169.
5 K.W. Pober and H.F. Bauer, in L.L. Anderson and D.A. Tillman (Editors), Fuels from Wastes, Academic Press, New York, 1977, p. 73.
6 D.S. Scott and J. Piskorz, Can. J. Chem. Eng., 60 (1982) 666.
7 D.S. Scott and J. Piskorz, Can. J. Chem. Eng., 62 (1984) 404.
8 D.S. Scott and J. Piskorz, in H. Egnéus and A. Ellegard (Editors), Bio. Energy 84, Vol. 3, Elsevier, London, 1985, p. 15.
9 Y. Solantausta and P. McKeough, in H. Egnéus and A. Ellegard (Editors), Bio. Energy 84, Vol. 3, Elsevier, London, 1985, p. 1.
10 D.C. Elliott, International Energy Agency Co-operative Project D-1, Biomass Liquefaction Test Facility, National Energy Administration, Stockholm, Vol. 4.
11 H. Ménard, D. Belanger, G. Chauvette, J. Khorami, M. Grisé, A. Martel, E. Potvin, C. Roy and R. Langlois, in S. Hasnain (Editor), Proc. 5th Bioenergy R & D Seminar, Elsevier, New York, 1984, p. 418.
12 G.M. Nicolaides, The Chemical Characterization of Pyrolysis Oils. MASc Thesis, Dept. of Chemical Engineering, University of Waterloo, Waterloo, 1984.
13 P. Elving and B. Warskowsky, Anal. Chem., 19 (1947) 1006.
14 M.J. Antal, Jr., H.L. Friedman and F.E. Rogers, Combust. Sci. Technol., 21 (1980) 141.
15 F.J. Kilzer and A. Broido, Pyrodynamics, 2 (1965) 151.
16 A. Broido, in F. Shafizadeh, K. Sarkanen and D. Tillman (Editors), Thermal Uses and Properties of Carbohydrates and Lignins, Academic Press, New York, 1976, pp. 19–36.

17 D.F. Arseneau, Can. J. Chem., 49 (1971) 632.
18 S.L. Madorsky, V.E. Hart and S. Straus, J. Res. Natl. Bur. Stand., 56 (1956) 343.
19 R.F. Schwenker, Jr. and E. Pascu, Ind. Eng. Chem., 50 (1958) 91.
20 S.L. Madorsky, V.E. Hart and S. Straus, J. Res. Natl. Bur. Stand., 60 (1958) 343.
21 J.B. Berkowitz-Mattuck and T. Noguchi, J. Appl. Polym. Sci., 7 (1963) 709.
22 G.A. Byrne, D. Gardner and F.H. Holmes, J. Appl. Chem., 16 (1966) 81.
23 P.C. Lewellen, W.A. Peters and J.B. Howard, Sixteenth International Symposium on Combustion, Massachusetts Institute of Technology, August, 1976.
24 F. Shafizadeh, Adv. Carbon Chem., 23 (1968) 419.
25 S. Glassner and A.R. Pierce, Anal. Chem., 37 (1965) 525.
26 F. Shafizadeh and Y.Z. Lai, J. Org. Chem., 37 (1972) 278.
27 H.-R. Schulten and W. Görtz, Anal. Chem., 50 (1978) 428.
28 R.J. Evans, T.A. Milne and M.N. Soltys, in Proc. 16th Biomass Thermochemical Conversion Contractors Meeting, Battelle Pacific Northwest Lab., PNL-SA-12403, 1984, p. 349.
29 A.G.W. Bradbury, Y. Sakai and F. Shafizadeh, J. Appl. Polym. Sci., 23 (1979) 3271.
30 F. Shafizadeh, J. Anal. Appl. Pyrol., 3 (1982) 283.
31 F. Shafizadeh, R.H. Furneaux, T.G. Cochran, J.P. Scholl and Y. Sakai, J. Appl. Polym. Sci., 23 (1979) 3525.
32 F. Shafizadeh and Y.L. Lu, Carbohydr. Res., 29 (1973) 113.
33 A.E. Lipska and F.A. Wodley, J. Appl. Polym. Sci., 13 (1969) 851.
34 J.C. Kang, P.H. Chen and W.R. Johnson, in F. Shafizadeh, K.V. Sarkanen and D.A. Tillman (Editors), Thermal Uses and Properties of Carbohydrates and Lignins, Academic Press, New York, 1976, p. 261.
35 H.-R. Schulten, U. Bahr and W. Görtz, J. Anal. Appl. Pyrol., 3 (1981) 137.
36 H.-R. Schulten, U. Bahr and W. Görtz, J. Anal. Appl. Pyrol., 3 (1981/82) 229.
37 O. Beaumont and Y. Schwob, Ind. Eng. Chem. Process Des. Dev., 23 (1984) 637.
38 D.S. Scott, J. Piskorz and D. Radlein, Ind. Eng. Chem. Process Des. Dev., 24 (1985) 581.
39 T. Funazukuri, Ph.D. Thesis, Dept. of Chemical Engineering, University of Waterloo, Waterloo, 1983.
40 T.C. Frankiewicz, Proc. Specialists Workshop on Fast Pyrolysis of Biomass, Copper Mountain, CO, October 19–22, 1980, Solar Energy Research Institute SERI/CP-622-1096, Golden, CO, 1980, pp. 123–136.
41 L.E. Sutton (Editor), Table of Interatomic Distances and Configuration in Molecules and Ions, The Chemical Society, London Spec. Pub. 11, 1958.
42 S.W. Benson, Thermochemical Kinetics, Wiley, New York, 2nd ed., 1976.

APPENDIX 6-B

On the Presence of Anhydro-Oligosaccharides in the Sirups from the Fast Pyrolysis of Cellulose

ON THE PRESENCE OF ANHYDRO-OLIGOSACCHARIDES IN THE SIRUPS FROM THE FAST PYROLYSIS OF CELLULOSE

DESMOND ST.A.G. RADLEIN *

Department of Chemistry, University of the West Indies, Mona,
Kingston, Jamaica W.I.

ANNA GRINSHPUN, JAN PISKORZ and DONALD S. SCOTT

Department of Chemical Engineering, University of Waterloo,
Waterloo, Ontario, Canada N2L 3G1

SUMMARY

Analysis by HPLC of the carbohydrate fraction of sirups obtained from the fast pyrolysis of Avicel cellulose (82% yield of organic liquid) indicated the presence of a considerable amount of an unknown oligosaccharide, presumably a di-saccharide. If this was formed from recombination of levoglucosan (the major product) it would be expected to be a mixture of di-saccharides, with maltosan as a major component. If the unknown di-saccharide was a primary product it should have a cellobiose structure. Maltosan and cellobiosan were synthesized and the unknown di-saccharide was identified as almost entirely cellobiosan in yields varying from 6-15% of the sirup product. It is postulated that the production of cellobiosan as a primary pyrolysis product lends support to recent theories that cellulose is a polymer of cellobioside units rather than of glucoside units.

ON THE PRESENCE OF ANHYDRO-OLIGOSACCHARIDES IN THE SIRUPS FROM THE FAST PYROLYSIS OF CELLULOSE

DESMOND ST.A.G. RADLEIN *

Department of Chemistry, University of the West Indies, Mona,
Kingston, Jamaica W.I.

ANNA GRINSHPUN, JAN PISKORZ and DONALD S. SCOTT

Department of Chemical Engineering, University of Waterloo,
Waterloo, Ontario, Canada N2L 3G1

Various authors have previously reported or speculated on the existence of oligosaccharides and their anhydro derivatives in the pyrolytic sirups obtained from cellulose.(1) However, to the best of our knowledge, no identification of specific oligomers has ever been made. For example, Shafizadeh and Fu [2], noted that these materials could be hydrolysed to glucose under acidic conditions and so simply lumped them all together under the category "Hydrolysable Materials".

In the course of development of a HPLC method for the analysis of pyrolysis sirups from biomass, a large peak - which was second in size only to that of levoglucosan in some samples - was observed, particularly in those sirups obtained from the fast pyrolysis of microcrystalline cellulose (Avicel PH-102 for 0.5 seconds at 500°C in a fluidized sand bed). Details of the Waterloo Fast Pyrolysis process used to prepare these sirups have been given in earlier publications [3]. A typical chromatogram of the oil is shown in Figure 1. On the basis of its retention time and the known characteristics of the column (Aminex HPX-87H

---

(1) Following Antal [1], the viscous liquids obtained from the pyrolysis of cellulosic materials have been termed "sirups" - a term which, with its peculiar spelling, is perhaps more descriptive than "oil" or "tar".

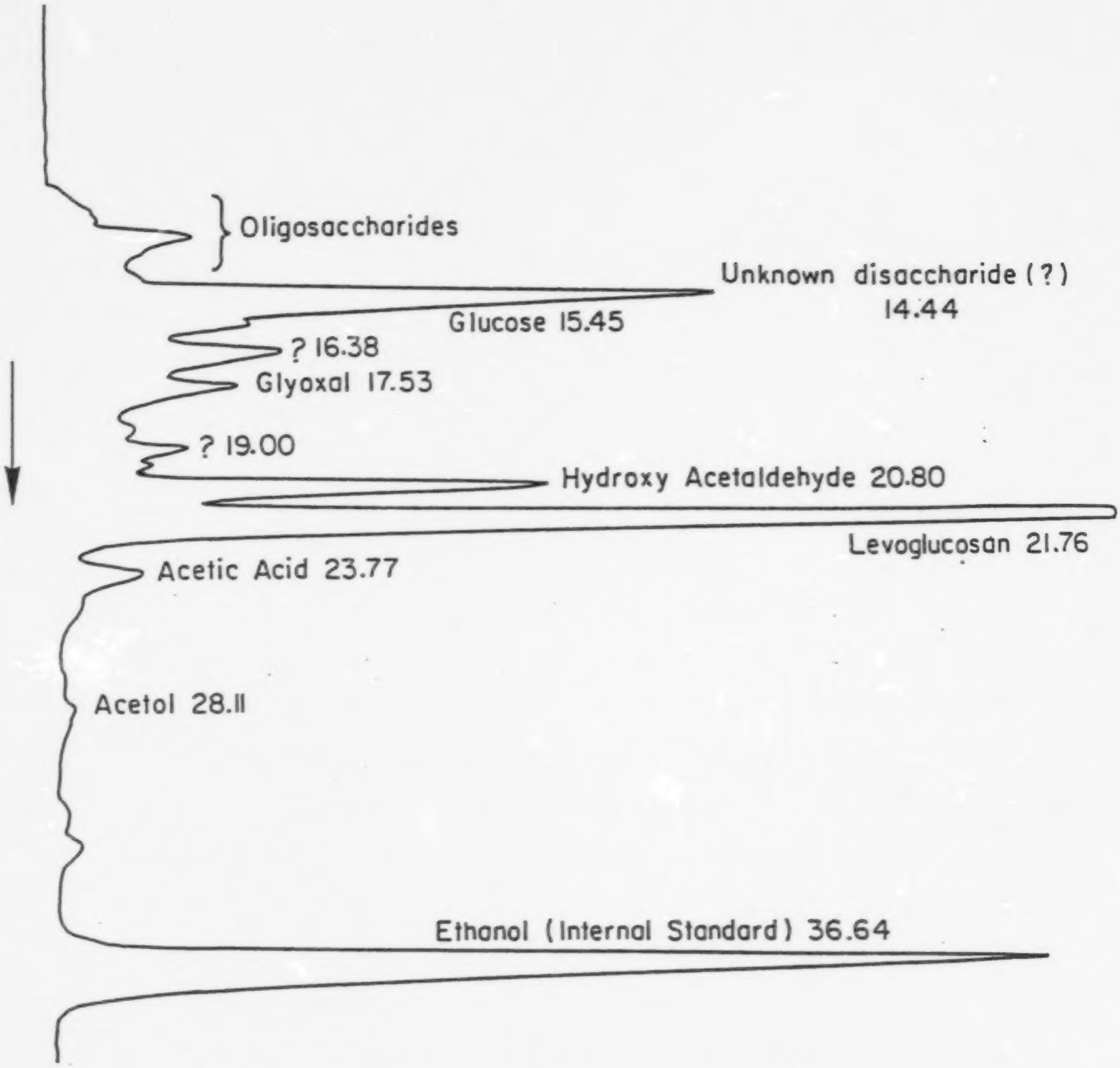

Figure 1 HPLC Chromatogram of Pyrolysis Oil from Avicel Cellulose, Run 66, Oil Yield (water free) 82.5%, Aminex HPX-87H ion exchange column, 2.25 ml/min, eluant 0.07 N H_3PO_4 at 25°C

ion exchange resin), the unknown material appeared to be oligomeric and probably a disaccharide or a disaccharide derivative. Oligomers in cellulose pyrolysis sirups have been regarded as formed by random condensation of primary monomeric units [2]. There is a wide range of possible oligosaccharides which can be formed by polymerisation of levoglucosan, which is the dominant monomeric entity in sirups derived from microcrystalline cellulose. For instance, Wolfrom et al. [4,5] studied the thermal polymerisation of levoglucosan and were able to identify various anhydro-disaccharides and tri-saccharides along with higher polymeric products in the resulting pyrodextrins. They also found that both α-D-1,4- and β-D-1,4-glucosidic links were present in both the dimers and the higher polymeric products. Other authors [6,7] have shown that the polymers contain about 50% of 1,6-glucosidic links.

Wolfrom et al. [4] identified four 1,6-anhydro-disaccharides in the products from their pyrolysis of levoglucosan (1,6-anhydro-maltose, 1,6-anhydro-kojibiose, 1,6-anhydro-sophorose and 1,6-anhydro-cellobiose). Although the ratios of yields of these four anhydro-disaccharides can only be approximately estimated from the results reported, it appears that 1,6-anhydro-maltose (maltosan) was obtained in the largest yield, possibly by a factor of three greater than any of the other disaccharides, which were all recovered in comparable amounts.

These facts can be explained by the mechanistic proposals of Houminer and Patai [8]. In particular, the predominance of maltosan among the dimers can be explained by the probable initial reaction which is a nucleophilic attack of a hydroxyl of one levoglucosan molecule on C-1 of another which would lead to inversion at that site and the formation of an α- instead of a β-glucosidic linkage (Figure 2). On the other hand, in cellobiosan (Figure 3) the monomers are linked in the β-D-glucosidic configuration typical of cellulose.

In summary, the unknown compound was concluded to be likely an oligomer of levoglucosan, and more specifically that it was likely to be a dimer, on the basis of its retention time. If this is the case, and if it arises by recombination of levoglucosan, then it is likely to be a mixture of anhydro-disaccharides with maltosan as a major component. Nevertheless, the large amount of the unknown product obtained in the cellulose-derived sirups also suggests that it might be primary in which case cellobiosan might be expected to predominate. If this were so, then it would be implied that, at least under fast pyrolysis conditions, the depolymerisation of cellulose is not the simple "unzipping" reaction which is widely held to be the case [1]. It was therefore of interest to identify and quantify this product.

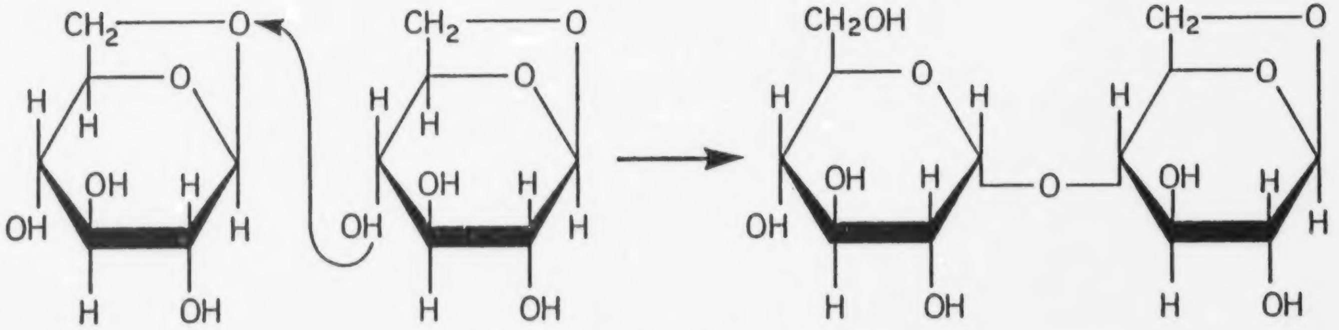
CH₂
O
OH
H
CH₂OH

Figure 2 Formation of Maltosan from Levoglucosan

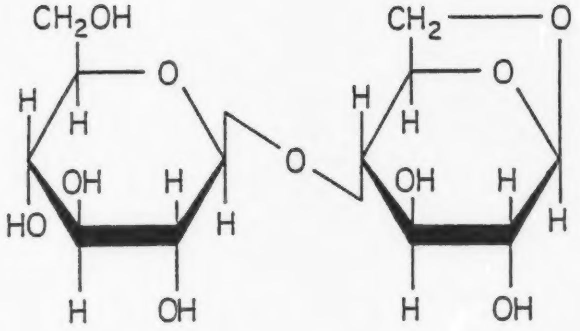
CH2OH
O
H
H
OH
H
HO
H
O
H
OH
CH2
O
O
H
H
OH
H
H
H
OH

Figure 3 Schematic Structure of Cellobiosan

Experimental

Cellobiosan was synthesized via the following scheme.

Cellobiose	Acetylation [9]
↓	
Octa-acetyl cellobiose	Glycosidation [10]
↓	
Phenyl hepta-acetyl cellobioside	Deacetylation [11]
↓	
Phenyl - cellobioside	Cyclisation [12]
↓	
Cellobiosan	

A similar procedure was followed for the preparation of maltosan starting from maltose.

In the first step, the procedure of Wolfrom and Thompson [9] was followed. The yield of the octa-acetyl maltose obtained was 115%, m.p. 155°C to 158°C (reported 158°C to 159°C). Similarly, the yield of octa-acetyl cellobiose was 110%, m.p. 198°C to 200°C (reported 202°C).

The phenyl hepta-acetyl derivatives were prepared from the procedure given by Asp and Lindberg [10]. The yield of the phenyl hepta-acetyl-β-maltoside was 42%, m.p. 155°C to 156°C (reported 155°C to 156°C). A yield of 33% of the phenyl hepta-acetyl-β-cellobioside was obtained, m.p. 200°C to 202°C (reported 206°C to 208°C).

Deacetylation of the phenyl-β-maltoside and phenyl-β-cellobioside was done using the method of Wolfrom and Thompson [11]. Yields of both products were about 50%, and the purity as reflected in melting points was not high. Great difficulty was experienced in recrystallizing these compounds, and indeed only the phenyl-β- cellobioside could be recovered in this way (yield 18%, m.p. 204°C to 206°C, reported 211°C to 213°C). No melting point value for the phenyl-β-maltoside could be found in the literature, possibly because of the difficulty in obtaining a crystaline product. Indeed, it was used as a sirup in the final step of this work.

The final cyclisation was carried out according to the procedure of Montgomery et al.[12]. The final yields of cellobiosan and maltosan were 50% and 60% respectively, based on the initial starting amounts of phenyl-cellobioside and phenyl-maltoside. Chromatograms of the two products are shown in Figures 4a and 4b. The major impurities are readily identified as levoglucosan as well as the initial cellobiose and maltose. A peak of H_2SO_4 appears, since it was used through the final step of preparation. The peak at 19.72 was not identified.

As a confirmation of the chromatographic identification, hexa-acetyl-cellobiosan was obtained by acetylation of 0.5 g of obtained cellobiosan using the method of Wolfrom and Thompson [9] with acetic anhydride and pyridine. The hexa-acetate was purified by recrystallization from water. The final product had a melting point of 144°C (reported 144°C).

The two isomers, maltosan and cellobiosan, have similar retention times on the HPLC column used. However, they were sufficiently different that a preliminary identification of their presence in the cellulose-derived sirups could be made. From examination of Figure 1 and of similar chromatograms, it was found that the unknown appeared to correspond more closely to cellobiosan and its concentration ranged from 6-15 mass % in

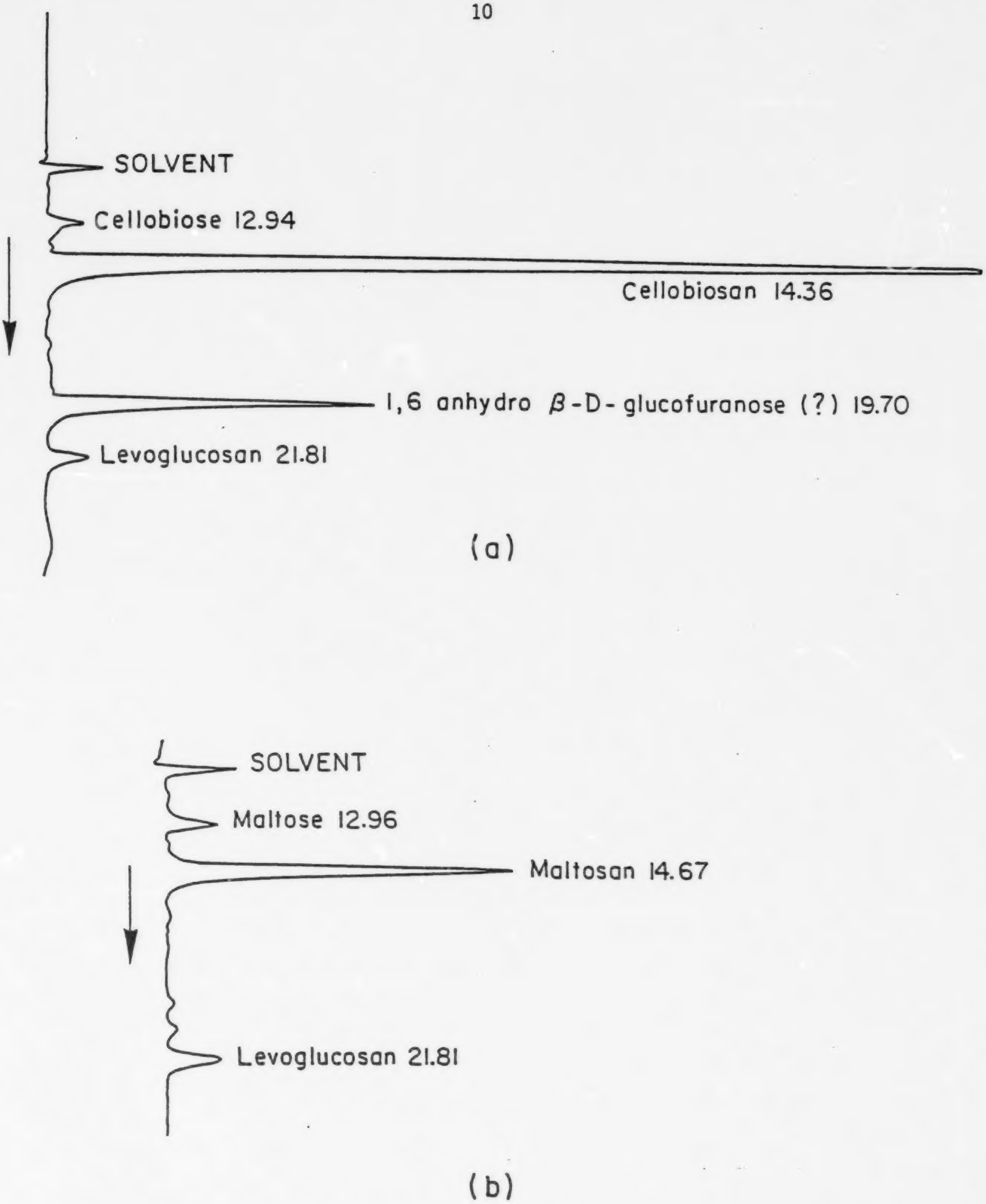

Figure 4 (a) Chromatogram of Cellobiosan Product
(b) Chromatogram of Maltosan Product
HPLC conditions as for Figure 1

various sirups obtained from the fast pyrolysis of Avicel microcrystalline cellulose. All sirups were produced using the fluid bed fast pyrolysis method developed by Scott and Piskorz [3]. The yield depended primarily on pyrolysis temperature, showing a decrease with increasing temperature over the range of 450°C to 550°C. Much smaller amounts of maltosan (<1%) were detected in some samples.

In order to obtain a more definite confirmation of the presence of large amounts of cellobiosan, gas chromatography of the trimethylsilylated derivatives of levoglucosan, maltosan and cellobiosan was carried out using a Hewlett-Packard model 5890/5970 GC/MS unit with a HP capillary column (12 m long, 0.20 mm inside diameter with 0.33 micron cross linked methyl silicone film). Good resolution was obtained for the three components using the following procedure.

To 10-20 mg. of the anhydrosugar was added 1 ml. of TRI-SILZ reagent [N-trimethylsilylimidanzole (TMSI) in dry pyridine], and the vial shaken until the sugar was dissolved. A sample was injected with the injection port at 250°C, initial oven temperature 150°C, heating rate 30°C/min with a final temperature of 250°C and a total time of 15 minutes. Retention times were pyridine, 0.9 min; imidazole, 1.2 min; TMSI, 1.4 min; levoglucosan, 3.45 min; maltosan 14.68 min; cellobiosan, 15.34 min. The mass spectra of the two silylated disaccharides were very similar, and therefore retention time was the principal identification. The separation achieved in a mixture of levoglucosan, maltosan and cellobiosan is shown in Figure 5.

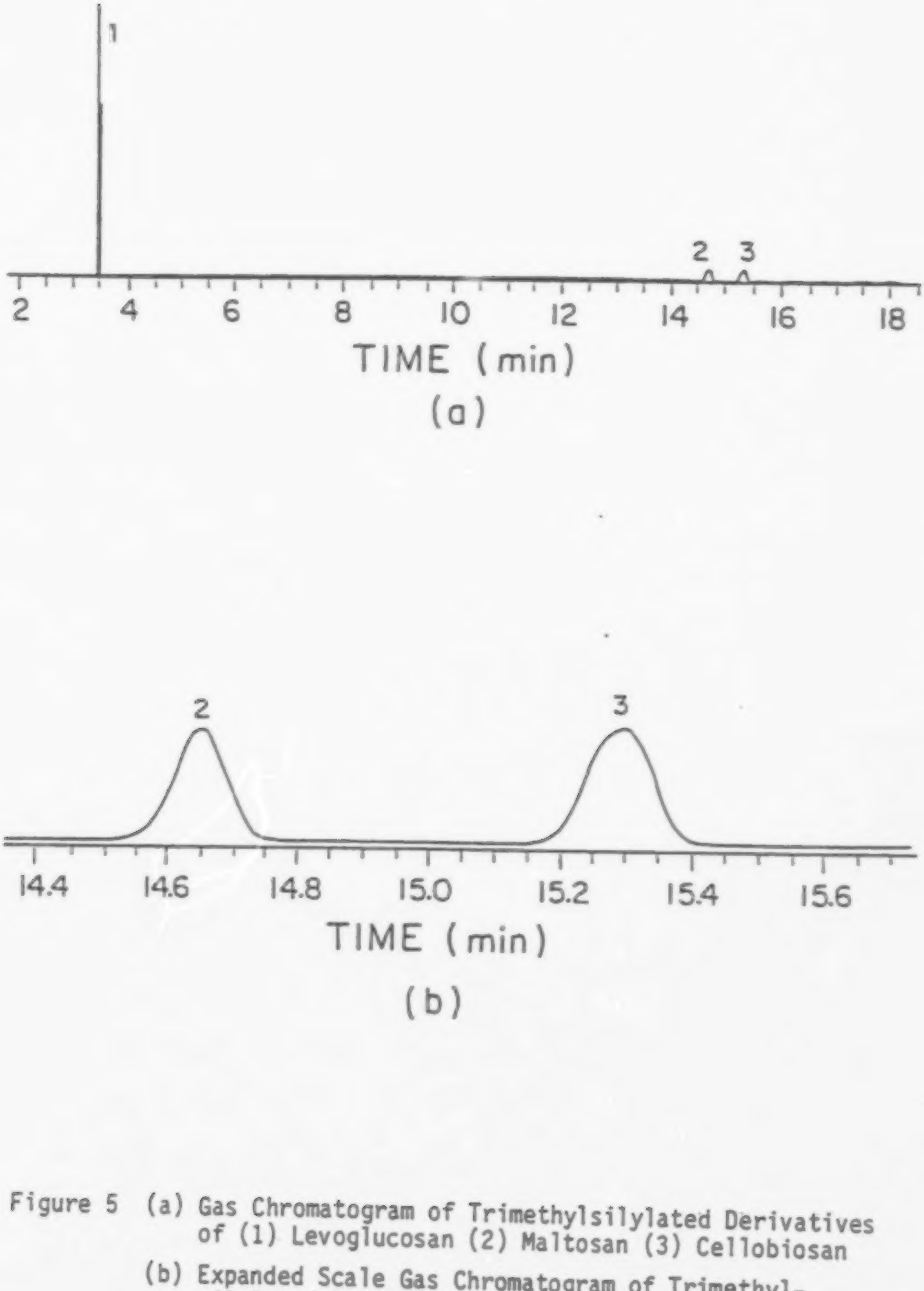

Figure 5 (a) Gas Chromatogram of Trimethylsilylated Derivatives of (1) Levoglucosan (2) Maltosan (3) Cellobiosan

(b) Expanded Scale Gas Chromatogram of Trimethylsilylated Derivatives of Maltosan and Cellobiosan

Three typical tars obtained from the fluidized bed pyrolysis of Avicel cellulose P-102 at temperatures from 400°C-500°C were selected for analysis, since the yield of disaccharides is highest at the lower pyrolysis temperatures. Chromatograms of the silylated tar samples for the region corresponding to disaccharides are shown in Figure 6. In sample P-62, obtained at 500°C from a large (3 kg/hr. feed rate) fluid bed unit, the major peak corresponding to cellobiosan and the minor peak corresponding to maltosan are readily identifiable. In addition, at least three other minor peaks of about the same yield as maltosan are apparent, probably representing other anhydro-disaccharides. Sample 14, obtained at 475°C from a small 50 gram/hr. fluid bed unit, shows a very similar analysis to sample P-62. Sample 20, obtained from pyrolysis at 400°C in the 50 gm/hr. unit, shows a more complex chromatogram, but again cellobiosan and maltosan are readily identified, with the cellobiosan remaining the only major anhydro-disaccharide product.

The TMSI derivatives of the disaccharides are known to be very volatile and to be thermally stable. Moderate amounts of water (these pyrolysis tars contained less than 10% water) do not affect the silylation reaction, and very little anomerisation has been observed. It can be concluded therefore, that the GC results confirm the fact that the major anhydrodisaccharide produced in the rapid pyrolysis of Avicel cellulose is cellobiosan with very much smaller amounts of other anhydro-disaccharides (little more than traces) being present.

As another test of the analytical results obtained, levoglucosan was polymerized according to the same procedure used by

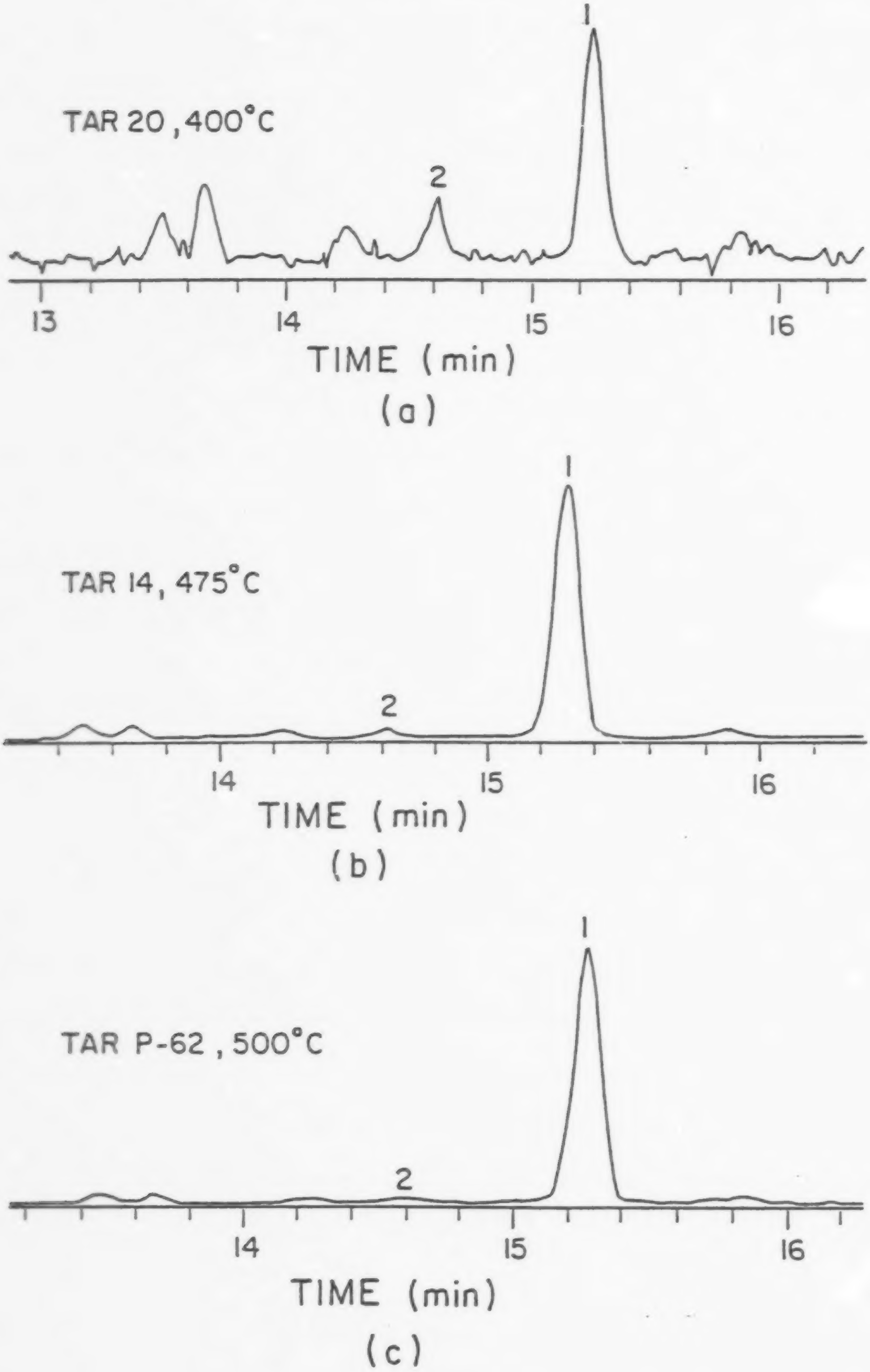

Figure 6 Gas Chromatogram of Trimethylsilylated Disaccharides in Three Pyrolysis Tars from Avicel Cellulose (1) Cellobiosan (2) Maltosan

Wolfrom et al. [5] (20 minutes heating at 230°C on an oil bath) and the disaccharide portion of the product was analyzed by both HPLC and GC/MS. In addition, in order to more closely approximate the conditions used in our flash pyrolysis reactor, another sample of levoclucosan was polymerized by heating in a furnace at 400°C for 1.5 minutes. At longer times, extensive charring occurred, but at 1.5 minutes reaction time a red-brown liquid resulted which on cooling became a glassy crystalline solid. (It was not possible to feed levoglucosan to our fluidized bed reactor, both because of the quantities required, and because of the relatively low melting point of the levoglucosan). Both reaction products were dissolved in water and then analyzed by HPLC (Aminex 87H column at 60°C with phosphoric acid eluent), and by GS/MS after reaction with TMSI to form the trimethylsilyl derivatives.

The HPLC chromatograms of the oligiosaccharide region of the two products showed qualitatively a very similar pattern, but one that was very different from that of the pyrolysis tars. Apart from unreacted levoglucosan, a major peak which appeared to represent two or more anhydro-disaccharides was obtained, as well as at least three lesser peaks in the disaccharide region. The HPLC analysis was carried out at the same conditions as those shown in Figure 1, except that the column temperature was held at 60°C to reduce analysis time (retention times are reduced by a factor of 1.99).

The two reaction products were also analysed by trimethylsilylation using the same procedure as that described previously for the cellulose pyrolysis tar products. Again the two polymerization products showed very similar GC patterns with good resolution of individual disaccharides. The portions of the chromatogram corresponding to the disaccharide retention zone are shown in Figure 7. The peaks corresponding to cellobiosan and maltosan are readily identifiable for both products, with maltosan apparently present in yields two or more times that of cellobiosan. In addition, four more disaccharides are also shown to be present in comparable yields. Wolfrom et al. [4] reported two anhydro-disaccharides in addition to cellobiosan and maltosan. From their data, it is probable that peak 3 is silylated kojibiosan and peak 4 is silylated sophorosan. Peak 6 is likely a disaccharide, possibly silylated iso-maltose or sophorose. In general, the GC analysis shown for the anhydro-disaccharides, for both products obtained by polymerization of levoglucosan of 230°C or 400°C, agrees both qualitatively and approximately quantitatively with that given by Wolfrom et al. [4].

The results obtained for the anhydro-disaccharide contents of pyrolysis tars from cellulose, and of the polymerization product of levoglucosan, show a great difference in yield of products. Therefore it is very unlikely that the high cellobiosan yields obtained in the cellulose pyrolysis tar can be the result of levoglucosan polymerization. In addition, the very low yields from the cellulose pyrolysis tar of other anhydro-disaccharides despite a high yield of levoglucosan also suggests that most of the cellobiosan yield is a primary product of pyrolysis, and not a secondary polymerization product of levoglucosan.

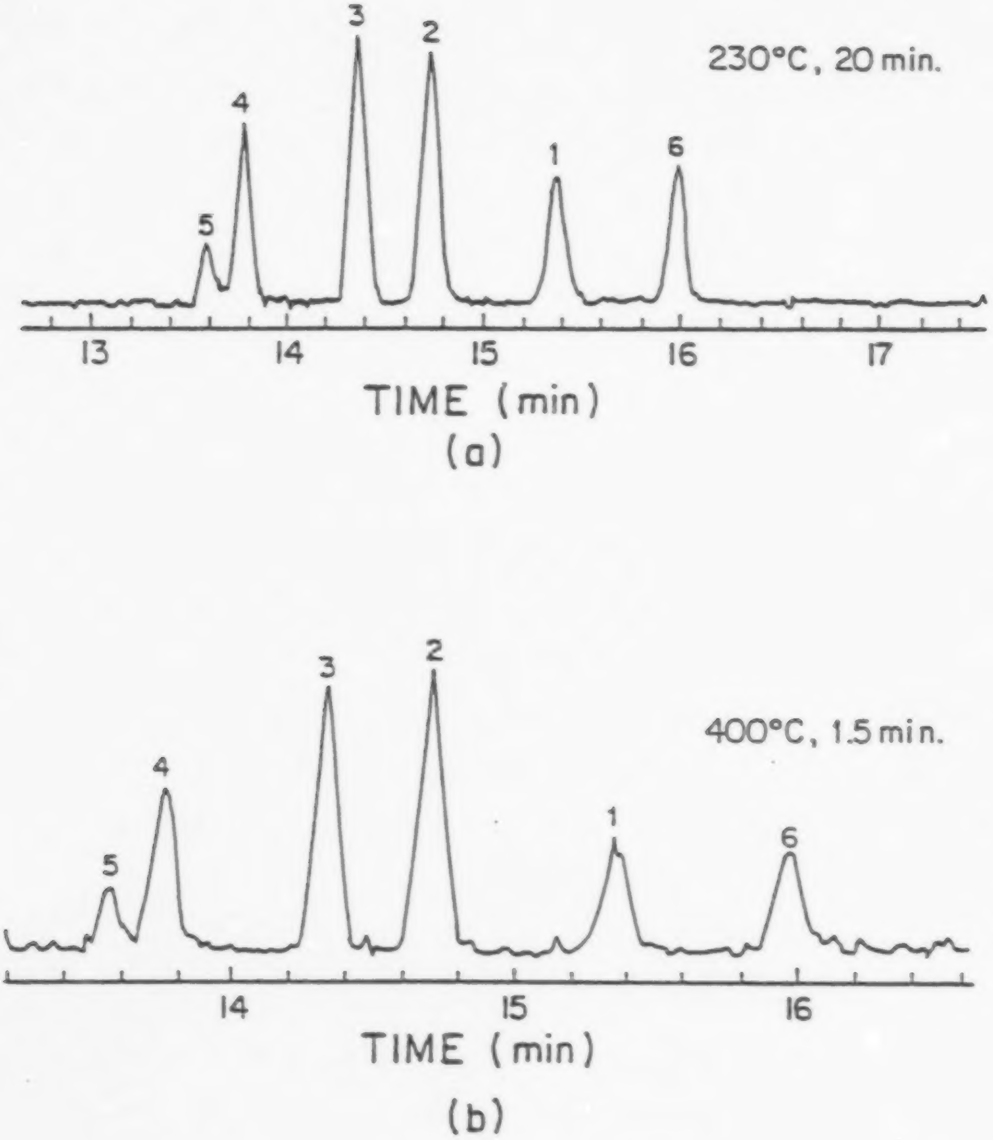

Figure 7 Gas Chromatogram of Trimethylsilylated Disaccharides Produced from Polymerization of Levoglucosan by Method of Wolfram et al. [5]
(1) Cellobiosan (2) Maltosan (3) Kojibiosan(?) (4) Sophorosan(?) (5) Iso-maltosan(?) (6) unknown Disaccharide

Discussion

The thermally induced recombination of levoglucosan is expected to produce more maltosan than cellobiosan, but the apparent near absence of maltosan in the pyrolysis tars obtained from the fast pyrolysis of cellulose, and the presence of relatively large amounts of cellobiosan, suggest that this latter compound is a primary pyrolysis product. The implications are important in speculating concerning the mechanism of rapid thermal depolymerisation of cellulose under conditions of high heating rates. The conventional view, based largely on the results of slow vacuum pyrolysis studies, is that cellulose depolymerises mainly through a concerted "unzipping" sequence of transglycosylation reactions in which levoglucosan monomers are sequentially released from a chain [1]. If cellobiosan is indeed a primary pyrolysis product then its production in such large amounts cannot be explained by such mechanisms. A more suitable mechanism might be the two-step process invoked by Chatterjee and Conrad [13], in which glycosidic bond scission is regarded as the initiation step and levoglucosan formation the propagation step. The former step was found to have the higher activation energy but it might be surmised that at high enough temperatures the initiation reaction is sufficiently fast to generate oligomeric fragments.

There is also interesting evidence that there are inherent tertiary-structural features of cellulose which might encourage the production of dimeric fragments. The conventional view is that cellulose is made up of anhydroglucose as the basic repeating unit with β-1,4-connections between them. Nevertheless, Atalla [14][15] has advanced the proposition that it may be more apt to regard anhydrocellobiose as the basic monomer, especially in the more crystalline forms of cellulose. In other words there may be two different kinds of β-1,4-connection which alternate in the cellulose chain. This can be illustrated as follows:

Conventional View : $G \cdot G \cdot G \cdot G$

Alternative View : $o \; \underbrace{G \; x \; G}_{C} \; o \; \underbrace{G \; x \; G}_{C} \; o$

Here G denotes an anhydroglucose and C an anhydrocellobiose unit. " · " denotes the conventional β-1,4-link while "o" and "x" denote the postulated two kinds of β-1,4-links. This conception was based on a review of Raman and infra-red spectral evidence along with the results of studies of cellulose hydrolysis.

This alternative viewpoint has received strong supporting evidence from an additional NMR study by Earl and VanderHart [16] and from a very recent and comprehensive conformational analytical study by Pizzi and Eaton [17]. These latter authors concluded that:

- Hydrogen bonds are the predominant stabilizing force in cellulose structures;
- The β-glucosidic linkage within a cellobiose-like monomer always has a different conformation from the β-glucosidic linkage that connects it to the preceding and following units along the cellulose chain;
- The cellobioside structure (in methyl cellobioside), rather than the cellobiose structure itself, is the monomer present throughout naturally occurring cellulose.

It should be appreciated that this last conclusion applies both to the crystalline zones as well as to the so-called "amorphous" zones. These authors also proposed that the cellulose chains exist in a helicoidal configuration in the amorphous regions.

Analysis of a series of six sirups obtained by fast pyrolysis of microcrystalline Avicel cellulose at temperatures between 450°C and 550°C gave a mean ratio of levoglucosan to cellobiosan of 2.62±0.46. Analysis of a sample of sirup from pyrolysis of SS-144 cellulose at 500°C gave 2.29 for the same ratio. (SS-144 cellulose which is a product sold for chromatography, contains both crystalline and amorphous zones and gives a significantly different spectrum of products than sirups from Avicel at the same pyrolysis temperature.) This constancy is consistent with the conclusions of Pizzi and Eaton which are outlined above.

We therefore conclude that these pyrolysis results offer strong support for the view of cellulose structure as proposed by Atalla [14][15] and by Pizzi and Eaton [17].

It is not clear at the present time how cellobiosan and other anhydro-disaccharides are removed from the decomposing cellulose and become a part of the liquid tar recovered in the condensers. The very rapid heating and low system total pressure (one atmosphere) would allow some vaporization to occur of pyrolytic fragments even as large as disaccharides. It is also possible that disaccharides could be removed when they form by mechanical entrainment in the tar mist generated on rapid heating of biomass. Further work is planned to investigate this aspect of rapid pyrolysis of biomass for the production of liquids.

REFERENCES

1 M.J. Antal, Jr., Adv. Solar Energy, 1 (1982) 61-112

2 F. Shafizadeh and Y.L. Fu, Carbohyd. Res., 29 (1973) 113-122.

3 D.S. Scott and J. Piskorz, Can. J. Ch. Eng., 62 (1984) 404.

4 M.L. Wolfrom, A. Thompson, R.B. Ward, D. Horton and R.H. Moore, J. Org. Chem., 26 (1961) 4617-4620.

5 M.L. Wolfrom, A. Thompson and R.B. Ward, J. Am. Chem. Soc., 81 (1959) 4623-4625.

6 J. da S. Carralho, W. Prins and C. Schuerch, J. Am. Chem. Soc., 81 (1959) 4045.

7 I.J. Goldstein and T.L. Hullar, Adv. Carbohyd. Chem., 21 (1966) 431.

8 Y. Houminer and S. Patai, J. Polym. Sci., A-1, 7 (1969) 3005-3014.

9 M.L Wolfrom and A. Thompson, Methods in Carbohydrate Chem., 1 (1962) 334.

10 L. Asp and B. Lindberg, Act. Chem. Scand., 6 (1952) 941.

11 M.L. Wolfrom and A. Thompson, Meth. Carbohyd. Chem., 2 (1963) 218.

12 E.M. Montgomery, N.K. Richtmyer and C.S. Hudson, J. Am. Chem. Soc., 65 (1943) 1848.

13 P.K. Chatterjee and C.M. Conrad, Text. Res. J., 36 (1966) 487.

14 R.H. Atalla, "Conformational Effects in the Hydrolysis of Cellulose" in Hydrolysis of Cellulose : Mechanisms of Enzymatic and Acid Catalysis, R.D. Brown and L. Jurasek (eds.), Adv. in Chem. Ser. No. 181, A.C.S. Wash., D.C. (1979) Chap. 3.

15 R.H. Atalla, J.C. Gast, D.W. Sindorf, V.J. Bartuska and G.E. Maciel, J.A.C.S. 102 (1980) 3249

16 W.L. Earl and D.L. VanderHart, J.A.C.S. 102 (1980) 3251

17 A. Pizzi and N. Eaton,
- J. Macromol. Sci. Chem., A21 (1984) 1443
- ibid. A22 (1985) 105
- ibid. A22 (1985) 139

Captions

Figure 1 HPLC Chromatogram of Pyrolysis Oil from Avicel Cellulose, Run 66, Oil Yield (water free) 82.5%, Aminex HPX-87H ion exchange column, 2.25 ml/min, eluent 0.07 N H_3PO_4 at 25°C

Figure 2 Formation of Maltosan from Levoglucosan

Figure 3 Schematic Structure of Cellobiosan

Figure 4 (a) Chromatogram of Cellobiosan Product

(b) Chromatogram of Maltosan Product
HPLC conditions as for Figure 1

Figure 5 (a) Gas Chromatogram of Trimethylsilylated Derivatives of (1) Levoglucosan (2) Maltosan (3) Cellobiosan

(b) Expanded Scale Gas Chromatogram of Trimethylsilylated Derivatives of Maltosan and Cellobiosan

Figure 6 Gas Chromatogram of Trimethylsilylated Disaccharides in Three Pyrolysis Tars from Avicel Cellulose
(1) Cellobiosan (2) Maltosan

Figure 7 Gas Chromatogram of Trimethylsilylated Disaccharides Produced from Polymerization of Levoglucosan by Method of Wolfrom et al.[5]
(1) Cellobiosan (2) Maltosan (3) Kojibiosan(?)
(4) Sophorosan(?) (5) Iso-maltosan(?) (6) unknown Disaccharide

APPENDIX 6-C

Lignin Derived Oils from the Fast Pyrolysis of Poplar Wood

LIGNIN DERIVED OILS FROM THE FAST PYROLYSIS OF POPLAR WOOD

DESMOND ST.A.G. RADLEIN

Dept. of Chemistry, University of the West Indies,
Mona, Kingston, Jamaica, W.I.

JAN PISKORZ and DONALD S. SCOTT

Dept. of Chemical Engineering, University of Waterloo,
Waterloo, Ontario, Canada

SUMMARY

A pyrolysis oil obtained from the fast pyrolysis of poplar wood was subjected to mild hydrolysis and an aqueous and a non-aqueous fraction recovered. The non-aqueous fraction (pyrolytic lignin), a brown powder, was 23% of the oil, or 16% of the wood, corresponding to about 80% volatilization of the lignin content. NMR spectra of this pyrolytic lignin were obtained, and its structure appears to be very similar to that of steam exploded poplar lignin. Methoxy content is relatively high and syringyl units appear to predominate over guaiacyl units. The pyrolytic lignin appears to be somewhat more degraded than steam exploded lignin and is probably lower in molecular weight.

INTRODUCTION

In recent years, a fast pyrolysis process for biomass has been developed at the University of Waterloo with a principal objective of maximizing liquid yields (Waterloo Fast Pyrolysis Process) [1][2][3]. This process uses an atmospheric pressure continuous fluidized bed reactor, and gives yields with wood sawdust feed at optimum conditions (about 500°C and 0.5 seconds gas residence time) of 75-80% total liquids, with about 65%

organic liquid yield on the dry wood basis. The oil is a single phase liquid containing from 10% to 25% water in solution, depending on the moisture content of the feed (normally under 10%). The oil is fluid, stable on storage, has a low pour point and is acidic with a pH of 2.5-3.5 depending on the feed material. Liquid density is about 1200 kg/m^3. A typical elemental analysis (moisture free) would show about 53.6% C and 6.97% H.

Recent work in our laboratories has been directed to a more complete analysis of the liquid product, and investigations of how the product composition varies with reaction conditions. Some of the results are described in recent publications [4][5][6]. Additional investigations of the aromatic fraction, presumably derived from lignin, are described here.

EXPERIMENTAL

An oil derived from the fast pyrolysis of a clean sawdust (Run 59) obtained from hybrid poplar-aspen was used in this work. Pyrolysis was carried out in the continuous 3 kg/hr. unit using recycle product gas for fluidization. Details of Run 59 are given in Table 1. The wood feed was the standard poplar sample supplied by the International Energy Agency for their Biomass Liquefaction Test Facility program (a plantation hybrid poplar-aspen from the Ontario Ministry of Natural Resources, Canada, about eight years old).

The oil comprised the total recovered pyrolytic liquids (77.0% of the dry wood fed). One sample of this pyrolyzate was treated with dilute HCl (2.5 g. of oil and 20 g. of 1 N HCl refluxed for 30 minutes), and a second sample was dissolved in methanol and then treated with a solution of La Cl_3 (2.0 g. of oil, 10 g. of methanol and 20 g. of 5% solution of La Cl_3 followed by refluxing for one hour and slow evaporation of the methanol). In both cases the product consisted of two phases which gave a clear separation into a dark brown viscous liquid, which solidified to a brittle solid on cooling, and a yellowish aqueous phase. The former dark phase will be referred to as pyrolytic lignin (PL). This material was washed and then dried at 105°C to give a hard brown solid which was readily powdered.

The yield of the pyrolytic lignin fraction was 24.1% and 22%, respectively, of the moisture free organic liquid, while the overall yield of the latter was 66.2% of mf wood. Typically aspen wood contains 16-21% of lignin. The NMR spectra to be discussed below showed no significant carbohydrate contamination in the pyrolytic lignin, so if the initial wood is assumed to contain 19% of lignin (mf basis) then the data imply that about 80% of the wood lignin was "liquified" during pyrolysis. This value is surprisingly high for a temperature of 504°C in view of published experimental results on the fast pyrolysis of wood lignins [7].

Spectra were recorded of 8-9% solutions of pyrolytic lignin in DMSO-d_6 at 62.9 MHz and 50°C with broad-band proton decoupling. Delay time between pulses was 10 s. Provided the material was sufficiently depolymerized, this delay would be expected to be sufficient for complete relaxation of all carbons so that the recorded relative line intensities should be quantitative. However, a small amount of a very fine black precipitate was observed to have been formed in the solutions after several hours so this may not be quite true. Acetone appears to be a much better solvent leading to lighter solutions which remain stable. Acetone-d_6 might therefore prove to be a superior solvent for this purpose.

RESULTS AND DISCUSSION

Nimz [8][9] has made assignments of all the important peaks in the spectra of milled wood lignin (MWL) from beech and spruce. On the basis of these, Marchessault et al. [10] have made assignments for milled wood lignin and steam exploded wood lignin (EXWL) from the aspen species populus tremula. The spectra of pyrolytic lignin may be interpreted in similar fashion.

The spectra of both the acid and metal ion hydrolyzed samples of pyrolysis oil were virtually identical. That of the latter was more noise-free and is shown in Figure 1. All chemical shifts are reported relative to TMS as reference. The broad features do confirm that the material isolated did in fact originate from lignin although it has clearly suffered extensive degradation. Thus the two main groups of peaks characteristic of beech and aspen lignin are present. These are from 20-90 ppm, characteristic of aliphatic side chains and 105-160 ppm, characteristic of olefinic side chain and aromatic carbons. In addition, the prominent methoxyl peak at about 56 ppm is also present.

Assignments for the more important peaks were made as follows. {To facilitate comparison, peaks are numbered in the same way as Marchessault [10] (see Figure 1). Chemical shifts are relative to TMS reference.}

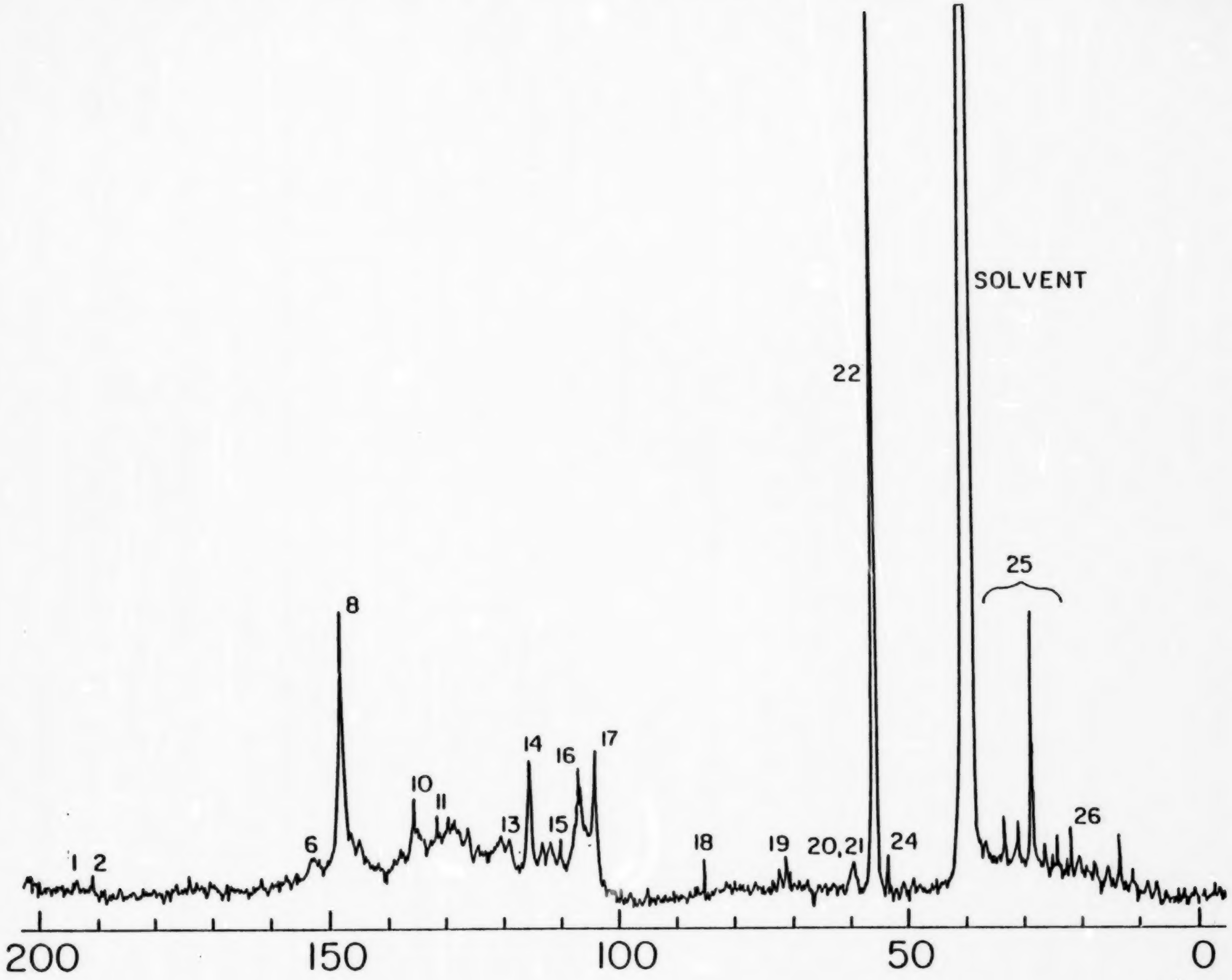

Figure 1 ^{13}C NMR Spectra of Pyrolytic Lignin from Fast Pyrolysis of Poplar wood

Peak No.	Chemical Shift	Assignment
1	~193	α-CHO
2	~191	γ-CHO in cinnamaldehyde
6	~152	C_3/C_5 in S (etherified)
8	148.3	C_3/C_5 in S (non-etherified) C_3 in G
10	135.4	C_1 in G (etherified)
11	131.7	[C_β in cinnamaldehyde]
13	~119	[C_6 in G (etherified)]
14	115.5	C_5 in G (non-etherified) C_3/C_5 in p-hydroxyphenl
15	~111	[C_2 in G (etherified)]
16	107.2	C_2/C_6 in S with α-CHO
17	104.3	C_2/C_6 in S
18	~ 86	C_β in β-0-4
19	~ 72	C_α in β-0-4
20, 21	~60-62	[C_γ in β-0-4 and phenylcoumaran]
22, 23	56.3	Methoxyl in S and G resp.
24	~54	C_β in phenylcoumaran units
25, 26	15-45	Saturated aliphatic side chain

In the above table, G denotes a guaiacyl and S a syringyl unit. The term "etherified" refers only to the link at C_4 and not to methoxyls. On account of the somewhat unsatisfactory signal to noise ratio the bracketed assignments should be regarded as tentative. The others seem well established by the works of Nimz and Marchessault [8][10].

Aspen lignin is a polymer made up largely of guaiacyl propane (57%) and syringyl propane (43%) units [11]. These basic configurations are illustrated in Figure 2(a). About 50-60% of the links joining these units are of the arylglycerol-β-aryl ether type (β-0-4) and this structure is also illustrated in Figure 2(a) [12]. In addition, aspen lignin is unique in that it contains about 10% of p-hydroxybenzoate groups [13a, 13b, 13c] which would be expected to pyrolyze readily to yield CO_2 and phenol, while any such unpyrolyzed groups would readily hydrolyze under the hydrolysis conditions used to give p-hydroxybenzoic acid which would be solubilized. Thus small losses of pyrolytic lignin can be expected to occur in this fashion.

Comparison of the spectra shown in Figure 3 of aspen milled wood lignin and steam exploded lignin [10] with that of pyrolytic lignin is instructive. A clear progression in degree of degradation is indicated. There are three principal indicators of this trend.

(i) Peak 6 is typical of C_3/C_5 in etherified syringyl units. It is strong in the milled wood lignin, much reduced in steam exploded wood lignin and reduced even more so in the spectra of pyrolytic lignin. Correspondingly, peak 8 (C in non-etherified guaiacyl and C_3/C_5 in non-etherified syringyl) is small in milled wood lignin, significantly increased in steam exploded wood lignin but is relatively largest in pyrolytic lignin. Taken together these changes indicate extensive scission of β-0-4 links with depolymerization being greatest in the pyrolytic lignin.

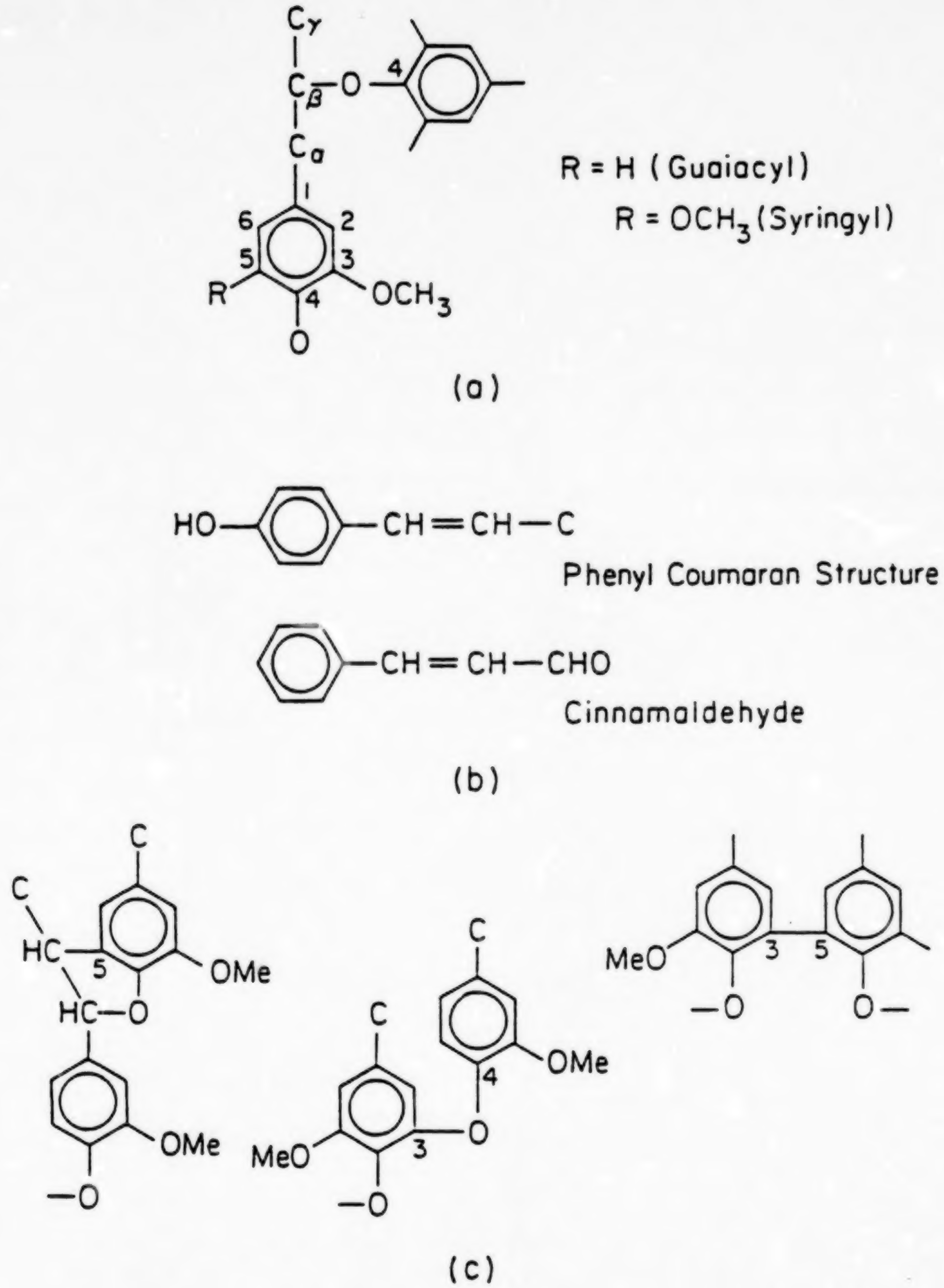
Cγ
Cβ
O
4
Cα
1
6
2
5
3
R
4
OCH3
O
R = H (Guaiacyl)
R = OCH3 (Syringyl)
(a)
HO
CH=CH—C
Phenyl Coumaran Structure
CH=CH—CHO
Cinnamaldehyde
(b)
C
C
HC
5
OMe
HC—O
OMe
—O
C
C
OMe
4
O
MeO
3
—O
MeO
3
5
—O
O—
(c)

Figure 2 (a) Representation of Guaiacyl and Syringyl Structures

(b) Representation of Coumaran and Cinnamaldehyde Structures

(c) Examples of Condensed Structures for Guaiacyl and Syringyl Units (from Nimz [8])

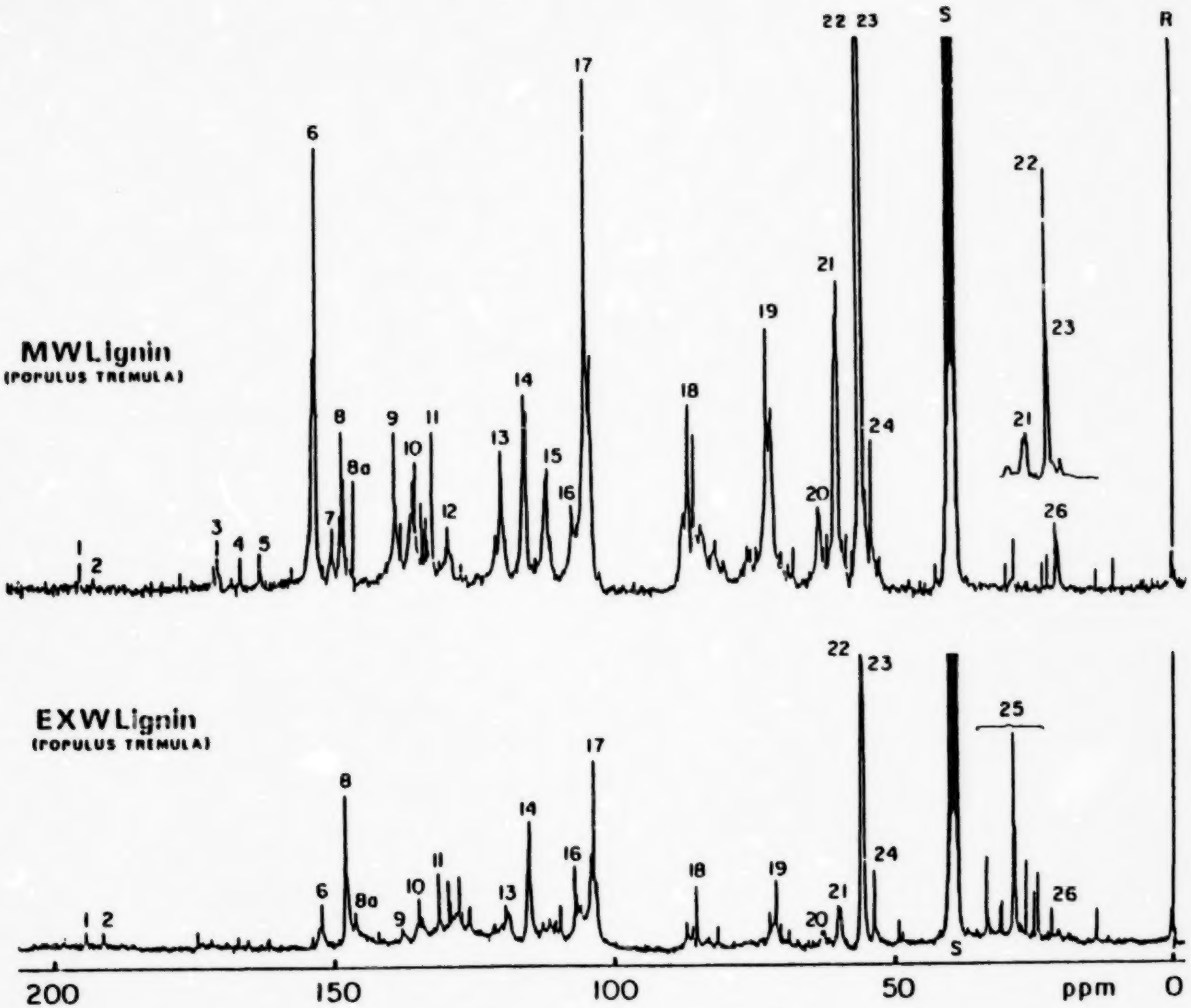

Figure 3 ^{13}C NMR Spectra of Milled Wood Lignin and Steam Exploded Lignin from Poplar Wood (from Marchessault et al. [10])

(ii) Peaks 18, 19 and 20 correspond to β, α and γ-carbons respectively, in the propyl side chain, when β-0-4 links are present. These peaks are relatively smallest in the pyrolytic lignin confirming the conclusion drawn above concerning the relative degree of depolymerization.

(iii) The group of peaks designated 25 are due to saturated aliphatic side-chain carbons. They are very weak in milled wood lignin, much increased in steam exploded wood lignin but again are relatively most intense for the pyrolytic lignin.

Other noteworthy features include the low intensity of peak 13, due to etherified guaiacyl units, and the relatively high value of peak 14 which can be attributed to non-etherified guaiacyl. Small amounts of olefinic materials appear to be present, for example, phenyl coumaran structures as indicated by peaks 20 and 24 and cinnamaldehyde as indicated by peaks 2 and 11 [these structures are shown in Figure 2(b)]. Peak 1 indicates the presence of small amounts of benzaldehyde derivatives.

There are apparently very significant amounts of methoxyl groups still existing in the pyrolytic lignin. This is interesting as such groups are thought to be a significant source of CH_4 in wood pyrolysis. Unfortunately, the quality of the spectrum was not sufficiently good to obtain a reliable integral for the relative amount of methoxyl carbon present.

Another point worthy of note is the apparently much greater abundance of syringyl (S) over guaiacyl (G) in the pyrolytic lignin units. This characteristic is also observed in steam exploded wood lignin [13a] in spite of the fact that there is a somewhat larger amount of guaiacyl than syringyl in the wood, as was pointed out earlier. In fact it is known [11] that on oxidation of hardwoods by nitrobenzene, only about 30% of guaiacyl units are converted to vanilin while about 90% of syringyl units are transformed to syringaldehyde. This difference in oxidation behaviour can be explained by the absence of condensed structures among syringyl units [11]. Such structures (C-C bonds or ether links at C_5 or C_6) appear mainly among guaiacyl units on account of the absence of a methoxyl group at C_5. Typical condensed structures taken from Nimz' model lignin [8] are shown in Figure 2(c). It seems quite possible that, because of this difference in behaviour, guaiacyl units will preferentially end up in the char product with syringyl units degrading more easily and ending up in the liquid.

This conclusion is consistent with the following observations made on the low molecular weight phenolic portion of a similar pyrolytic oil. In Run No. 58 a whole-tree hybrid poplar (Brockville Poplar) was pyrolysed under identical conditions to those outlined in Table 1. The high molecular weight fraction of the pyrolytic lignin was precipitated by diluting the oil with three parts of cold water. After filtration the dark brown aqueous phase was clarified by adsorption on activated carbon which was filtered off and extracted with acetone. After evaporation of the bulk of the acetone the viscous red-brown residue was examined by GC-MS. The results are shown in Figure 4 and Table 2.

The 3-methyl-1,2-cyclopentane dione and pyrocatechol are believed to be derived from carbohydrates by known "browning"

Table 1

Details of Pyrolysis Test

Run No.	59
Reaction Temperature	504°C
Feed	IEA hybrid poplar wood, air dried to 4.6% moisture C 49.45% H 6.05% N 0.07% O 44.4% Ash 0.46% *
Particle Size of Feed	-1000 microns
Apparent Vapour Residence Time	0.48 seconds
Feed Rate	1.85 kg/hr
Yields, weight % of mf wood fed	
Organic Liquid	66.2
Water	10.8
Char	11.8
H_2	0.01
CO	4.44
CO_2	5.75
CH_4	0.37
C_2H_4	0.13
C_2H_6	0.05
C_3	0.08
C_4+Light Volatiles	0.19
Total Gas	11.0
Total Product Recovery	99.8%
pH of pyrolysis oil	2.45
Density of pyrolysis oil	1.23 g/ml
Water Content of Oil, %	18.6

* Elemental Feed Analysis maf basis

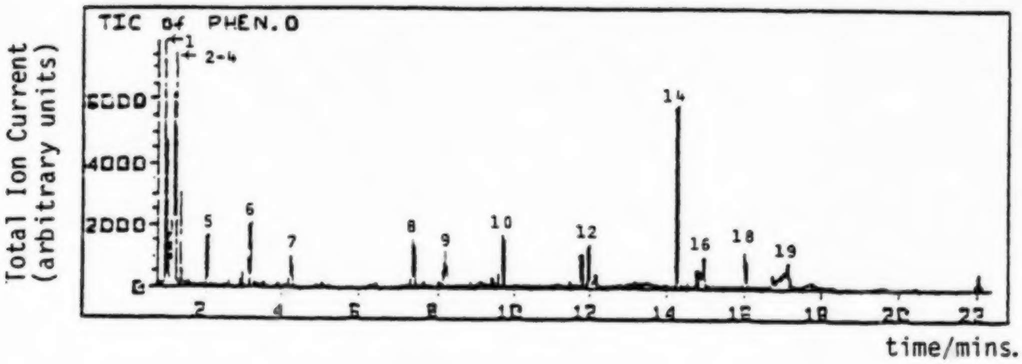

Figure 4 Chromatogram of a Low Molecular Weight Fraction of Pyrolytic Oil from Run 58 (see text).
Column: Hewlett-Packard (HP) DB-1 Fused Silica Capillary (12 m x 0.20 mm).
Carrier Gas: He at 54 cm³/min, split ratio = 1/9.
Temperature Program: 60°C for 5 mins., 10°C/min to 150°C.
HP 5970 Mass Selective Detector.

Table 2

Compounds Identified in the Chromatogram of Fig. 4

Identification was made by comparison of mass spectra with standards in the NBS Mass Spectral Libraries. If the match was not excellent the compound is bracketed and should be regarded as tentative.

Peak No.	Substance
1	Acetone
2 - 4	Hydroxyacetaldehyde, acetic acid and acetol. (These arise from the carbohydrate portion of the wood.)
5 - 7	(Linear and cyclic acetals of hydroxyacetaldehyde.)
8	Phenol
9	3-Methyl-1,2-cyclopentane dione
10	(Guaiacol)
12	Pyrocatechol
14	Syringol
16	(4-hydroxy-3-methoxy benzaldehyde)
18	(1-[4-hydroxy-3-methoxyphenol] ethanone)
19	(4-hydroxy-3,5-dimethoxy benzaldehyde)

reactions [15]. Acetol, acetic acid and hydroxyacetaldehyde arise directly from holocellulose during pyrolysis. Acetone is extraneous. The remaining compounds identified all appear to derive from lignin. It is evident that among these syringol is by far the most abundant. A preliminary quantitative estimate suggests that it may constitute of the order of 1-2% of the whole oil.

Finally, it is of interest that Marchessault et al. [10] found a number average molecular weight of 700 and a mass average molecular weight of 1700-1900 for steam exploded wood lignin. This value should be compared to the typical milled wood lignin molecular weight of 11000. On the evidence of the NMR spectra, pyrolytic lignin, being even more degraded, should have a still smaller molecular weight. Insofar as this is favourable for copolymerization applications [11], pyrolytic lignin should be even more suitable than steam exploded wood lignin for such reactions. On the other hand if pyrolytic lignin is indeed relatively enriched in syringyl units, then this might be unfavourable for generation of phenolformaldehyde resins as the critical ortho-positions are blocked. A higher content of syringyl groups should, however, be no obstacle in the formation of polyols and urethane foams by the methods outlined by Glasser [14a, 14b].

It appears that the oils produced by the Waterloo Fast Pyrolysis process from wood contain a fraction derived from the lignin content which represents nearly 80% of the lignin. This pyrolytic lignin is relatively richer in syringyl groups than the original lignin, and has an appreciable methoxy content. The general structure of the pyrolytic lignin is very similar to that of lignin from steam exploded wood, although the average molecular weight of the former may be somewhat lower because of its apparent greater degree of depolymerization.

ACKNOWLEDGEMENTS

The authors would like to express their thanks to the National Research Council of Canada and to the Natural Sciences and Engineering Research Council of Canada for the financial support of this work. The assistance of A. Grinshpun and P. Majerski is also gratefully acknowledged.

REFERENCES

1 D.S. Scott and J. Piskorz, Can. J. Chem. Eng. (1984) 62, 404-412

2 D.S. Scott, J. Piskorz and D. Radlein, Ind. Eng. Chem. Process Des. Dev. (1985) 24, 581-588

3 D.S. Scott and J. Piskorz, Bio. Energy 84, Vol. 3, H. Egnéus and A. Ellegard (Editors), Elsevier, London (1985) 15

4 J. Piskorz, D. Radlein and D.S. Scott, J. Anal. Appl. Pyrolysis (in press)

5 D.S. Scott and J. Piskorz, "The Composition of Oils from the Fast Pyrolysis of Cellulosics" submitted to J. Anal. Appl. Pyrolysis, Nov. (1985)

6 D. Radlein, A. Grinshpun, J. Piskorz and D.S. Scott, "On the Presence of Anhydro-Oligosaccharides in the Sirups from the Fast Pyrolysis of Cellulose", submitted to J. Anal. Appl. Pyrolysis, Nov. (1985)

7 T.R. Nunn, J.B. Howard, J.P. Longwell and W.A. Peters, Ind. Eng. Chem. Process Des. Devel. (1985) 24, 844

8 H. Nimz, Angew. Chem. Int. Ed., 13 (1974) 31

9 H.-D. Ludemann and H. Nimz, Biochem. Biophys. Res. Commun. 52 (1973) 1162

10 R.H. Marchessault, S. Coulombe, H. Morikawa and D. Robert, Can. J. Chem., 60 (1982) 2372

11 Lignins: Occurrence, Formation, Structure and Reactions K.V. Sarkanen and C.H. Ludwig (eds.), Wiley-Interscience N.Y. (1971) p.43

12 I.S. Goldstein in "The Chemistry of Solid Wood", R. Rowell (ed.), Adv. in Chem. Ser. 207, A.C.S. (1984) p.575

13 (a) D.S.C. Smith, J. Chem. Soc. (1955) 2345
  (b) I.A. Pearl et al., Tappi 40 (1957) 374
  (c) J. Nakano et al., Tappi 44 (1961) 30

14 (a) O.H.-H. Hsu and W.G. Glasser, Appl. Polym. Symp. 28 (1975) 297
  (b) Chem. Eng. News., Sept. 24 (1984) pp 19-20

15 K. Olsson, P.A. Pernemalm and O. Theander, Prog. Fd. Nutr. Sci., 5 (1981) 47

Captions

Figure 1 ^{13}C NMR Spectra of Pyrolytic Lignin from Fast Pyrolysis of Poplar Wood

Figure 2
(a) Representation of Guaiacyl and Syringyl Structures
(b) Representation of Coumaran and Cinnamaldehyde Structures
(c) Examples of Condensed Structures for Guaiacyl and Syringyl Units (from Nimz [8])

Figure 3 ^{13}C NMR Spectra of Milled Wood Lignin and Steam Exploded Lignin from Poplar Wood (from Marchessault et al. [10])

Figure 4 Chromatogram of a Low Molecular Weight Fraction of Pyrolytic Oil from Run 58 (see text).
Column: Hewlett-Packard (HP) DB-1 Fused Silica Capillary (12 m x 0.20 mm).
Carrier Gas: He at 53 cm^3/min, split ratio = 1/9.
Temperature Program: 60°C for 5 mins., 10°C/min to 150°C.
HP 5970 Mass Selective Detector.

7. PRELIMINARY CONCEPTUAL DESIGN AND ECONOMIC FEASIBILITY STUDY FOR THE WFPP

7.1 Executive Summary and Comments

The economic feasibility study was carried out by John Black of BBC Engineering & Research Ltd. under a subcontract placed in mid-1985. Basic material and energy balances, as well as compositions, reaction parameters etc. were supplied by the Waterloo Pyrolysis group.

A study of two possible plant sizes was requested - 500 dry tonnes/day and 100 dry tonnes/day. In addition, some preliminary consideration of potential markets was to be done. A copy of the original letter of enquiry to consultants is attached as Appendix 7-A.

Executive Summary of the consultant's report is attached, together with the Table of Contents of the report. One full copy has been submitted as Section 7.2 with the original of this report to the Renewable Energy Division of Energy, Mines and Resources Canada.

In general, we are satisfied with the work done and the conclusions reached, although they are very decidedly conservative, and the costs quoted can therefore be taken as near maximum or "worst case" values. We do not agree with the consultant's statement at the top of the second page, as our annotation shows. Our studies show that up to a capacity of 50-100 tonnes/day, a fluidized bed reactor with a 1 m deep bed could be readily designed from current scale up knowledge to give a 0.7 second gas residence time. The fast fluidized or circulating fluid bed reactor suggested by the consultant would apply therefore only for the larger scale plants. Inasmuch as one of the basic proposals for the WFPP is that it be operated as multiple small scale units located at the site of the biomass supply, the ability to use the standard fluidized bed technique in the WFPP is important. However, as the consultant points out, the cost of the pyrolysis reactor is not a major cost item, regardless of its particular design.

It is worthwhile to quote a statement concerning manufacturing costs (p.49 of full report)

"The resultant manufacturing costs, as shown in Table VIII, can be competitive with other fuel prices, at least for the smaller plant (our emphasis), in areas with low labour costs and low biomass costs. This tends to suggest that the technology would be well suited to developing countries with little indigenous petroleum fuel."

The major capital cost items are the feed preparation and drying system. The annual fixed costs for the assumptions made include interest and return on investment charges which amount to 25% of the total annual cost of production. Therefore, reduction in capital costs would not only reduce normal fixed costs but these financial costs as well. Hence, if drier feed stock could be found, or inexpensive (e.g. air drying) used, and if a larger particle size could be used, a much more economical process would result. Also for smaller plants, labour costs are 40%-30% of the total annual production cost. If a nearly automatic integrated small scale processing unit could be devised, the process would again be rendered much more economic.

It would appear that the factors identified as high cost contributors are likely to be of less importance in special situations in Canada or generally in less developed countries. It is also evident that in the demonstration or PDU stage, significant improvements in costs in these areas could be made to the Waterloo Fast Pyrolysis Process.

However, on a larger scale, the WFPP is presently marginally competitive for the production of an alternative fuel oil. Given special circumstances, or some modest increase in petroleum prices, this process could very quickly become competitive generally.

APPENDIX 7-A

PRELIMINARY EVALUATION
OF THE
WATERLOO FAST PYROLYSIS PROCESS

Prepared for

Professor D.S. Scott
University of Waterloo

by

John W. Black

BBC ENGINEERING & RESEARCH LTD.
Markham, Ontario

June 1986

EXECUTIVE SUMMARY

Using fluidized bed technology, Professor D.S. Scott and his associates at the University of Waterloo have developed a process for the production of liquid fuels from biomass.

In the present study, the conceptual process, originated by D.S. Scott and his co-workers, was modified and then developed into a formal process flow-sheet, complete with mass and energy balances. The capital and operating costs for two plant sizes (100 B.D.T.P.D. and 500 B.D.T.P.D.) were estimated and a preliminary evaluation of the market completed.

In designing the plant, a number of alternative techniques for providing process energy were examined including indirect heat exchange, in-bed heat exchange and direct heat exchange with partially combusted char. Because of its simplicity, the char combustion alternate was ultimately incorporated into the final process flow-sheet. For the most part, the design employed equipment and operational conditions that are typical of conventional petrochemical practice with two exceptions. The char combustor was designed to operate at a very high temperature (1370°C). This, however, was considered acceptable. A major difficulty was encountered in the design of the fluidized bed reactor which was constrained by the requirement for a gas residence time of 0.7 seconds. In the pilot plant, this is achieved with a velocity of about 0.6 m/s and a total reactor height of 0.4 metres. In a commercial reactor with a large

Not true. A 1 m deep, fluidized bed can be used for 100 t/d plant

diameter, it is extremely difficult to limit the reactor height to less than 3 metres. For design and estimating purposes, the fluidizing velocity was increased to 3.3 metres/sec i.e. the bed was projected to be a fast fluid bed with its concomitant large bed recirculation rates. While this configuration may not prove to be the final design arrangement, it was thought adequate for preliminary estimating purposes. An alternative approach of rapid quenching of the gas in the dilute phase above the bed, while feasible, was not investigated in detail in this report. Much more work is needed in this area in order to define a commercial sized reactor.

Not a large cost factor.

For the larger 500 B.D.T.P.D. plant, a capital cost of ($9.5 million) was estimated by quotations and from literature sources. The major elements of cost were the feedstock processing (50% of T.I.), the reactor including feeding system (20% of T.I.), and the product recovery and cooling module (30% of T.I.) where T.I. is the total investment.

Subsequently, the operating costs (O.C.) were estimated and for a 500 B.D.T.P.D. plant, the major costs were identified as: raw materials at 55% O.C. and capital related items at 30% O.C. Thus the final production cost is most sensitive to raw material price which, in the present instance, was taken to be $40/B.D. tonne. These operating costs translate into product prices, at the plant gate, of: $92/tonne (including 24% moisture) or 10.8 ¢/litre (S.G. = 1.18) or $5.7/million BTU. The debt/equity ratio was assumed to 50/50 with a return on investment of 30% before tax.

These values are only marginally competitive in some areas of Canada but are quite competitive in many areas of the world.

For the smaller plant (100 B.D.T.P.D.), the major operating costs were associated with labour and capital related charges. The resulting product price, $143/tonne ($8.9/M.M.B.T.U.) was not considered viable in Canada or the U.S.A.

With a raw material such as municipal refuse, which is well suited to the technology, the process can be very competitive especially at larger plant sizes.

If it is possible to separate lignins, anhydro-sugars, aldehydes, ketones and the carboxylic acids which are all present in significant amounts, then the readily available markets for these commodities would enhance the viability of the technology.

One very positive aspect of the on-going work at the University of Waterloo, is that the reactions can be made more specific by wood pretreatment and selection of reactor parameters. This will permit higher yields of valuable products, easier separation from by-products and ultimately greater marketability for the process.

TABLE OF CONTENTS

Page

EXECUTIVE SUMMARY i
TABLE OF CONTENTS iv
LIST OF TABLES v
LIST OF FIGURES vi

1.0 INTRODUCTION 1

2.0 PROCESS DESIGN CRITERIA 4

2.1 Design Conditions 6

2.1.1 Design Temperature 7
2.1.2 Particle Size 8
2.1.3 Gas Phase Residence Time 9
2.1.4 Solids REsidence Time 9
2.1.5 Heat Transfer Rate 10

2.2 Process Design Basis 11
2.3 Reactor Model 15
2.4 Initial Conceptualization 16
2.5 Alternate Flowsheets 17

2.5.1 Indirect In-Bed Heat Exchange 17
2.5.1.1 Limiting Fluidizability Conditions 19
2.5.1.2 In-Bed Heat Exchange Bundle 21

2.6 Combustion of Pyrolysis Gas 22
2.7 Combustion of Char 23
2.8 Summary of Alternate Heating Systems 24

3.0 PLANT DESIGN 29

3.1 Materials Processing 29
3.2 Pyrolysis System 31

3.2.1 Alteration of Fluidizing Regime 32
3.2.2 Shock Cooling 34

3.3 Char Combustor 37
3.4 Gas Cooling and Vapour Condensation 38
3.5 Gas Cleaning 40
3.6 Dryer Combustor 40
3.7 Mass and Energy Balances 41

4.0 COST ESTIMATE 42

- 4.1 Capital Cost Estimate 42
- 4.2 Operating Cost 43
  - 4.2.1 Raw Material Costs 43
  - 4.2.2 Labour 45
  - 4.2.3 Utilities 45
  - 4.2.4 Capital Related Charges 46
- 4.3 Discussion 47
  - 4.3.1 Capital Cost 47
  - 4.3.2 Manufacturing Costs 49
- 4.4 Cost of a Mini Plant 52

5.0 MARKET EVALUATIONS 53

- 5.1 Direct Fuel Replacement 53
- 5.2 Modified Fuel Market 58
- 5.3 Non Fuel Uses 59

6.0 CONCLUSIONS 64

7.0 RECOMMENDATIONS 66

8.0 REFERENCES CITED 67

APPENDIX A Flowsheets

LIST OF TABLES

			Page
Table	1	Pilot Plant Tests at 500°C	7a
	2	Reactor Design Parameters	12
	3	Estimated Physical Properties	13
	4	Comparison of Results with Waterloo Data	15a
	5	Comparison of Alternate Reactor Heating Schemes	28
	6	Capital Cost Estimate	44
	7	Shift Operator Requirements	45a
	8	Estimate of Operating Costs	48
	9	Physical Properties of Fuel	55
	10	Resource Recovery Plants	57
	11	Product Categories in Pyrolysis Oils	60

LIST OF FIGURES

		Page
Figure 1	Flow Sheet of Pilot Plant	2
2	Preliminary Plant Concept	5
3	Inlet Temperature vs Recycle Ratio	16a
4	Effect of In-Bed Heat Exchange on Recycle Ratio	18a
5a	Energy Input by Indirect Heat	25
5b	Energy Input by In-Bed Heat Exchange	25
6a	Energy Input by Direct Heat	25a
6b	Energy Input by Char Oxidation	25a
7a	Effect of Capital Cost on Product Price	50
7b	Effect of Feedstock Cost on Product Price	50
8a	Effect of Labour Cost on Product Price	51
8b	Effect of R.O.I. on Product Price	51
9	Chemicals Derived from Biomass	61

University of Waterloo

Waterloo Ontario Canada
N2L 3G1

Faculty of Engineering
Department of Chemical Engineering
519 885-1211

Telex Number
069 55259

May 29, 1985

Mr. John W. Black
BBC Engineering and Research Ltd.
P.O. Box 388
Markham, Ontario
L3P 3J8

Dear John,

As you are aware, we have been engaged for some time at the University of Waterloo in developing what is now known as "The Waterloo Fast Pyrolysis Process". As a part of our current research program (sponsored originally by NRC but now under the direction of the Renewable Energy Division of the Energy Research Laboratories, EMR) we have agreed to carry out a preliminary economic feasibility study of our process. In preparation for this, we have carried out reactor optimization studies, and have some solid data for pyrolysis reactor design. Product collection technology is more of a question mark, but we have decided on the most desirable method even though some data is lacking.

We have funds in our present budget to allow a sub-contract with a value up to $18,000 to carry out this study. We have neither the time nor expertise to do the study ourselves, so we are asking two or three engineering firms such as yours to submit a short proposal (about two pages) to carry out the study. The questions the study should answer are listed below, and are intended mainly as guidelines. The study should be completed by about December 31, 1985.

1. On the basis of two plant sizes, 100 oven dry tonnes/day and 500 oven dry tonnes/day, what is the capital cost and the production cost in energy terms of a crude pyrolysis oil? What are the major cost factors?

2. Supply conceptual flow sheets and complete material and energy balances for the two plant sizes.

3. Give an analysis of possible market areas for the pyrolysis oils, or of potential markets for the flash pyrolysis technology.

We would supply details of our investigations so far, and data concerning the process, feed materials, product characteristics, etc. A copy of one publication on the process is enclosed, but it should be remembered that the information given is nearly two years old. However, it describes the central concept.

Please feel free to call me or to visit us at Waterloo if you wish to do so. We would like to receive your proposal, if you are interested, by about July 15, 1985.

Yours sincerely,

Donald S. Scott
Professor

Encl.

8. CONCLUSIONS AND RECOMMENDATIONS

In the last two years (1984-86), as a result of the work done under this contract, as well as from some fundamental studies, it is fair to say that the Waterloo Fast Pyrolysis Process has proven itself to be one of the most promising routes for the conversion of cellulosic biomass to alternative fuels or chemicals. Indeed, the potential of the fast pyrolysis method as a way of preparing feedstocks for the recovery of chemicals, or other by-products of value, is just now being appreciated. The studies reported here show at least four major applications for the liquid products produced by the WFPP. These are discussed in turn in the following.

As a source of an alternative fuel oil, the WFPP is competitive with oil at $20-$25/bbl if wood costs about $40 per dry tonne. Conversion to a fuel oil, which is used directly as produced from the WFPP, has many advantages. The oil stores well, if air is excluded. The WFPP can be economically used on a smaller scale, that is, multiple units could be located at the sources of the biomass, and if this led to low costs for the feed material, the operating cost of a small unit would be competitive also. Liquid product can be readily transported to a central facility, for further processing, if desired. The oil has a low heating value, but is 50% denser than a hydrocarbon oil, and thus the volumetric heating value is reasonable. The oil can be burned as produced in conventional pressure or air atomizing oil fired equipment. Given the right economic circumstances - a cheap source of biomass, and high local prices for fuel, the WFPP would be economic even today. It is recommended, therefore, that more extensive combustion tests of the oil should be carried out. Consideration should be given to a possible demonstration unit with a capacity of 5-10 t/day. The cost is estimated to be about $1.5 million, and a mechanical design is now being prepared. In particular, it is expected that a ready market exists today for this technology in many third world countries that have no indigenous fossil fuel supplies.

The WFPP pyrolysis oil has been more fully analyzed in this present study than any previously reported thermal biomass product. We have identified 85%-90% of all the liquid components, and more recent work has indicated that most of the missing 10%-15% are not unknown components, but are losses of some of the major components occurring in our analytical procedures. Roughly, the pyrolysis oil at optimal condition contains about 25% lignin derived aromatic materials, 22% water and 53% carbohydrate derived compounds. The carbohydrate based fraction is interesting because of its high contents of hydroxyacetaldehyde (10%-15%) and acetic acid (about 10%). Both of these have commercial value. In addition, a number of other compounds of present and potential commercial value are present. Many of these are fermentable sugars, and the carbohydrate containing fraction could be used as a fermentation substrate, if desired.

The separation of the crude pyrolysis oil into a lignin and a carbohydrate fraction is readily carried out by a water extraction. The lignin fraction can be recovered as a solution or as a powder. The lignin fraction from poplar shows an NMR spectra which is virtually identical to that of the lignin from steam-exploded poplar (Stake process), but the molecular weight of the WFPP product appears to be somewhat lower. Initial tests of this "lignin" product as a constituent of plywood or chipboard glues shows considerable potential. This lignin product could be produced very cheaply.

Recent work has shown that the nature of the carbohydrate derived fraction can be controlled by a mild pretreatment of the wood to give a much higher yield of anhydrohexoses at the expense of hydroxyacetaldehyde and acetic acid. A liquid can be readily produced in which 30%-40% of the dry wood weight has been converted to fermentable sugars, with the sugar content at 10%-15% by weight. Further, this substrate is produced very cheaply. Fermentation tests are currently underway, as are investigations for the recovery of single compounds from the pyrolysis oil, particularly amhydrosugars and hydroxyacetaldehyde.

Given the low cost of producing these specialty chemicals from waste wood, or producing a cheap fermentation substrate, the potential of the pyrolysis oils for these uses should be explored with vigor. It is probably appropriate to consider encouraging other research groups to engage also in studies of this type, using oils supplied from our pilot plant.

The Waterloo Fast Pyrolysis Process itself has been fully optimized in this study from the viewpoint of determining the best reaction conditions for maximum liquid yields, using either hardwood or softwood feed. However, this work was in essence a suboptimization study based on reactor behaviour and design. The study showed that temperature was the single most important controllable variable in the feasible ranges of reactor operating conditions. Depending on the end use of the oil, it might be desirable to modify operating conditions. For example, higher feed moisture contents might be used when the oil is intended as a source of chemicals or lignin, rather than as a fuel oil. Depending on grinding costs, larger particle sizes than 2 mm might be economic, even if liquid yields were slightly lower. In fact, it is recommended that a study be done using larger feed particles of two kinds - one with a small dimension across the grain (pin chips) and one with the small dimension parallel to the grain (conventional chips).

The yield of oils as a function of temperature has been measured for poplar (and for cellulose) over the temperature range of 450°C-850°C, and this yield curve has been successfully modelled and kinetic parameters derived. The residence time of wood particles and char particles in the fluid bed pyrolyzer have been measured, as has the heat of the pyrolysis reaction. In effect, the wood particle is fully mixed at all times and is not eluted from the bed until its density approaches that of the char. As a result, the required solid particle residence time required for full decomposition is self-regulating in the fluidized bed reactor.

Scale-up parameters and mixing behaviour in fluid beds with height/diameter ratios <1.0 were investigated (shallow fluid beds) and successful models developed for pyrolysis reactions in such shallow beds. It is our present belief that a fluid bed could be successfully used for the WFPP at throughputs up to 50-100 t/day. A PDU unit would allow further testing of these kinetic models and mixing correlations.

It should be stressed that the pyrolysis oil mixture obtained from the WFPP was found to be unexpectedly rich in several interesting multifunctional chemicals, especially hydroxyacetaldehyde and hydroxy propanals. Useful yields of carboxylic acids and hydroxy acids are also obtained; as well as of anhydrosugars. Further, our mixture does not appear to be as complex a mixture as others have reported for other processes. These facts have allowed us to publish some speculations on the mechanisms of fast pyrolysis of cellulose. It is recommended that the potential of this oil as a chemical feedstock should be evaluated as quickly as possible.

The lignin product may be useful in the existing lignin derivatives market (over one billion lbs. per year), and product tests are recommended, and are now being done to a limited degree. Selling prices of commercial lignin are such that this product alone could support the process.

A high sugar content fermentation substrate can be prepared from the carbohydrate derived fraction of the pyrolysis oil. This would be a very cheap cellulose-to-sugar conversion process, and it is recommended that the economics of this modification should be evaluated.

APPENDIX "C"

TITLE: Technical Evaluation of the Waterloo Fast Pyrolysis Process

CONTRACTOR: Waterloo Research Institute

SCIENTIFIC AUTHORITY: Dr. R.P. Overend
Mr. E. Hogan

PRINCIPAL INVESTIGATOR(S): Dr. Donald S. Scott
Dept. of Chemical Engineering
University of Waterloo
(519) 885-1211 Ext.2914

DURATION: One Year

COST:

OBJECTIVE(S):
Optimization of the Waterloo Fast Pyrolysis Process
Characterization of the Liquid Pyrolysis Oil
Modeling of the Process
Preliminary Economic Feasibility Study

RESULTS: The WFPP shows the potential of being the cheapest current process for the conversion of biomass to an alternative liquid fuel oil. The crude pyrolysis oil also appears to be a good potential source of several valuable chemical compounds and of other by-products.

CONCLUSION: Further work is warranted to expand the scope of this promising process, and some of this work is currently underway.

RECOMMENDATIONS/ COMMENTS: A demonstration scale plant (5 to 10 tonnes/day) should be designed and sources of funding sought.
Some unique and significant contributions to the understanding of the mechanisms of the fast pyrolysis of cellulose and wood have come from this study. Unfortunately, this work cannot be pursued because of lack of funds.